

Upgrading of an Automated Micron Level
Measurement System for Sub-micron
Measurement

by

Brendan Phelan

Submitted for the degree of Master of Engineering

Supervisor: Mr. Joe Phelan

School of Engineering
Waterford Institute of Technology

Submitted to Waterford Institute of Technology, September 2010

Declaration

UPGRADING OF AN AUTOMATED MICRON LEVEL MEASUREMENT SYSTEM
FOR SUB-MICRON MEASUREMENT

Presented to: Mr. Joe Phelan

Department of Engineering Technology

Waterford Institute of Technology

This Thesis is presented in fulfilment of the requirements for the degree of Masters of Engineering. It is entirely of my own work and has not been submitted to any other college or higher institution, or for any other academic award in this College. Where use has been made of the work of other people it has been fully acknowledged and fully referenced.

Signed: _____

Brendan Phelan

Date: _____

Acknowledgements

I would like to thank those who gave help and advice during the course of this project. Their help proved invaluable.

I would like, in particular, to thank my supervisor, Mr. Joe Phelan for his continuous help, encouragement and guidance and also the following people whose help I greatly appreciated:

Mr. David Walsh	Lecturer
Mr. Tom Wemyss	Post graduate student
Mr. Paul Allen	Lecturer
Mr. Liam O' Shea	Lecturer
Mr. Milo Ó' Rathaille	Lecturer
Mr. Albert Byrne	Head of Department of Engineering Technology
Mr. Mark Maher	Manufacturing Technician
Mr. Seamus Scully	Engineering Manager, NN Euroball
Mr. David Madigan	Post graduate student
Mr. Colman Shouldice	Post graduate student
Enterprise Ireland	Grant No. IP/2001/735

Table of contents

DECLARATION.....	II
ACKNOWLEDGEMENTS.....	III
TABLE OF CONTENTS.....	IV
LIST OF FIGURES	VI
LIST OF TABLES	VIII
ABSTRACT	IX
1. INTRODUCTION	10
1.1. PROJECT INTRODUCTION.....	10
1.2. BALL BEARINGS [52]	10
1.3. BALL BEARING MANUFACTURE AT NN EUROBALL KILKENNY [51],[52]	11
1.4. MANUAL MEASUREMENT SYSTEM	13
1.5. THE PROBLEM	14
1.6. AUTOMATED MEASUREMENT SYSTEM.....	15
1.7. STARTING POINT OF PROJECT	16
1.8. PROJECT OBJECTIVES.....	17
1.9. THESIS STRUCTURE.....	17
2. LITERATURE REVIEW	18
2.1. INTRODUCTION	18
2.2. PRECISION MEASUREMENT.....	18
2.3. KEY STATISTICAL TERMINOLOGY IN MEASUREMENT	20
2.3.1. <i>Introduction</i>	20
2.3.2. <i>Measurement accuracy, precision, and error</i>	21
2.3.2.1. Location Variation – Accuracy.....	22
2.3.2.2. Width Variation - Precision	22
2.3.2.3. Error.....	23
2.4. REVIEW OF CONTACT MEASUREMENT OPTIONS	26
2.4.1. <i>Precision movement technologies</i>	26
2.4.2. <i>Contact detection in precision measurement</i>	30
2.4.3. <i>Precision position measurement</i>	32
2.5. ENVIRONMENTAL EFFECTS.....	34
2.5.1. <i>Humidity</i>	35
2.5.2. <i>Temperature</i>	37
2.5.3. <i>Vibration</i>	38
2.6. SUMMARY	39
3. RELOCATION & MODIFICATIONS	40
3.1. INTRODUCTION	40
3.2. REPLACEMENT OF FLUID NORMALISING MEDIUM	41
3.3. RECONFIGURATION OF SAMPLE CIRCULATION	41
3.4. SAMPLE ORDER CONTROL	47
3.5. FLUID LEVEL CONTROL AND CIRCULATION	49
3.6. NEW BRACKET FOR BALL IN PLACE SENSOR	51
3.7. PLC REWIRING & REPROGRAMMING.....	52
3.8. MONITORING AND CONTROL PROGRAM UPDATES	53
3.8.1. <i>Multiple touch measurement (LabVIEW)</i>	53
3.9. ADDITIONAL SENSORS.....	56
3.9.1. <i>Humidity and temperature</i>	56
3.9.2. <i>Fluid circulation status and air line pressure</i>	57
3.9.3. <i>Logging</i>	59
3.9.4. <i>Status board and interface modifications</i>	59
3.10. CONCLUSION.....	60

4.	POSITIVE PRESSURE PIEZO PROTECTION SYSTEM	61
4.1.	INTRODUCTION	61
4.2.	PHASE 1: PROOF OF CONCEPT.....	62
4.3.	PHASE 2: PROTOTYPING.....	63
4.4.	PHASE 3: PRIMARY EQUIPMENT IMPLEMENTATION	65
4.5.	SYSTEM TESTING.....	67
4.6.	CONCLUSION.....	68
5.	SAMPLE LOCATION AND FEED MECHANISM DEVELOPMENT	70
5.1.	INTRODUCTION	70
5.2.	CLAMPING	71
5.3.	CLAMPING AND SAMPLE LOCATION	71
5.3.1.	<i>Locating forces analysis</i>	72
5.3.2.	<i>Active clamping design</i>	78
5.3.3.	<i>Design study</i>	79
5.3.4.	<i>Active clamp implementation</i>	84
5.3.5.	<i>Testing</i>	86
5.4.	SAMPLE INSERTION MECHANISM.....	87
5.4.1.	<i>First implementation & issues with</i>	87
5.4.2.	<i>Design study</i>	88
5.4.2.1.	<i>Rotary</i>	89
5.4.2.2.	<i>Vertical</i>	90
5.4.2.3.	<i>Horizontal</i>	91
5.4.3.	<i>Implementation</i>	92
5.5.	CONCLUSION.....	93
6.	PROGRESSIVE MEASUREMENT IMPROVEMENTS.....	94
6.1.	INTRODUCTION	94
6.2.	SOURCES OF MEASUREMENT ERROR.....	94
6.2.1.	<i>12bit DAQ hardware</i>	95
6.2.2.	<i>Touch detection and step sizing</i>	95
6.2.3.	<i>Line Noise</i>	97
6.2.4.	<i>Measuring platform locking mechanism</i>	98
6.2.5.	<i>Sample seating</i>	99
6.2.6.	<i>In process damage</i>	102
6.2.7.	<i>Sample temperature variation</i>	102
6.2.8.	<i>Environmental temperature</i>	103
6.3.	EXPERIMENTATION	105
6.3.1.	<i>Measurement strategy and test methodology</i>	106
6.4.	RESULTS	107
6.4.1.	<i>Accuracy and Precision</i>	107
6.4.2.	<i>ANOVA Analysis</i>	110
6.4.3.	<i>Regression Analysis</i>	111
6.5.	CONCLUSION.....	112
7.	OUTCOMES, CONCLUSION, AND FURTHER WORK	113
7.1.	INTRODUCTION	113
7.2.	OBJECTIVES AND OUTCOMES	113
7.3.	CONCLUSIONS.....	114
7.4.	RECOMMENDATIONS FOR FUTURE WORK TO ACHIEVE AIMS AND OBJECTIVES	115
7.4.1.	<i>Temperature normalisation fluid filtration</i>	115
7.4.2.	<i>Cycle time</i>	115
7.4.3.	<i>Accuracy improvement - regression analysis</i>	116
7.4.4.	<i>Rebuild sample return system</i>	116
7.4.5.	<i>Sample queuing upgrade</i>	116
7.4.6.	<i>PLC wiring/communication</i>	116
7.4.7.	<i>LabVIEW control improvements</i>	117
7.4.8.	<i>Temperature normalising station reconstruction</i>	118
7.4.9.	<i>Secondary position measurement</i>	119
7.4.10.	<i>Improved stage height locking mechanism</i>	119

7.4.11. Temperature control of normalising fluid	119
7.4.12. Mass based measurement	120
8. REFERENCES	121
APPENDIX A – TEST RESULTS	125
APPENDIX A.1: SINGLE SAMPLE, SINGLE TOUCH	125
APPENDIX A.2: SINGLE SAMPLE, MULTIPLE TOUCH.....	126
APPENDIX A.3: SINGLE SAMPLE, MULTIPLE TOUCH, UNDER FLUID	127
APPENDIX A.4: SINGLE SAMPLE, MULTIPLE TOUCH, ACTIVE CLAMPING	128
APPENDIX A.5: SINGLE SAMPLE, MULTIPLE TOUCH, WEIGHTED STAGE	129
APPENDIX A.6: M. TOUCH, WEIGHTED STAGE, ACTIVE CLAMPING, UNDER FLUID.....	130
APPENDIX B – PLC PROGRAMS	132
APPENDIX B.1: COOLING STATION PLC PROGRAM.....	132
APPENDIX B.2: MEASUREMENT STATION PLC PROGRAM.....	134

List of figures

Fig. 1 Types of bearings [51]	11
Fig. 2 Ball bearing appearance at stages of manufacture [52]	12
Fig. 3 Heidenhain-Dorsey gauge elements. L-R Clockwise: Dorsey versatile snap gauge, Heidenhain ND221 display unit, Heidenhain MT12 length gauge.....	14
Fig. 4 First and second prototypes.....	15
Fig. 5 Characteristics of measurement process variation	22
Fig. 6 Bias illustration	24
Fig. 7 Stability	25
Fig. 8 Linearity	25
Fig. 9 Linear motor [20].....	27
Fig. 10 Exploded side view of linear motor [20]	27
Fig. 11 Hysteresis curve of an open-loop piezo actuator for various peak voltages. The hysteresis is related to the distance moved, not to the nominal travel range [22]...29	
Fig. 12 Creep of open-loop PZT motion after a 60µm change in length as a function of time. Creep is on the order of 1% of the last commanded motion per time decade [22]	30
Fig. 13 LVDT Diagram	33
Fig. 14 Piezo electric actuators in aluminium flexure.....	35
Fig. 15: Current leakage of piezo actuator exposed to 70% RH, 25°C, and 100V applied [39]	36
Fig. 16 Piezo actuator with water proof enclosure and connection for flushing/cooling air [22]	36
Fig. 17 Linear thermal expansion of different PZT ceramics [22].....	38
Fig. 18 Vibration isolation assembly [51]	39
Fig. 19: Station installed at NN Euroball (L) and subsequently at WIT (R).....	41
Fig. 20: PLC control and timing program	42
Fig. 21: Damage caused to steel elbow piece by samples.....	46
Fig. 22: Render of sample capture box showing base reinforcements	47
Fig. 23: Cage for ball order control	48
Fig. 24: "bounce out" protector installation	48
Fig. 25: Traditional notch weir.....	50
Fig. 26 Cutaway showing inner tank weir arrangement.....	51

Fig. 27: Original bracket for "ball in place" optics	52
Fig. 28: Replacement bracket for "ball in place" optics	52
Fig. 29: Cantilever dimensional diagram (not to scale)	54
Fig. 30: Part one of changing step size program	55
Fig. 31: Part two of changing step size program	55
Fig. 32 Single vs. multiple touches	56
Fig. 33: LabVIEW code for humidity and temperature sensors.....	57
Fig. 34: LabVIEW temperature normalising process run status and down time counter code	59
Fig. 35: LabVIEW status board showing main air failure.....	60
Fig. 36 Piezo electric actuator construction	61
Fig. 37: Mock-up piezo chamber in a water bath.....	62
Fig. 38: Front view of flexure with air protection system installed	63
Fig. 39: Flexure in water bath showing water level and thermocouple	64
Fig. 40 Render of air protection system as installed on working equipment	66
Fig. 41: Relative humidity (%) vs Time after fluid is drained	68
Fig. 42 Sample location diagram [51].....	70
Fig. 43 Previous prototype clamp mechanism [51].....	71
Fig. 44: Diagram illustrating 13.5mm sample and locating sphere relationship.....	72
Fig. 45: Free body diagram about sample	72
Fig. 46: Resolved forces about sample.....	73
Fig. 47 Diagram illustrating 10.5mm sample and locating sphere relationship.....	74
Fig. 48: Illustration showing flexures and piezos.....	76
Fig. 49: Prototype/Concept clamp mechanism.....	78
Fig. 50: Identification of clamp working height.....	79
Fig. 51: Side elevation showing clamp position (left) and sample handling position (right).....	80
Fig. 52: Clamped 13.5mm sample showing perpendicular distances (mm) between pivot and forces	81
Fig. 53: Freebody diagram about 13.5mm sample with the clamping force L	82
Fig. 54: Component forces	82
Fig. 55: Side view showing hinge and pneumatic ram.....	84
Fig. 56: Clamp in insert/remove position.....	85
Fig. 57: Clamp in home position with sample ball clamped	85
Fig. 58: Pneumatic ram in both positions showing position sensors.....	86
Fig. 59: Original vertical queue diagram [51].....	87
Fig. 60: Original queuing system overview showing working sequence [51]	87
Fig. 61: Attempted multiple sample insertion	88
Fig. 62: Render of rotary indexer	90
Fig. 63: Render of vertical feeding and storage mechanism	91
Fig. 64: Render of horizontal storage showing all areas open	92
Fig. 65 Horizontal sample insertion mechanism	93
Fig. 66 Perceived causes of measurement error	94
Fig. 67 Rise time during a single touch measurement.....	96
Fig. 68: Large strain gauge line noise	98
Fig. 69 Plan view of measuring platform showing location of different sized samples	100
Fig. 70 Surface roughness illustration [51]	100
Fig. 71 Slip gauges installed [51].....	101
Fig. 72 Damage to sample.....	102
Fig. 73 Temperature log over 48 hour period	104

Fig. 74 Temperature over randomly selected five minute period	105
Fig. 75 Accuracy vs. precision diagram[41]	107
Fig. 76 Comparison of measurement range (precision)	108
Fig. 77 Accuracy comparison chart.....	109
Fig. 78 Suggested program layout for a single workstation.....	118
Fig. 79 Twin workstation program layout.....	118

List of tables

Table 1: Equivalent pipe fitting lengths [49].....	43
Table 2: Kinetic energy results.....	43
Table 3: Kinetic energy absorption options comparison.....	44
Table 4: Fluid level control methods.....	49
Table 5: Temperature control "rules of thumb" [unknown source]	103
Table 6: Extract from results (13.50mm ball)	108
Table 7: Precision	108
Table 8: Accuracy (13.50mm sample ball)	109
Table 9: Combined precision and accuracy.....	110
Table 10: ANOVA analysis of 'single touch' experiment	110
Table 11: Compiled 'P values'	111
Table 12: Regression formulae.....	111

Abstract

Upgrading of an Automated Micron Level Measurement System for Sub-micron
Measurement by Brendan Phelan

This thesis presents a systematic program of improvements to an automatic micron level precision ball bearing measurement instrument system to achieve sub-micron measurement performance. Progressing from relocation of instrumentation and its subsequent reinstallation and re-commissioning, it describes the upgrade work to achieve the targeted performance improvements and the subsequent testing and experimentation to identify the improvements achieved. A significant body of work aimed at improving the reliability of the overall system has also been completed.

The end result is a very significantly improved measurement system. Key factors leading to the targeted single micron performance level have been identified and tested and other factors affecting the final performance have been identified.

Keywords: Sub-Micron Measurement; Flexure Stage; Piezo Actuation

1. Introduction

1.1. Project Introduction

The economics of steel ball bearing production largely hinges on the efficient control of batch grinding and lapping processes (for minimum cost) and the effective production and classification of finished balls into tight tolerance ranges (to maximise value). Ball diameter is the critical metric in both of these. This project, run in conjunction with the NN Euroball manufacturing facility located in Co. Kilkenny, was developed to improve the two factors mentioned above (cost and value).

Measurement in the ball bearing industry throughout the world (as in NN Euroball Ltd., Kilkenny) is performed manually on laboratory type instruments. The NN-WIT project (as the project was called) focussed on the development of a prototype high speed piezo measurement instrument, to service a representative section of production at NN (2 machines) in a closed-loop production system.

The effectiveness of the concepts and the technology has been successfully demonstrated with the measurement equipment returning repeatable results in the micron range.

This thesis presents the work done in improving apparatus performance in terms of repeatable, sub-micron results. A range of improvements were identified, implemented, and assessed.

1.2. Ball Bearings [52]

The purpose of a bearing is to reduce friction and to support radial loads (Load applied perpendicular to the bearing axis of rotation) and axial loads (thrust load, applied to the bearing parallel with the bearing axis of rotation). Ball bearings reduce friction by providing smooth metal balls or rollers and a smooth inner and outer metal surface for the balls to roll against. These balls or rollers "bear" the load, allowing the device to spin smoothly. Generally one of the races is fixed; this allows the second race to rotate which also causes the balls to rotate. As one of the bearing races rotates it causes the balls to rotate as well. This rotation results in a lower coefficient of friction, than if the two flat surfaces were rotating on each other. Fig. 1 below shows some

typically seen bearing types; ball bearings (a), roller bearings (b), needle bearings (c), and tapered roller bearings(d) and (e) from left to right.

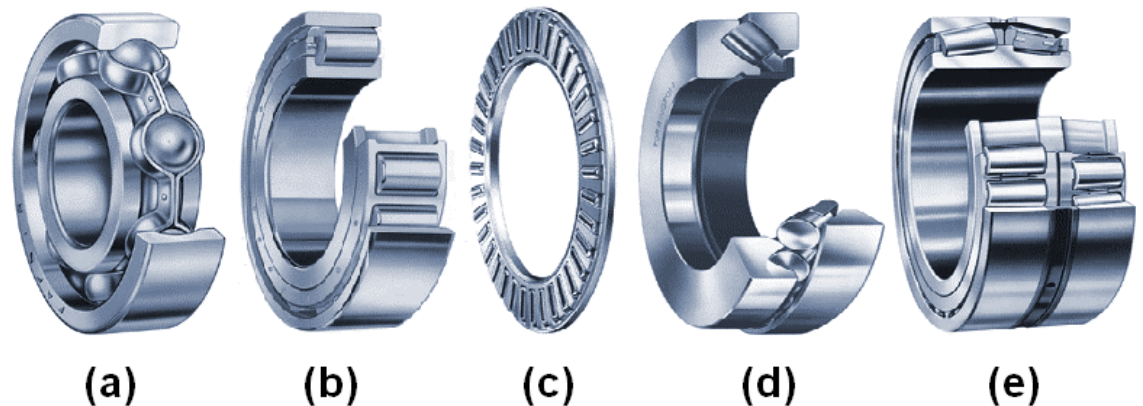


Fig. 1 Types of bearings [51]

Ball bearings, as shown in Fig. 1(a), are probably the most common type of bearing. These bearings can handle both radial and thrust loads and are usually found in applications where the load is relatively small; for lightly loaded bearings, balls offer lower friction than rollers. In a ball bearing, the load is transmitted from the outer race to the ball and from the ball to the inner race. Since the ball is a sphere, it only contacts the inner and outer race over a very small area, which helps the bearing to rotate very smoothly. On the other hand this means that load is spread over a very small area and if the bearing is overloaded, the balls can easily deform.

1.3. Ball bearing manufacture at NN Euroball Kilkenny [51],[52]

Manufacturing at NN Euroball, Kilkenny Ltd. concentrated on steel ball bearings only. The Kilkenny plant produced the “ball” component which is shipped to a client for installation in the bearing housing shown in Fig. 1(a).

Before the steel used for ball bearing manufacture enters the production process it is annealed. Here the steel is heat treated at high temperature and control cooled to soften the metal and provide change in its microstructure to improve machine-ability during the cold working process. The steel is then introduced to the 5 stages of manufacture beginning with cold forging and ending with lapping. Fig. 2 below displays a typical example of the appearance of the bearing ball at each stage of production.



Fig. 2 Ball bearing appearance at stages of manufacture [52]

The stages of production are described below:

1. Cold Forging:

A calculated length of wire is sheared and cold forged in a close die to give spherical shape to the work piece.

2. Flashing:

During this production step the work pieces are rolled between plates with concentric grooves to eliminate the seam formed during cold forging and to correct the spherical shape of the work pieces.

3. Heat treat:

The balls are hardened and tempered to attain the desired microstructure and level of hardness.

4. Grinding:

Here the hardened balls are ground to improve surface finish and geometrical parameters. Several careful grinding processes with ceramic wheels lead to improved balls for the next final lapping operation.

5. Lapping:

The final lapping operation gives the ball a bright, compact surface free from defects. These balls have a very low surface roughness and very low deviations from spherical form.

6. Quality Control:

Each finished ball is tested using a Krob ball scanner; this is a testing and sorting machine for the non-destructive examination of the surface-quality of ball bearings.

7. Packaging

Each gauge lot is packed separately and is supplied with corrosion protection applied. The packaging is marked with the ball nominal diameter, grade, gauge, and material number or material designation and is now ready to be shipped.

1.4. Manual Measurement System

The measurement instrument used by NN Euroball was a combination of a Dorsey versatile snap gauge, a Heidenhain MT12 digital length gauge, and a Heidenhain ND221 control unit (Fig. 3).

The purpose of a snap gauge is to remove operator skill from the measuring process. Unlike a handheld micrometer there is no “feel”, skill, or high level of technical ability required from the operator to achieve consistent measurements [1]. The operator first pulls a lever to separate the two contact platens and then places the sample on a holding stage. Using a micrometer an operator would manually close the distance between the contact platens, whereas with the snap gauge they release the lever holding the platens apart and a spring return mechanism is used to close platens on the sample.

The Heidenhain MT12 length gauge is a precision linear optical encoder which interfaces with the ND221 control unit. The gauge has a stroke length of 12mm and an accuracy of $\pm 0.2\mu\text{m}$ [2]. The probe is normally extended and is returned to this state after compression by a spring.



Fig. 3 Heidenhain-Dorsey gauge elements. L-R Clockwise: Dorsey versatile snap gauge, Heidenhain ND221 display unit, Heidenhain MT12 length gauge

In practice it was found that the Heidenhain-Dorsey gauge would achieve a nominal measurement accuracy of $1\mu\text{m}$ [3]. It is thought that the stated capabilities of the Heidenhain optical encoder are greater than the inherent capabilities of the Dorsey snap gauge. The friction in the snap gauge is a particular performance reducing factor. Friction presents a major design challenge for sub-micron measurement [3] and introduces uncertainties during the precision movement of parts.

To this end a monolithic piezo electric actuator driven flexure was developed [51]. These flexures have the advantages of frictionless movement, no wear and tear, and completely predictable movement within their elastic limits. It is these improvements in certainty of movement that make a sub-micron measurement a realistic proposition.

1.5. The problem

The objective as presented by NN Euroball, Ltd., at its subsidiary manufacturing facility in Kilkenny was to make a step improvement in its competitiveness. It was identified that this could be done by 1) improving the control of the batch grinding and

lapping processes in order to reduce cost and improve product accuracy and 2) by improving the classification of finished balls into tight tolerance ranges to maximise value (tightly toleranced ball batches command a higher price than loosely toleranced balls). Rapid, high accuracy measurement of both in-process product and finished product was identified as the key to both of these issues.

1.6. Automated measurement system

The current system of measurement was developed through two prototyping stages which will be labelled as ‘first’ and ‘second’ prototype (the current system) in the following discussion. It consists of two piezo electric actuators in a specifically designed high-grade aluminium cantilever monolithic-flexure stage. Both ‘first’ and ‘second’ prototypes are illustrated in Fig. 4 below.

Piezo electric actuators were selected to drive the flexure and to detect contact with the samples. The ‘first’ prototype measurement system (Fig. 4(a)) used a single piezo actuator to service both the movement and the touch detection functions [4], [31].

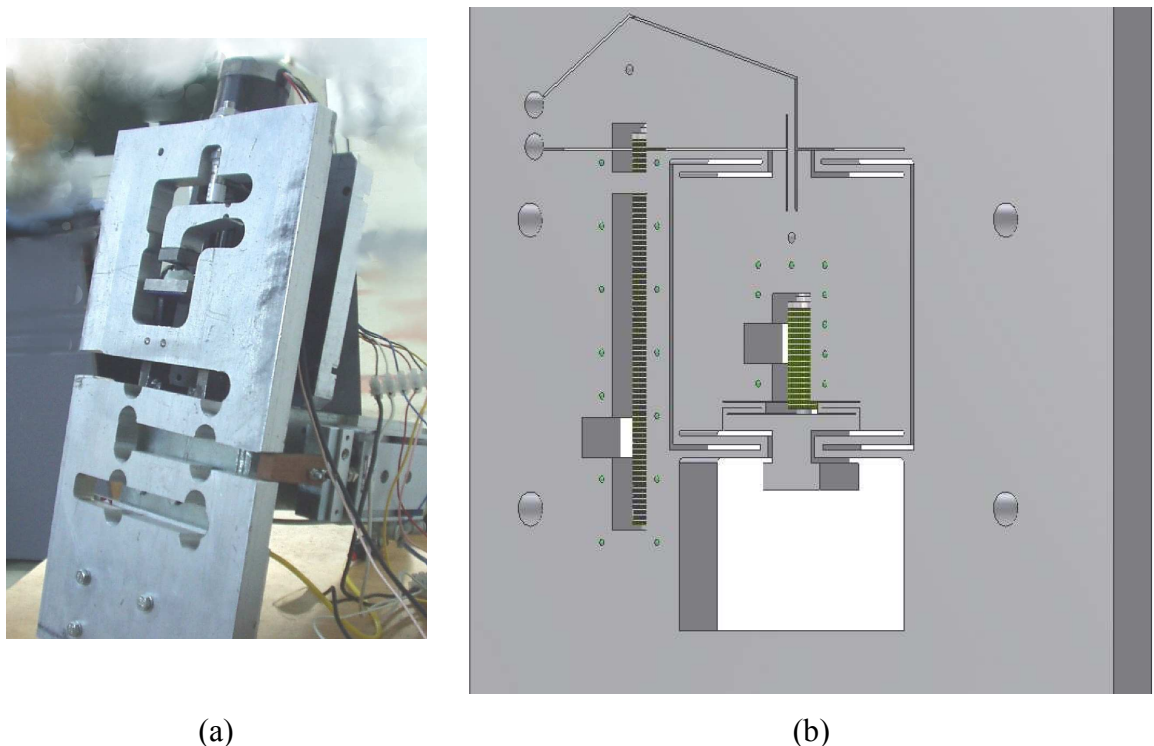


Fig. 4 First and second prototypes

The piezo used here was much smaller than in the present working apparatus; 15 μ m vs. 90 μ m operating ranges respectively. The subsequent move to an actuator with

a longer stroke was to accommodate a large variation in sample diameter with fewer reference balls. Also the cantilever arrangement of this first prototype allowed for approximately 30 μm movement range [51] vs. the 167 μm range of the large piezo/cantilever arrangement used in the present implementation (Fig. 4(b), also see section 3.8.1).

The move from a single to a dual piezo arrangement in the ‘second’ prototype also saw a move from resonance to strain based contact detection. The first prototype used a sudden change in system stiffness [31] to detect contact between the measuring platen and the sample. The dual piezo arrangement in Fig. 4(b) uses the changing force transferred to the “small” piezo by the flexures to detect contact between measuring platen and sample. The strain gauge feedback from the large piezo is used to calculate the sample diameter. The calculation system is based on comparative measurement system mimicking the manual system which it was replacing. The system first measures a large and small reference ball of known diameter. Using the voltages measured from these ‘calibration’ balls the diameter of the production balls to be measured is inferred.

One key issue here is that measurement resolution is limited by the step size taken by the ‘large’ or ‘driving’ piezo. In the implementation at the outset of this masters a single step of the driving piezo translated to 252nm vertical displacement at the measuring platen (see Section 3.8.1 for supporting calculation). The driving piezo cannot be stopped mid-step so once contact was made between measuring platen and the sample, that contact could occur anywhere in a 252nm range. With a stated measurement precision target of 0.1 μm (100nm) this 0.252 μm (252nm) clearly has to be improved upon.

1.7. Starting point of project

At the outset of the project the measuring and cooling stations were located at the NN Euroball facility where they had been undergoing testing and evaluation side by side with, and at the final stage, interlinked with live production [51,52]. Unfortunately circumstances at the plant (see Chapter 2.6) necessitated moving the equipment back to WIT at the outset of this project. The measurement unit was working successfully but not at the accuracy and precision levels considered suitable to achieve the desired step improvement in process control and with a level of reliability somewhat less than necessary for live production.

1.8. Project Objectives

The objectives of this project can now be outlined as follows:

- To improve the overall reliability of the station. Reliability improvement was an ongoing process while the station was in the plant.
- To establish a benchmark for measurement performance. Although considerable effort had already been spent defining the system performance while in the plant, much work remained. Again, the removal and recommissioning would necessitate this to be re-established.
- To investigate and implement methods of improving measurement performance. Prior to the start of this project the measurement station had not reached its targeted precision level (0.1 μ m). The project had reached a point where it was obvious that major design and environmental changes would be necessary before further real progress could be made. The effect of these changes on the working instrument would have to be proven systematically.
- To redefine the instrument capabilities post improvements. The final task would be the redefinition of the instrument design and its operating environment for optimum performance and the establishment of its expected new level of precision.

1.9. Thesis Structure

The structure of this thesis is as follows

- 1) Two chapters (Chapters 2 & 3) devoted to literature review and technical issues related to significant aspects of the original design of the instrument and its relocation and modification for operation and testing in the Laboratory
- 2) Two chapters (Chapters 4 & 5) devoted to specific technical studies and subsequent major modifications to the instrument
- 3) Two chapters (Chapters 6 & 7) devoted to the identification of potential performance improvements, their selection and implementation and subsequent experimentation and proving, and finally to the project conclusions.

2. Literature review

2.1. Introduction

This chapter outlines the concepts of measurement, accuracy, precision, and their associated errors. It reviews the important technologies and techniques related to the design of a precision movement system. Precision movement, precision contact detection, and precision measurement are specifically addressed. The key environmental issues of humidity, temperature variation, and vibration in the context of the targeted sub-micron performance of the as-built system are reviewed.

2.2. Precision measurement

Researchers [5] define precision measurement as the subset of measurement ranges which lie between 1-0.1 μm while even greater levels of precision are generally termed '*ultra precision*' [5],[6].

As stated in Chapter 1 the target of this project is the upgrading of an automated measurement system to an accuracy of 0.1 μm . The difficulty of achieving this can be gauged from the effective target resolution of 0.01 μm (10nm) required (based on the common rule of thumb of any inherent system variability being less than 1/10th of the required accuracy).

Measurements can be either qualitative or quantitative in nature. Qualitative measures describe objects using words and are subjective while quantitative measures use numbers to define physical attributes of an item and are objective. This thesis is focussed on quantitative measures.

Quantitative measures can be taken as either an absolute measure or a relative measure. An absolute measure requires knowing an exact (and uniquely identifiable) position of the measuring tip. Grey scale encoders, for instance, are often used to determine a unique position. This measuring method does not require reference to a home position. A relative measure involves measuring the distance the measuring tip moves from a known home position (often using hard stops for the home position). Both methods are capable of the same precision levels. However the relative measuring system normally requires frequent recalibration for a high level of confidence in the results.

The prototype system in this project utilises an absolute positioning system (the strain gauges always report a specific voltage for a specific extension). However to convert these absolute voltage figures into measurements the system must be calibrated each time by first measuring the voltage of two calibrated balls (one larger and one smaller than the samples to be measured). Once this calibration is complete the system has established the relationship between the distance travelled (by the measurement tip) and the diameter of the sample being measured. This is called comparative measurement as the samples are compared to known references.

One classification of the available measurement techniques is the contact or non-contact approach. Common non-contact techniques are, for instance, optical and ultrasonic. Vision systems (an optical technique) utilise a camera with a macro lens (a lens which is capable of representing the image of the component at a 1:1 ratio on the sensor) or a microscopic lens (greater than 1:1 ratio) to see the sample. These systems rely on carefully controlled lighting and software processing to interpret what they are seeing. The ultimate resolution of a vision system would be limited by the size of each pixel in the camera's sensor. These resolutions are currently larger than a micron (for example the Nikon D3x, a high resolution, high performance camera, has a pixel size of $5.49\mu\text{m}$ [7]). When considering the goal of submicron measurement it is clear that a vision system would not meet the requirements.

Laser measuring techniques (another optical technique) 'bounce' a laser off of the component to be measured and the reflected beam is picked up by a sensor. Oka et al. [8] demonstrate a micro-optical sensor with a measurement range of 1mm and a repeatability error of less than $3\mu\text{m}$. The system uses an optical triangulation system to measure the distance to the measurement target. However measurement accuracy using laser techniques are heavily dependent on the surface reflectivity of the measured object [9]. As the samples taken from production, in the ball bearing industry, would exhibit differing surface finishes due to the different stages of production (and therefore different surface reflectivities) laser based systems would not be suitable for this project. Ultrasonic techniques suffer from the same dependency on surface reflectivity.

The contact measurement approach is used in this project: this approach had already been chosen and was largely implemented long prior to the start of this project. Contact measurement in this case involved a movement system, contact sensing/detection, and position measurement. A variety of technologies could be considered for each of the three elements; these are discussed in section 2.4.

2.3. Key statistical terminology in measurement

2.3.1. Introduction

Measurement is defined as '*a process of empirical, objective assignment of symbols to attributes of objects and events of the real world, in such a way as to describe them*' [10].

The process of assigning numbers is defined as the measurement process and the value assigned is defined as the measurement value. The measurement process consists of a set of operations for the purpose of determining the value of a quantity to establish the magnitude of some attribute of an object, such as its length or weight, relative to a unit of measurement [11]. Measurement usually involves using a measuring instrument, such as a ruler or scale, which is calibrated to compare some standard, such as a meter or a kilogram to the object being measured. Finkelstein [10] states that '*all measurement involves a comparison of the measured with a standard*'.

This measurement data can be used in a variety of ways; most commonly it is used in the decision to adjust a manufacturing process or not based on measurement data from a specific process parameter. Measurement data can also be used to determine if a relationship exists between variables e.g. the relationship between material removal rate and pressure applied to the work pieces by the grinding plates in a grinding process. Key to utilising measurement data as a process control is ensuring that the measurements are good. Bullock et. Al [12] identify six characteristics shared by "*good measures*". These are:

- Timely – measures should be collected and processed in a timeframe required to be relevant to the context.
- Objective – measurements should be easy to understand, be the same regardless of the assessor, and be the same under similar circumstances.
- Economical – collection and processing of measurements should provide benefits that off-set the burden of measurement activities.
- Complete – measures should address all areas of concern in enough detail to discern reasons for differences in actual and expected system results.

- Measureable – measures should hold for the representation (any empirical relational system which purports to measure (by a simple number) a given property of the elements in the domain of the system is isomorphic* (or possible homomorphic**) to an appropriately chosen numerical relational system [13]), uniqueness (determine the scale type of the measurements resulting from the procedure [13]), and meaningfulness (A numerical statement is meaningful if and only if its truth (or falsity) is constant under admissible scale transformations of any of its numerical assignments [13]) conditions of measurement theory.
- Strategically linked – measures should be traceable to the system strategic purpose or behaviour.

*Isomorphic [14]: A one-to-one relation onto the map between two sets, which preserves the relations existing between elements in its domain.

**Homomorphic [15]: An into map between two sets that preserves relations between elements.

2.3.2. Measurement accuracy, precision, and error

The analysis and conclusions of a process or analytical study are often based upon the assumption that measurements are exact (accurate and precise). It is often forgotten that there is variation in the measurement instrument which effects the individual measurements and subsequently the decisions based upon the data.

Bullock et al [12] identify three primary sources of error in a measurement system: random error or ‘noise’ from any source impacting the system; systemic error which derives from construction of the attribute measures and comes in the form of measurement bias; and observational error which is the oversight of a key system attribute requiring measurement or using the wrong measure for an identified system attribute. These errors can affect the accuracy and/or precision of the measurement system.

Variation is one of the most frequent explanations for low quality measurement data. The characteristics of measurement process variation consists of location variation and width variation, Fig. 5. Location variation is related to the trueness of a measurement; trueness refers to the closeness of agreement between the arithmetic mean of a large number of test results and the true or accepted reference value [16].

Width variation is related to the precision of a measurement; precision refers to the closeness of agreement between test results [16].

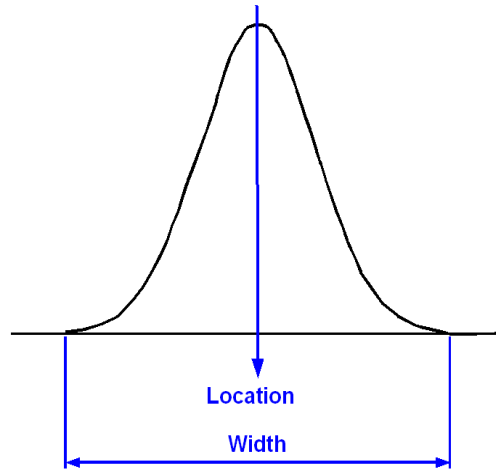


Fig. 5 Characteristics of measurement process variation

2.3.2.1. Location Variation – Accuracy

Accuracy is a generic term to describe the concept of exactness related to the closeness of agreement between the average of one or more measured results and a reference value [17]. In the past the term accuracy was used to describe the component now named as “trueness”. A comparison between the measurement results and the accepted reference value is used to examine the trueness of a measurement method. It is desirable to have individual measurements as close to the true value as possible. For many measurement processes this value is often unknown. In these cases the accepted reference value is used as an approximation of the true value.

2.3.2.2. Width Variation - Precision

Tests performed on presumably identical materials in presumably identical circumstances (it is difficult to guarantee identical circumstances outside of a controlled environment) generally do not give identical results. The general term for variability between repeated measurements is precision. Precision is the closeness of agreement between independent test results obtained under stipulated conditions [16]; the closeness of repeated readings to each other. A precise measuring instrument will give very nearly the same result each time it is used.

Precision measures the dispersion of a set of results, usually computed as a standard deviation of the test results. It depends only on the distribution of random errors inherent in every measurement and does not relate to the true value or the

accepted reference value: a random error is a deviation of an observed from a true value, which behaves like a random variable in the sense that any particular value occurs as though chosen at random from a probability distribution of such errors [18]. The variability due to random errors must be taken into account when interpreting measurement data, e.g. comparing test results from two batches of ball bearings will not indicate a fundamental quality difference between them if the difference can be credited to the inherent variation in the measurement process.

Many different factors other than variations between supposedly identical parts may contribute to the variability of results from a measurement method including the operator, equipment used, calibration of the equipment, environment (temperature, humidity etc.), and the time between measurements. The variability between measurements performed by different operators and/or with different equipment will usually be greater than the variability between measurements carried out within a short interval of time by a single operator using the same equipment [16].

2.3.2.3. Error

Trueness is normally expressed in terms of bias. Bias is the difference between the true value (accepted reference value) and the observed average of measurements of the same characteristic on the same part [17], see Fig. 6. Bias is the measure of systematic error as contrasted to random error e.g. an incorrectly calibrated thermostat may consistently read (i.e 'be biased') several degrees hotter or colder than the actual temperature. There may be one or more systematic error components contributing to the bias. A larger systematic difference from the accepted reference value is reflected by a larger bias value. Some possible causes for excessive bias are:

- Instrument not properly calibrated.
- Wear and tear to instrument or fixture.
- Wear and tear to reference standard.
- Distortion of instrument or part.
- Environmental influences such as temperature, humidity, vibration and cleanliness
- Location error due to sample/reference seating in fixtures.
- Operator skill.

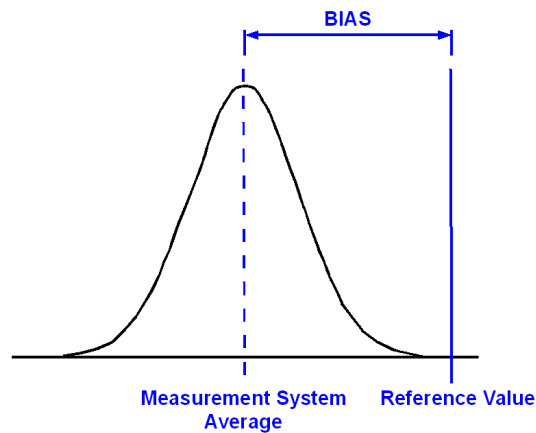


Fig. 6 Bias illustration

The change in instrument bias over time is known as stability. Fig. 7 illustrates how bias might change over time in a system. Stability is the total variation in the measurements obtained with a measurement system on the same master or parts when measuring a single characteristic over an extended time period [17]. Instability of the measuring instrument is evident, if the biases of a group measurement vary over time. Stability measures the change in systematic errors over time. Systematic errors, which change during an experiment, are usually easy to detect; measurements show trends with time rather than varying randomly about the mean. Long-term instability should not be a problem for comparator measurements, but short-term can be a problem.

The factors, which frequently contribute to the instability of the observed values obtained, are:

- Excessive time interval between calibration cycles.
- Normal aging or obsolescence of the measuring instrument.
- Poor maintenance of the measuring instrument.
- Worn or damaged reference standard.
- Improper calibration or use of the reference standard.
- Measuring Techniques differ- setup, loading, clamping.
- Environmental drift- temperature, humidity, vibration, cleanliness.
- Application: part size, position, operator skill, fatigue, observation error (readability).

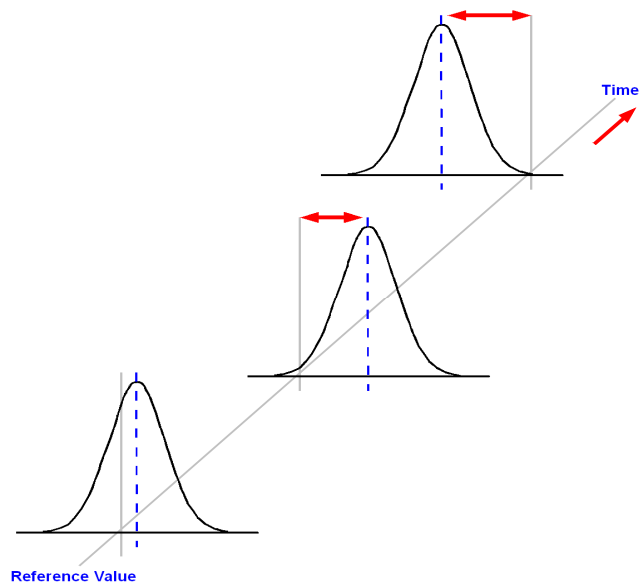


Fig. 7 Stability

Linearity is the change in bias over the measurement range of the instrument, Fig. 8; it is the difference of bias throughout the expected operating (measurement) range of the equipment [17]. Linearity can be thought of as a change in bias with respect to size and it is the correlation of multiple and independent bias errors over the operating range. If the instrument bias remains constant throughout the measuring range, the instrument is said to have constant bias, on the other hand if the bias varies over the operating range the instrument has non-constant bias (non-constant linearity). All the possible causes of excessive bias and instability can also cause linearity inconsistencies.

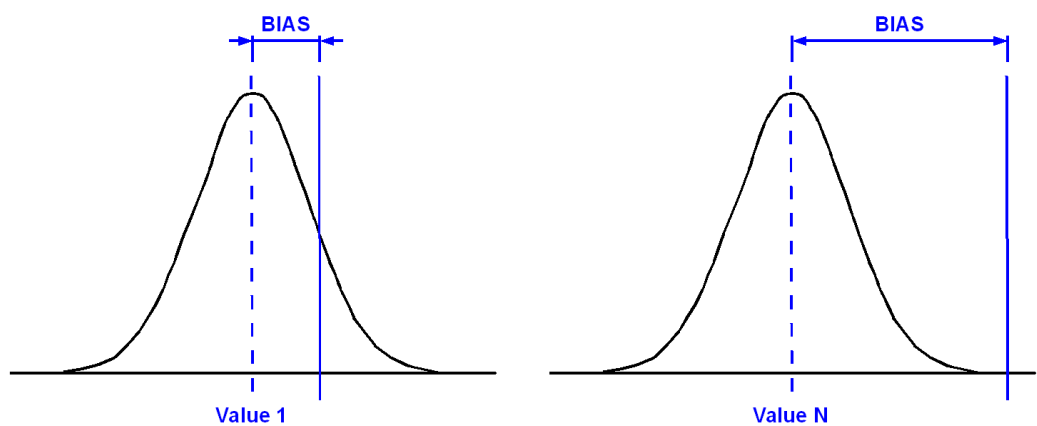


Fig. 8 Linearity

2.4. Review of contact measurement options

As stated in Section 2.2 sub-micron contact measurement requires a precision movement device, a sensitive contact detection system, and a precision position measurement system. This section provides a brief review of some of the key technical options in relation to each of these system elements.

2.4.1. Precision movement technologies

- **Lead screw/Ball screw:** A lead screw is a mechanical device for translating rotational motion to linear motion. A ball screw is a development of the lead screw which utilises ball bearings on the threaded shaft to minimise friction. Ball screws are typically bulkier than lead screws as they require a mechanism to re-circulate the ball bearings. These technologies are commonly used for positioning work tables over large distances [19] but are precision positioning systems which can be considered for the task of positioning a touch sensing system in contact measurement. The primary disadvantages of lead/ball screws are [19]:
 - Transmission errors due to pitch tolerances of the lead screw.
 - Dead zone and friction induced backlash.
 - Elasticities.
 - Additional large inertias (inertia of the work table).
 - Position, velocity, and acceleration limitations due to mechanical characteristics of the leadscrew.
 - Wear.

It is important to note that lead/ball screws do not by design report their position to a controller. To achieve this an encoder is typically added to the assembly. This can report position as either absolute (gray scale encoder) or relative (requiring frequent recalibration for high levels of certainty). With a lead screw the resolution achievable is determined by the pitch on the screw thread and the increments the drive motor is capable of rotating it through.

- **Linear drive motor:** Linear motors are widely deployed in industry for tasks requiring high speed and high precision [20], two of the key requirements of this project. Similarly to the lead screw; linear motors typically have a large working envelope. These motors have the advantage of their force acting

directly on the payload without mechanical transmissions which can introduce nonlinearities associated with backlash and friction. However external disturbances act directly on the translator which degrades positional accuracy and the method of movement can introduce speed ripple, mechanical vibration, and noise. Fig. 9 shows an overview of a typical linear motor assembly. The base contains the stator and permanent magnet while the top assembly contains the coil and translator. The translator is kept from contact with the base by a series of air bearings to minimise friction.

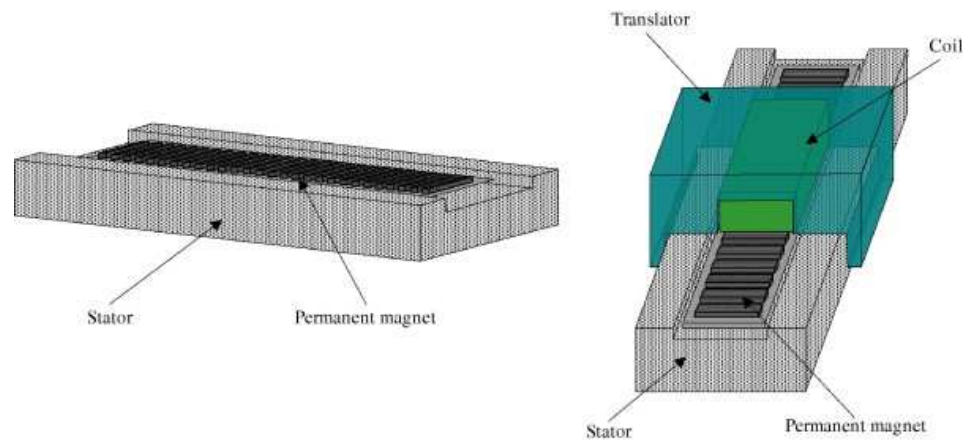


Fig. 9 Linear motor [20]

Fig. 10 shows a side on view of the translator and permanent magnet interface. The translator is moved across the surface of the permanent magnet by controlling the voltage direction in the coils.

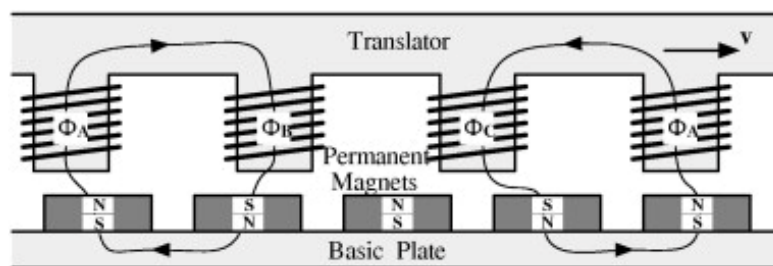


Fig. 10 Exploded side view of linear motor [20]

Similar to the lead/ball screw this type of positioning motor requires an encoder to report on and allow for control of its position. Baldor [21] claims repeatability to $0.1\mu\text{m}$ and positional accuracy of $2.5\mu\text{m}/300\text{mm}$ for their linear motors.

- **Piezoelectric actuator:** A piezoelectric material is a material which changes its dimensions when a voltage is applied and produces a charge when pressure is applied. Certain ceramic materials, which are used to build actuators, such as lead- zirconium-titanate (PbZrTi or short PZT), have very large piezo-electric strains. Those materials are permanently polarized by a strong electric field during the production process.

Piezoelectric systems have a number of beneficial features for submicron positioning. These include [22]:

- Unlimited resolution (limited only by the capabilities of the controlling and monitoring hardware. No moving parts to limit resolution).
- Fast expansion (A piezo with a 10kHz resonant frequency can reach its nominal displacement within 30 μ s).
- No magnetic fields (piezoelectric actuators do not produce and are not affected by magnetic fields).
- No wear and tear (after billions of operations under suitable conditions).

Travel range for piezo actuators are from a few tens to a few hundreds of microns depending on construction. By using the actuators in a lever system millimetre level actuation can be achieved (at the expense of resolution at the end of the lever).

Two types of piezo actuators have become established: low voltage actuators and high-voltage actuators. Monolithic low-voltage actuators (LVPZT) operate with potential differences up to 100V and are made from ceramic layers from 20 to 100 μ m in thickness. High-voltage actuators (HVPZT) on the other hand, are made from ceramic layers of 0.5 to 1mm thickness and operate with potential differences of up to 1000V. HVPZT can be made with larger cross sections, making them suitable for larger loads than the more compact LVPZT.

Piezo ceramics are not subject to the stick-slip effect and therefore offer theoretically unlimited resolution. In practice, the resolution actually attainable is limited by electronic and mechanical factors [22]: Sensor and servo-control electronics (amplifier) noise and sensitivity to electromagnetic interference affect the position stability. Mechanical parameters such as the design and

mounting precision issues (concerning the sensor, actuator and preload) can induce micro-friction which limits resolution and accuracy.

There are several drawbacks to using piezo elements in an open-loop fashion. The voltage-to-displacement relationship is non-linear and exhibits hysteresis, see Fig. 11; hysteresis is based on crystalline polarization effects and molecular effects within the piezoelectric material. The non-linear relationship implies that for a given increase in voltage, the piezo will expand by a varying amount across its full range of extension. The amount of hysteresis increases with increasing voltage applied to the actuator; from this it can be concluded that the smaller the move the smaller the uncertainty.

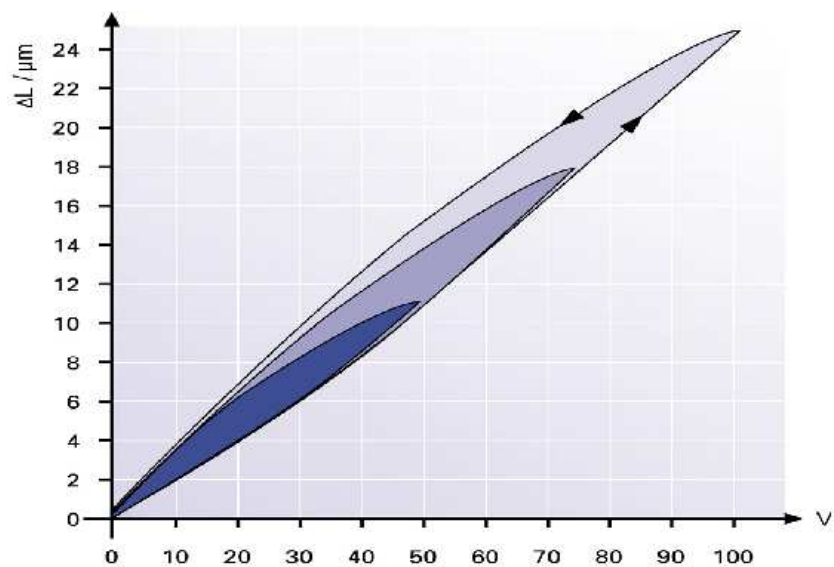


Fig. 11 Hysteresis curve of an open-loop piezo actuator for various peak voltages. The hysteresis is related to the distance moved, not to the nominal travel range [22]

The same material properties responsible for hysteresis also cause drift or creep; creep is a change in displacement with time without any accompanying change in the control voltage. If the operating voltage of a piezo is changed the piezo gain continues to change, manifesting itself in a slow change of position. The rate of creep decreases logarithmically with time [22]. In general use, maximum creep after a few hours can add up to a few percent of the commanded motion. Fig. 12 shows creep vs. time for a piezo electric actuator in open loop mode.

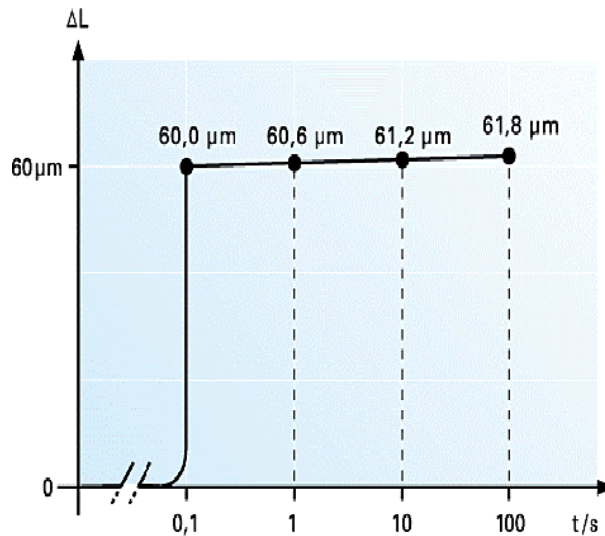


Fig. 12 Creep of open-loop PZT motion after a 60μm change in length as a function of time. Creep is on the order of 1% of the last commanded motion per time decade [22]

It should be noted that for periodic motion, creep and hysteresis have only a minimal effect on repeatability [22] and so are not major concerns for this research project as the apparatus is frequently recalibrated.

Piezo electric actuators typically include an integrated strain gauge and so do not require a secondary positioning measurement device such as an encoder.

- **Piezoelectric motor:** A piezoelectric motor utilises an ‘ultrasonic drive’. A piezoceramic plate is excited to a high frequency and a friction tip attached to the plate moves along an inclined path at the ‘eigenmode frequency’. These motors cannot produce the theoretically unlimited resolution of the linear piezoelectric actuators however they have a much larger work envelope (theoretically unlimited) and are capable of 0.1μm resolution when coupled with a linear encoder [23].

2.4.2. Contact detection in precision measurement

A variety of techniques exist which facilitate detection of the point of contact between a sample and a probe or measuring platen. The techniques outlined below are the key ones used in the area of precision measurement.

- **Elasto-resistive:** An elastoresistive material consists of an elastomer embedded with conductive particles [24]. When the material is compressed at the point of

contact a change in resistance is detected and this effect can be used to identify, with great precision, the probe to surface contact event.

- **Capacitive:** Muhammad et al. [25] describe a MEMS (micro electro mechanical system) capacitive tactile sensor. The sensor consists of a thin silicon diaphragm ($2\mu\text{m}$), a capacitance gap ($2\mu\text{m}$), and a bottom electrode made of silicon. Signals from the capacitance sensor were converted using a high resolution capacitance-to-digital converter (AD7747) and monitored via a graphical user interface on a PC. With this sensor setup it was possible to detect contact forces of approximately 0.1N.
- **Piezo- resistive:** A piezo resistive tactile sensor is based on the '*possibility of quantifying the electrical resistance changes in an element of material as a function of the applied mechanical strain*' [26]. Shikida et al. [27] discuss a piezo-resistive sensor capable of detecting contact force and object hardness.
- **Piezo-electric:** Dargahi [28] describes the use of a membrane tactile sensing system using a PVDF (polyvinylidene fluoride) to detect touch. In the discussed implementation Dargahi utilises three sensing elements to determine not only that touch had occurred but also to locate where it had occurred on a 2-D plane using triangulation. This triangulation method overcomes some of the problems associated with matrix array PVDF elements; namely cross talk (undesireable responses from neighbouring sensing elements), complexity, and fragility.
- **Strain gauge:** A strain gauge is commonly used to detect and measure (when calibrated) strain in a component subject to stress. In the apparatus which is the focus of this thesis a strain gauge is inbuilt into both piezo electric actuators where they are used to detect contact between probe and sample as well as movement (discussed later).
- **Resonance detection:** Researchers [29], [30], [31] have utilised resonance based touch sensors to detect contact between a measuring probe and measuring surface. Vidic et al. [29] utilise a pairs of piezoelectric (PZT) elements cemented at either side of the beam holding a spherical probe tip. One PZT element is used to actuate (oscillate) the beam while the other is used to monitor the strain. When oscillated near its (the probe assembly) resonant frequency a change in either frequency or phase (depending on the operating mode) can be observed when the probe contacts the sample. Gao et al. [32] also describe a

significant increase in probe sensitivity when the force is converted to an AC signal and found that the output of the force sensor corresponds with the oscillation frequency of the sample upon contact.

2.4.3. Precision position measurement

An important consideration in precision measurement is the issue of direct or indirect metrology. Indirect metrology involves inferring the position of the platform by measuring position or deformation at the actuator (by utilising the strain gauge integrated into many piezo actuators for example) or other component in the drive train. Motion inaccuracies which arise between the drive and the platform cannot be accounted for.

With direct metrology motion is measured at the point of interest which is sometimes difficult due to space limitations and/or the range of movement involved. Typical technologies used in this manner for precision measurement are interferometry, capacitive sensors, or LVDT. Direct metrology is inherently more accurate (due to the absence of inaccuracies created by translating motion from the point of movement to the measurement device) than indirect metrology. Due to the continuous referencing against standard balls carried out in this project the issue of direct vs. indirect metrology is not of major significance.

- **LVDT:** A LVDT (linear variable differential transformer) is used primarily as a device for monitoring position. Fig. 13 shows the workings of a LVDT. It is essentially a transformer with multiple output (secondary) coils. As the iron core moves it causes the voltage measured across the secondary coils to vary. This varying voltage allows the position of the iron core to be determined. Note that only two of the three components need to be fixed in place meaning the iron core does not necessarily have to be the moving component. A sub-micron positioning system can be achieved by an LVDT equipped piezo actuator [33].

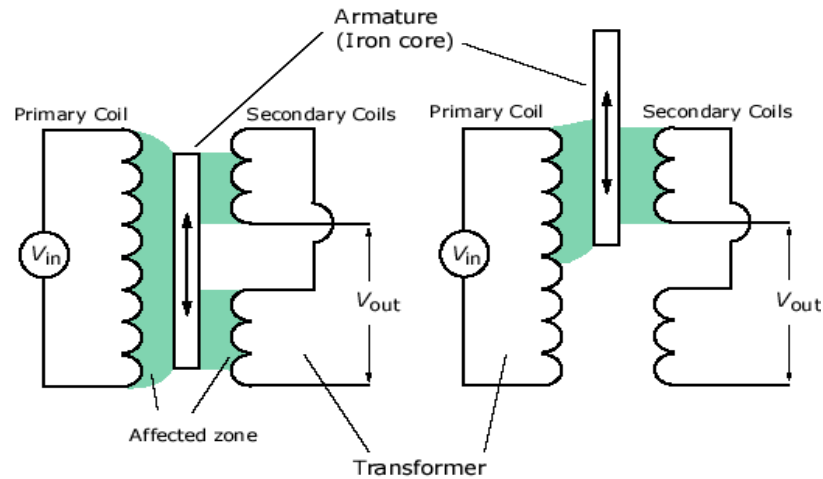


Fig. 13 LVDT Diagram

- Interferometry:** Laser interferometry utilises a split laser beam and the principles of constructive and destructive interference to measure changes in displacement. Researchers [34], [35] have reported precisions in the order of $2\mu\text{m}$ over large distances under ‘*realistic and deliberately generated hostile conditions of air flow and vibration*’ using laser interferometry and a measurement precision of better than 1nm under laboratory conditions. Yang et al. [34] demonstrate a system utilising multiple lasers to yield increased precision over a single laser setup. Using only a single laser precisions in the range of $3\text{-}11\mu\text{m}$ over 0.41m were achieved. The introduction of the second laser improved this to $2\mu\text{m}$ over the same distance under realistic conditions. Wang et al. [35] utilise a feedback control system to reduce measurement errors and to give a measurement repeatability of 1nm .
- Capacitive:** Two plate capacitance sensors are capable of resolutions better than 0.1nm [37]. By utilising two plates (one fixed, one free to move) the distance between the plates can be measured by monitoring the capacitance value. Capacitance and displacement have an inverse relationship.
- Metallic strain gauge:** A strain gauge converts mechanical motion into an electrical signal [36]. The change in length of the gauge is proportional to its resistance. A strain gauge is usually adhered to component which is experiencing the strain. Piezo actuators are often equipped with an integrated strain gauge which can be used to measure position indirectly by monitoring the deformation they undergo when a voltage is applied. Typical resolution is in the

range of 5nm [37]. Used in this manner the strain gauge is an implementation of indirect metrology.

2.5. Environmental effects

The constructed prototype [51] utilises two piezo electric actuators housed in an aluminium flexure to provide drive, position measurement, and sample sensing capabilities. This arrangement is shown in Fig. 14 below. The larger piezo (on the left of the illustration) is used to drive the measuring platen towards the sample and its integrated strain gauge is used to monitor its extension. The small piezo is used to detect contact between the measuring platen and the sample. It detects a sudden change in strain, when the measuring platen contacts the sample, utilising its integrated strain gauge. This ‘small piezo’ is not driven during the measurement process nor is its strain gauge signal used to provide measurement data.

The prototype system must use a comparative measurement system as the position of the stage that samples are held on during measurement is not monitored. Before a series of measurements can be taken the system is first calibrated by detecting two calibrated samples. The signal from the large strain gauge is recorded for each calibrated sample which gives a relationship between strain gauge voltage and sample size. Next the samples are measured and the voltages recorded are used to calculate their diameters.

This setup was selected to provide the high speed, high precision requirements of the project and to give the targeted ability to measure to 0.1µm. However, as mentioned earlier, issues arise particularly in relation to humidity, temperature and vibration in the use of the technologies selected and the targeted accuracies. These issues will be briefly reviewed in the following paragraphs.

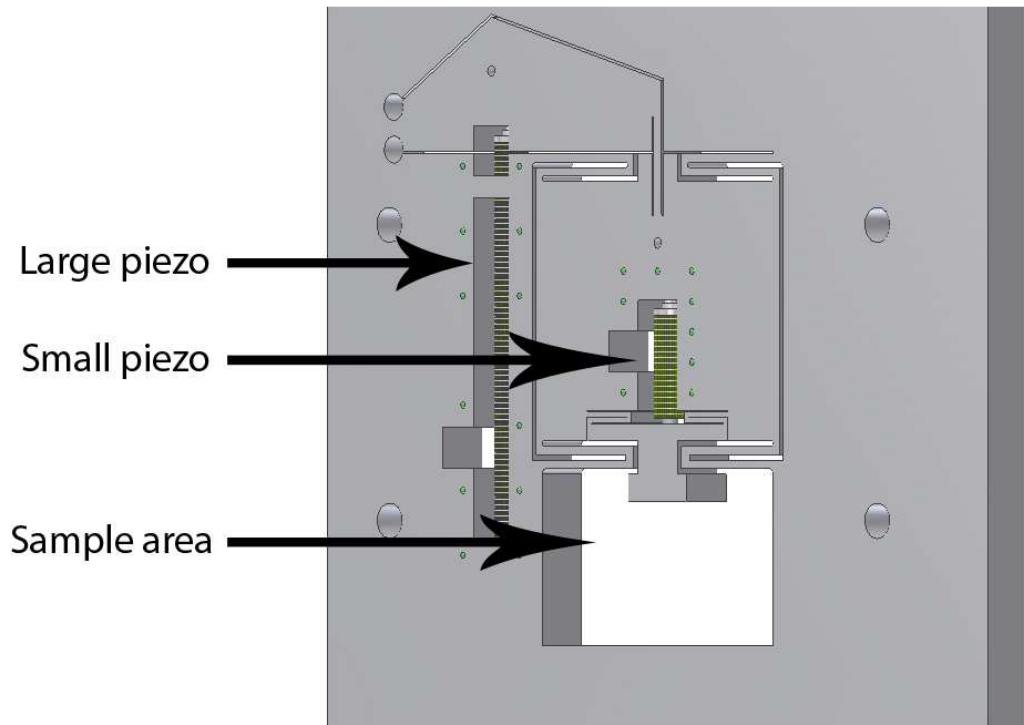


Fig. 14 Piezo electric actuators in aluminium flexure

2.5.1. Humidity

The piezo electric actuators used in the measurement stage to provide the rapid contact and the high accuracy measurement capability required [3] are sensitive to high humidity levels. High humidity is known to reduce the lifespan of, or even destroy polymer, insulated piezo electric actuators [22], [38], [39]. Any deterioration occurring due to break down of the insulation as water molecules diffuse through the polymer layer when the actuator is exposed to a high humidity environment is permanent [38]. It is uncertain exactly what effect this deterioration would have on measurement results prior to total failure of the piezo. Fig. 15 shows the reported effect of exposing a piezo electric actuator to high relative humidity. In the test, 100V was applied to the piezo in a 70% RH environment at 25°C. After approximately 8 hours in this environment the polymer insulator used in the piezo construction started to break down and current began to leak. The leakage continued to increase until approximately 100 hours into the test at which point it reached its maximum; about 4000 times the initial leakage current [39]. The figure also shows PICMA insulated piezo-actuators under the same test conditions. They show no adverse reaction to the high humidity environment.

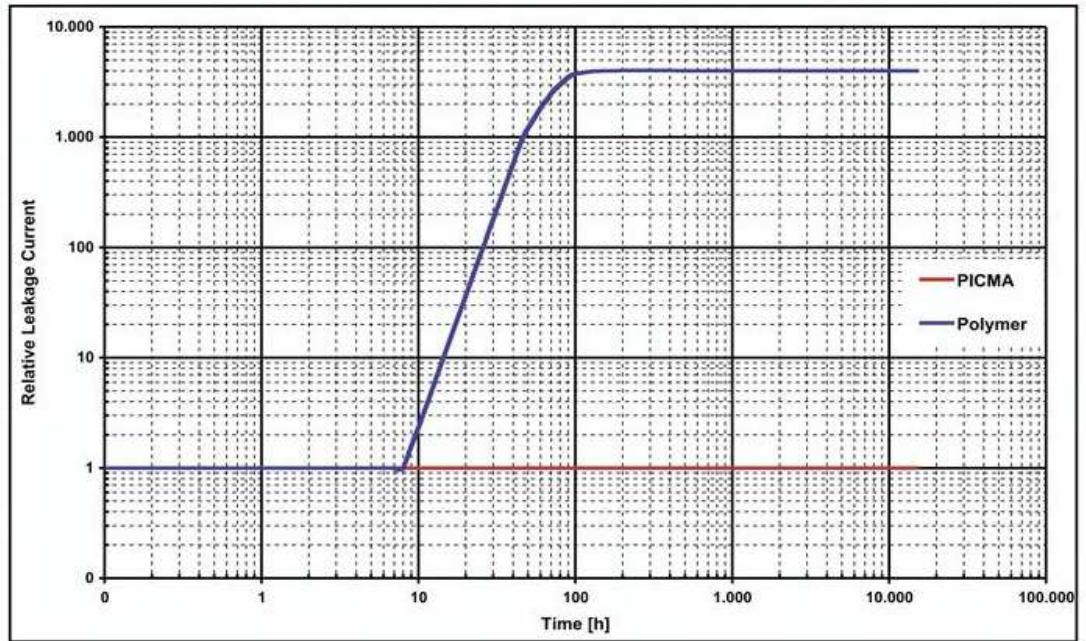


Fig. 15: Current leakage of piezo actuator exposed to 70% RH, 25°C, and 100V applied [39]

Protection of Piezo actuators using an air protection system is offered as an extra on actuators supplied by PI (Physiks Instrumente) [22]; however this option as presented by PI (show in Fig. 16) would not fit within the space constraints presented by the apparatus used for this research project.



Fig. 16 Piezo actuator with water proof enclosure and connection for flushing/cooling air [22]

The tolerance of the piezo actuators to high local humidity is important in the case of under fluid measurement. Given the susceptibility of polymer type piezos to humidity, the cost and availability issues surrounding PICMA actuators, and the fact

that PI's 'in-house' solution would not be possible to implement a decision was taken to develop an in house humidity protection system to work with the polymer type piezo actuators used in the measuring stage. The design and development of this system is discussed in detail in Chapter 4.

2.5.2. *Temperature*

Researchers have highlighted the effects of temperature on tooling [40], [53], work pieces [42], [52], [53], and piezo actuators [38].

Zhao et al. [53] state the primary effects of temperature fluctuation are errors in interferometer beam paths and thermal expansion of the work piece and metrology frame. As the measurement technology utilised in this project does not make use of interferometry the key concerns are thermal expansion of work piece of measurement hardware.

Shouldice [52] defines the maximum allowable temperature changes on 10mm and 13.5mm diameter ball bearings as 0.943°C and 0.7°C respectively to ensure less than 0.1µm change in diameter of the samples. Alternatively this means a 143nm/°C and 106nm/°C change in diameter for 13.5 and 10mm balls respectively. This calculation is shown below.

$$\Delta L = (L_o)(\alpha_L)(\Delta T) = (0.0135)(10.6 \times 10^{-6}) = 143 \times 10^{-9} m$$

Where: α_L is the linear coefficient of thermal expansion for chrome steel 52100 [52]; L_o is the original length (m); and ΔT is the change in temperature (K).

Working on the common rule of thumb that any inherent system error should be less than 1/10th of the target accuracy, this would suggest a requirement for temperature stability of the samples of $\pm 0.07^\circ$ [41].

In this project measurement under fluid makes up one element of a strategy to achieve a targeted measurement precision of 0.1µm. The purpose the fluid is to reduce the effects of thermal expansion of the waiting samples as a source of error in the results [42]. The effectiveness of fluid based thermal control has been demonstrated previously by M.E. Harvey of the National Standards Board (USA) [43] and separately by Hiromitsu Ogasawara of the University of Iwate [44]. Harvey and Ogasawara presented temperature stabilities of $\pm 0.025m^\circ C$ and $0.01m^\circ C$ respectively. In the case of the system used by Ogasawara a method of control using flowing water was presented to

achieve stated temperature stability at near room temperature, utilising thermistors, proportional controllers, proportional-integral controllers, heating elements, and Peltier elements. The requirement for this project being less than $\pm 0.01\text{m}^\circ\text{C}$ demonstrated by Ogasawara it was considered that a much simpler passive thermal control system would be adequate. This passive system uses the thermal inertia of a large volume of water to act as a buffer to sudden room temperature changes [52]. The samples would be held for a specific period of time in the temperature normalisation tank before measurement. In this arrangement (illustrated Fig. 19, Section 3.1) fluid is circulated between the temperature normalisation tank and the measurement tank to minimise thermal variation in the fluid.

The piezoelectric actuators used in the apparatus exhibit low levels of linear thermal expansion and no performance degradation due to temperature changes. Fig. 17 shows that large temperature shifts from the calibration temperature (22°C) are required for even small changes in length of the actuators.

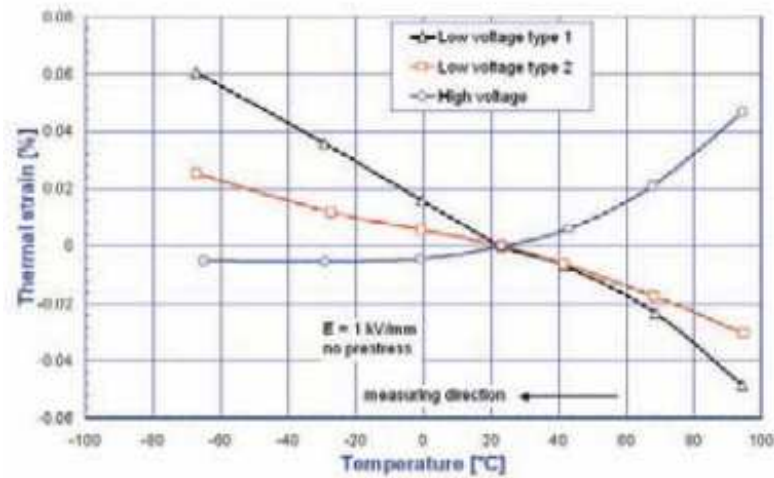


Fig. 17 Linear thermal expansion of different PZT ceramics [22]

2.5.3. *Vibration*

Researchers [45], [46], [47], [48], [51] have identified the importance of vibration control for precision measurement and manufacturing applications.

Chen et Al. [46] identify sources of vibration as internal and external. Internal disturbances originate from within the manufacturing facility (e.g. HVAC systems, heavy machinery, conveyor systems, etc) while external disturbances can include

vibrations from the ground (passing trucks, nearby construction site, etc), people walking, and machine operation.

Madigan [51] describes the passive system developed for the apparatus used in this research project. It is a passive structure which relies on its mass to lower its resonant frequency. The assembly is show in Fig. 18. It utilises:

- “Instrument base” of granite.
- “Support frame” made from steel.
- “Instrument table” constructed using cast iron beams, four steel side plates and an aluminium top.

The combined weight of the assembly is approximately 600kg [51].

An anti-vibration material was also placed between the feet of the instrument table and the floor. The anti-vibration material chosen was an elastic vibration damping material with high shock and vibration damping properties moulded from high-grade nitrile (NBR) rubber.

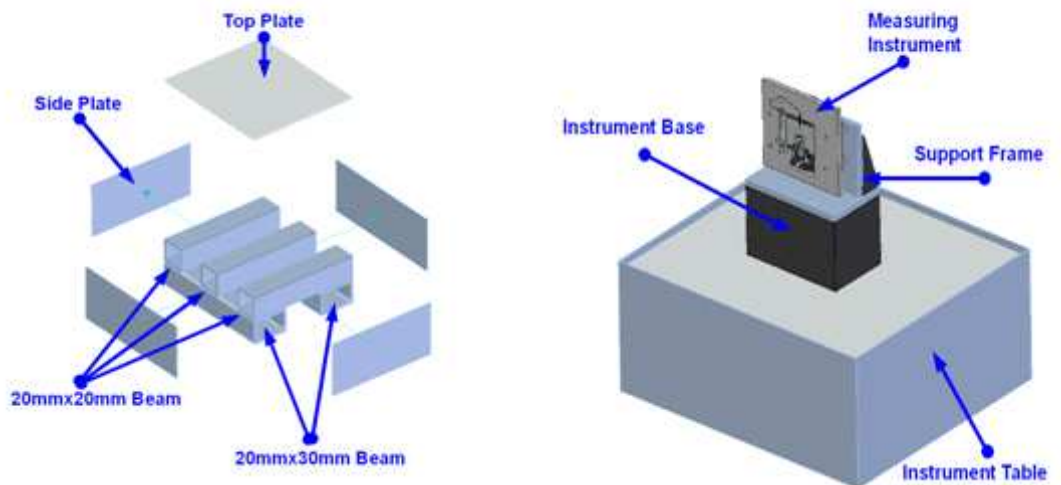


Fig. 18 Vibration isolation assembly [51]

2.6. Summary

This chapter reviewed the concepts of measurement, accuracy, precision, and their associated errors as well as precision movement, precision contact detection, and precision measurement technologies in the context of the literature. The concepts and literature associated with the key environmental issues of humidity, temperature variation, and vibration as related to the performance of the instrument at the targeted sub-micron level were also reviewed.

3. Relocation & modifications

3.1. Introduction

At the outset of the project the measuring and temperature normalising stations were based in the NN Euroball facility in Co. Kilkenny and were achieving a measurement precision of $1\mu\text{m}$ [51]. The relocation of the equipment to the Ultra Precision Research Laboratory at Waterford Institute of Technology became essential due to the imminent closure of the NN Euroball Kilkenny facility. Apart from the disruption and obvious disappointment in terms of the long term prospects for project viability this move was attractive as it meant bringing the equipment back into a stable environment (the area in NN Euroball was subject to drastic and sudden temperature swings; for example if the loading dock door was opened) where the targeted measurement accuracy of $0.1\mu\text{m}$ could be more realistically addressed.

The relocation highlighted problems with the delicacy of the plant. More specifically water leaks, control difficulties, and sample ball circulation problems all combined to prove a serious reliability issue.

This chapter deals with the difficulties encountered during the relocation and re-commissioning of the equipment. It also details the various physical upgrades and software modifications made for improved reliability and performance with the ultimate goal of achieving the targeted measurement capability of $0.1\mu\text{m}$. Fig. 19 below shows photographs of the equipment when installed in NN Euroball and WIT respectively.



Fig. 19: Station installed at NN Euroball (L) and subsequently at WIT (R)

3.2. Replacement of fluid normalising medium

The temperature normalising fluid used while installed in the NN facility was the oil based temperature normalising fluid used in the various manufacturing processes in the plant. The reason for this was to reduce fluid cross contamination in the plant. Prior to transportation of the equipment to Waterford IT the fluid was removed from the system.

Water was used as the temperature normalising fluid when re-installed in Waterford IT; the fluid used in the NN facility was no longer readily available and the issue of contamination from differing fluids was, of course, no longer relevant.

While running commissioning tests on the equipment it was discovered that the samples were corroding in the fluid. To combat this, an anti-oxidation agent was added to the fluid.

3.3. Reconfiguration of sample circulation

While in use in the NN facility the station was configured to store the calibration balls locally and to take samples for measurement from production machinery as required. Calibration balls would be returned to storage in the normalising fluid while measured production balls were sent to a reject bin and then manually returned to

production. Large and small calibration balls were sorted and stored separately upon returning to the storage area. Similarly the incoming sample balls were stored separately from the calibration balls while being cooled. This mechanism was originally built to sort two different size samples; one set of 13mm nominal diameter balls, and one set of 11mm nominal diameter balls. This meant there were 6 storage areas (4 for calibration balls and 2 for incoming samples). When installed at WIT this mechanism was altered to suit continuous recirculation of calibration and sample balls.

Over time, issues related to the kinetic energy of the samples were observed. These included:

- Damage to various parts of the pipe work, most notably any 90° elbows.
- “Bouncing out” of the collection pyramid in the storage tank.
- Denting of the collection pyramid in the storage tank.

A study of the kinetic energy was undertaken. A section of pipe work equal in length to the ball return pipe work was set up with an inductive type sensor at the end to detect the arrival of the sample. A PLC was connected to control the “firing” of the sample and record the time taken for it to arrive at the destination. This program is illustrated in Fig. 20 below. The input X7 is used to start the process. It initialises the timer T247 and turns on Y0 which controls the air blast. T247 is used as it counts in milliseconds and is the highest resolution offered by the PLC. T247 triggers counter C1 every 3ms. So the figure stored in C1 multiplied by a factor of 3 is the transit time recorded for the sample. Input X6 is the input from the inductive sensor which detects arrival of the sample at the end of the piping.



Fig. 20: PLC control and timing program

The overall length of the pipe work was calculated using standard pipe equivalent lengths for fittings as shown in Table 1 below.

Table 1: Equivalent pipe fitting lengths [49]

Pipe Size	System Components	Equivalent Length of Component (m)
3/4in (DIN20)	Tee	0.4
3/4in (DIN20)	90 deg Elbows	0.8

Using this information the following table of results was compiled.

Table 2: Kinetic energy results

Time (s)	Mass (kg)	length (m)	Velocity (m/s)	Air Line Pressure (kPa)	KE (J)	J/kg
1.545	0.01	5.8	3.75	100	0.070464	7.046428
1.857	0.01	5.8	3.12	100	0.048776	4.877555
1.365	0.01	5.8	4.24	150	0.090274	9.027358
1.389	0.01	5.8	4.17	150	0.087181	8.718093
1.116	0.01	5.8	5.19	200	0.135051	13.50509
1.107	0.01	5.8	5.23	200	0.137256	13.72558
1.068	0.01	5.8	5.43	250	0.147463	14.74631
1.035	0.01	5.8	5.6	250	0.157016	15.70165
0.789	0.01	5.8	7.35	300	0.270192	27.01917
0.843	0.01	5.8	6.88	300	0.236685	23.66851
0.663	0.01	5.8	8.74	400	0.382648	38.26475
0.603	0.01	5.8	9.61	400	0.462585	46.25848

It was concluded that the kinetic energy inherent in the system design had to be removed before the balls reached the temperature normalising station to prevent damage to fixtures and fittings.

Three options were considered:

1. A method of absorbing the kinetic energy before the ball reaches the tank.
2. Sections of meandering pipe work as used in the NN installation [52]
3. Re-design the sample return system to use a carrier on a pneumatic ram or electric motor driven pulley system to carry the ball to the required height and allow the ball to drop into the tank.
4. Installation of stronger 90° elbows.

These are considered in more detail in Table 3 below.

Table 3: Kinetic energy absorption options comparison

	Absorption	Meandering pipe work	Mechanical return	Tougher elbow sections
Space requirements	Minimal. No more space than existing piping.	High.	Minimal. No extra vertical space needed and there is adequate space around the equipment for installation.	No additional requirements.
Complexity	Simple.	Moderate.	Complex installation and control programming required.	Simple.
Reliability	No extra moving parts or elbows required. Reliability should be high.	Adds additional elbows which were a primary source of failure in initial design.	Moving parts could have a negative impact on reliability.	Unknown until tested.
Ease of installation/ part availability	Parts readily available.	Parts readily available.	Not all parts available. Would require time for programming and testing also.	Parts readily available.

The options presented in Table 3 would help to reduce or remove the kinetic energy problem and result in the samples entering the tank using only the energy gained by acceleration due to gravity.

Despite the comparatively complicated installation and control difficulties associated with a mechanical return system this was the preferred solution. With a mechanical lifting mechanism there would be little or no kinetic energy added to the

sample during transportation. However component availability meant this was not a viable option.

The meandering pipe work presents a tried and tested approach to the issue of kinetic energy dissipation however it does not go far enough towards solving the problem and would add more potential failure points to the system. The approach here would take up a great deal of vertical space, for which there would not be adequate clearance in it's present installation as illustrated in Fig. 19. There were also problems with the samples breaking through corner pieces and various sections of the plastic pipe work.

With this in mind a combination of Option 1 (absorption) and Option 4 (tougher elbows) was installed. First the tougher elbow pieces were installed. Then the issue of energy absorption was examined. A first prototype was constructed, consisting of a single acting pin cylinder inserted into a part of the pipe work and held in place using a metal epoxy. The PLC code governing the ball return system was modified to utilise the extra cylinder and, once the epoxy cured, the system was tested. The first prototype was a failure. The force of the ball impacting the cylinder bent the rod out of shape and cracked the epoxy holding the cylinder in place.

A tougher second model was envisaged and constructed. Instead of placing a small cylinder in the pipe work, a larger pneumatic ram was placed under the exit of the piping. So as to avoid denting the ram or damaging the balls a thick rubber covering was applied to the ram to absorb any kinetic energy carried by the ball. This solution, along with tougher 90° elbows, remained in use until it became apparent that the samples were still damaging the elbows when passing through the pipe work. This is illustrated in Fig. 21 below.



Fig. 21: Damage caused to steel elbow piece by samples

At this point it was decided to modify the system further to remove the elbow joints in use. A large storage box was utilised. The base was reinforced with an aluminium framework with steel sheeting above it. Fig. 22 below shows a 3D render of the framework with one side of the box removed. The steel sheet was covered with 25mm thick rubber. The open end of the box was covered with a sheet of Perspex with an entry and exit hole cut into it. The assembly was positioned over the temperature normalising tank to allow the balls to fall into the tank after their kinetic energy had been absorbed by the rubber on the impact surface in the box.

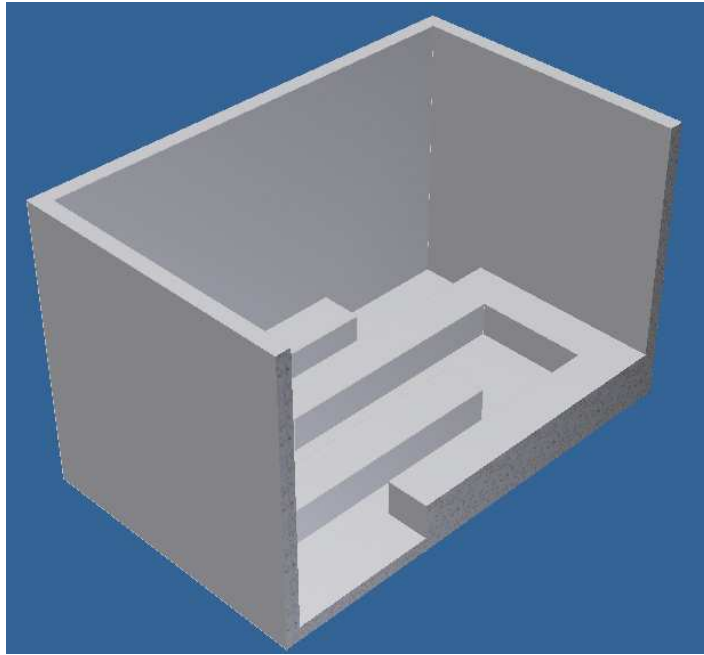


Fig. 22: Render of sample capture box showing base reinforcements

3.4. Sample order control

Samples are gravity fed from the temperature normalising tank to the measuring stage. They must arrive at the measuring stage in a pre-determined order. From time to time the samples would arrive at the measuring station out of sequence. An investigation revealed an open section of pipe work delivering balls from the temperature normalisation tank to the measuring tank as the only place in the system where the delivery order of the samples could change. This section of pipe work is open to allow the fluid to drain before it can reach the measuring station which helps to prevent rippling in the fluid close to the measuring stage and hence limits vibrations and removes a potential source of measurement error.

To prevent the balls swapping position, by moving over or around each other, a temporary cage was created over the top opening in the pipe using two lengths of M3 threaded bar and two ties to hold them in place, as illustrated in Fig. 23 below.



Fig. 23: Cage for ball order control

Occasionally when a sample was ejected from the measuring station it would bounce forwards into the temperature normalising fluid instead of falling backwards towards the sample return pipe. After installation of the new “ball in place” sensor bracket, discussed in section 3.6 below, this issue became more frequent. To combat this, a Perspex guard, illustrated in Fig. 24 below, was put in place. The balls which would have bounced out now bounce off the guard and return to the normal exit path.

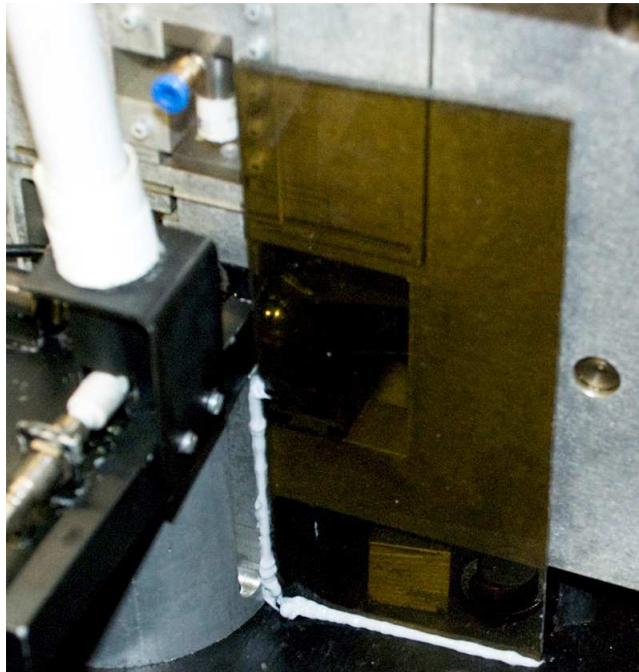


Fig. 24: "bounce out" protector installation

3.5. Fluid level control and circulation

A part of the experiments undertaken in enhancing measurement precision of the stage include the removal/reduction of the influence of outside factors on the thermal expansion of the samples. To this end a system was implemented to immerse the samples in the temperature normalising fluid during the measuring process. This fluid would be circulated continuously between temperature normalising and measuring stations to try to ensure a uniform temperature throughout.

Given the proximity of the piezo actuators to the fluid, reliable control of the fluid level was required. It was envisaged that the fluid would be kept at a constant height close to the top of the sample being measured. Precise level control would be required to ensure consistency between measurements. Two options were examined: a weir and an electronic level control system. Their relative pros and cons are examined in Table 4 below.

Table 4: Fluid level control methods

	Weir	Electronics
Flexibility	Infinitely adjustable fluid level with variable height gate.	Limited by adjustability of level switch.
In operation level variation	None.	Lag time between switch closing and valves opening/closing may make level control difficult.
Complexity	Extremely simple.	May require complex control programming to achieve a stable level with minimal disruption.

The weir option presented a number of attractive benefits over an electronic control system and so was implemented. Fig. 25 below shows what a traditional notch type weir would look like installed in the tank holding the measurement stage. This

image shows that wall into which the weir is cut would need to be sealed along three edges with the measuring tank.

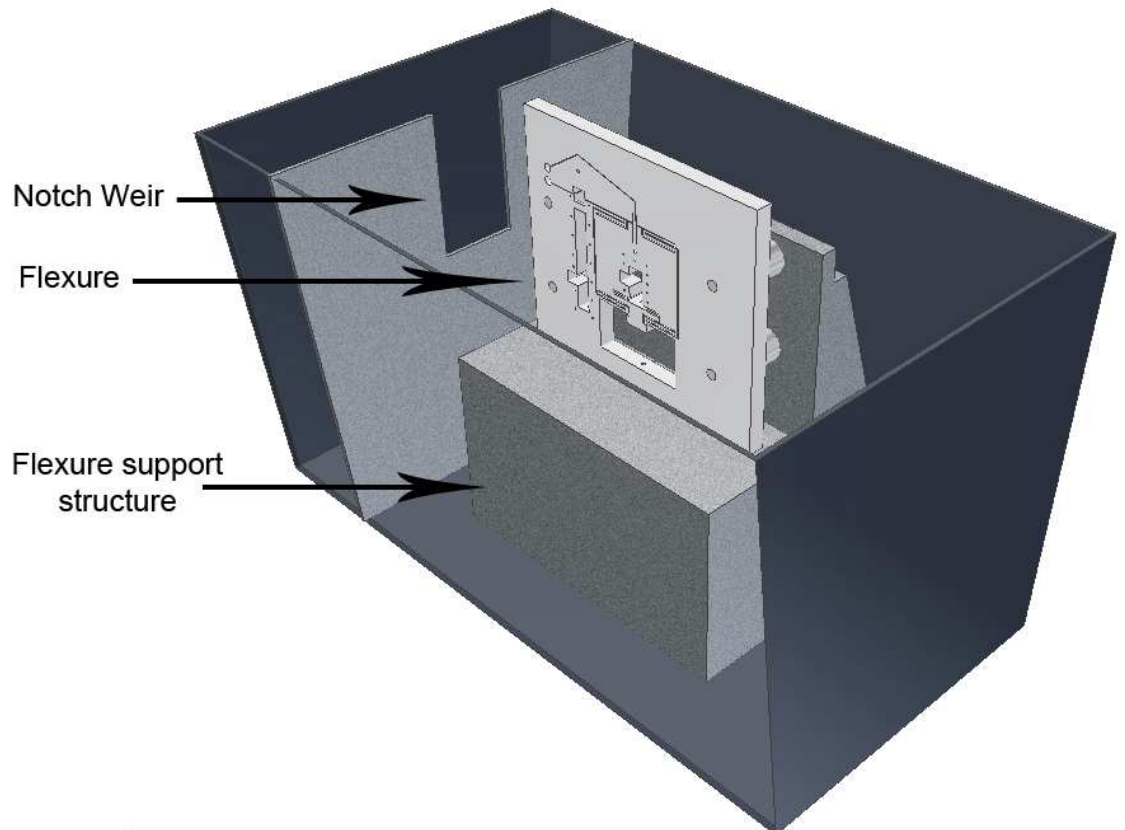


Fig. 25: Traditional notch weir

Rather than attempt to seal these leak points it was decided to create a “tank-in-tank” arrangement as illustrated in Fig. 26 below. The inner tank can be drained through a pipe which passes through the walls of both inner and outer tanks. As can be seen the use of an inner tank removes the risk of leaks between the controlled area and the drain area. The fluid level in the controlled area can be set using a vertical sluice gate to adjust the working height of the notch.

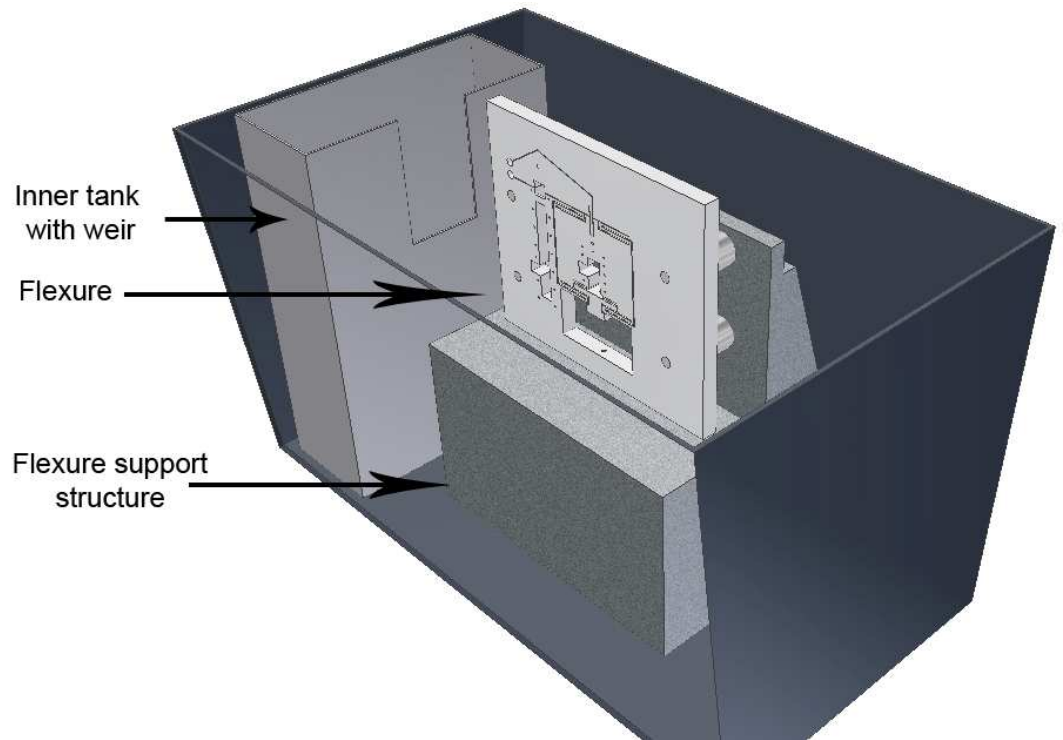


Fig. 26 Cutaway showing inner tank weir arrangement

Electrically actuated spring return ball valves were installed on the inlet and outlet pipes to allow the control system to stop flow either as required by the user or if there is a problem with the air protection system as discussed in Chapter 4.

3.6. New bracket for ball in place sensor

The “ball in place” sensor utilises a Keyence FS-V21RP optical sensor. This sensor uses fibre optic cables to transmit light to the seating area and measure reflected light from the seating area. When a sample is inserted the magnitude of reflected light increases greatly and triggers the sensor to output a “high” signal indicating a sample is in place and waiting to be measured. The fibre optic cables are positioned behind the sample locating spheres and held in place by a custom made bracket. The original bracket is shown in Fig. 27 below. It was made from a single thin piece of folded sheet metal. Once moved it proved almost impossible to return to the same position and so as part of the apparatus reliability upgrades was replaced with a new bracket.

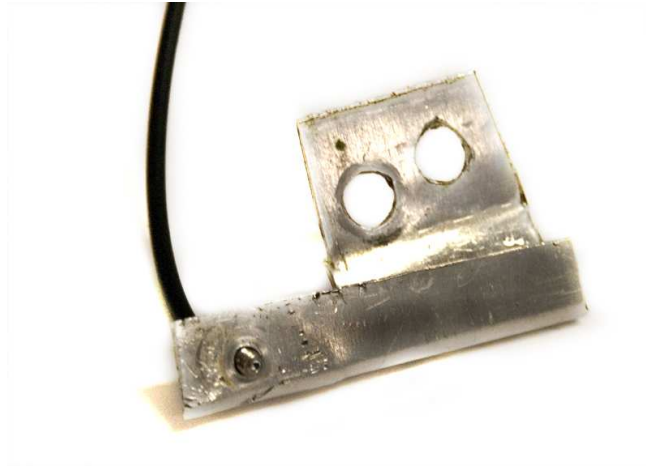


Fig. 27: Original bracket for "ball in place" optics

Fig. 28 below shows the replacement bracket which is made from much thicker materials. Although it uses multiple components it can be returned to the same position with greater ease and is significantly more rigid than the original. If it is necessary to alter the position of the optics there is now a greater range of adjustability.



Fig. 28: Replacement bracket for "ball in place" optics

3.7. PLC Rewiring & Reprogramming

With the switch from production plant to laboratory based measurement some features utilised in the production installation became unnecessary and were removed to reduce complexity.

Components no longer necessary included:

- The ball sort mechanism for returning calibration balls to their holding positions in the measuring tank was removed as all samples would now be cycled continuously between temperature normalising and measuring stations instead of

only calibration balls returned and the rest rejected. Part of the purpose of this system was to allow for queued temperature normalising of samples from several machines. This was no longer needed in laboratory conditions as only a single set of samples would be in use at any one time.

- Removing the above allowed for a large PLC controlled valve island (collection of electrically actuated 3/2 way valves) and it's wiring loom to be taken out.
- Induction sensors for detecting samples arriving from the process and all their associated wiring were removed.
- Extra water valves to allow for fluid control were added to the system, as discussed in section 3.5 above.

The combination of the above allowed for a greatly simplified PLC program be written to govern the control of the temperature normalising station; reducing the program from over 300 ladder logic lines to just over 100 lines. The wiring loom providing communication between temperature normalising station and measuring station PLCs was also reduced from 17 to 7 wires. The ladder diagram can be seen in Appendix B – PLC Programs.

3.8. Monitoring and control program updates

3.8.1. Multiple touch measurement (LabVIEW)

The moving block (with its touching surface) is driven forward in increments (step sizes) by signals from the LabVIEW control program. This step size was originally fixed and represents a compromise between measurement speed and resolution. The piezo control can only send a signal to move in full increments. The fixed step size was originally set at 0.015V.

The piezo actuator used to drive the cantilever is a P-841.60 supplied by Physik Instrumente. This actuator has a maximum displacement of 90 μ m. However when used in a stiff flexure the maximum stroke length will decrease. The stiffness of the flexure in which the piezo is installed reduces the maximum stroke to 57.97 μ m [51]. This gives rise to the value d_2 in Fig. 29 below, the linear vertical travel at the end of the cantilever due to d_1 being the 57.97 μ m extension of the piezo actuator.

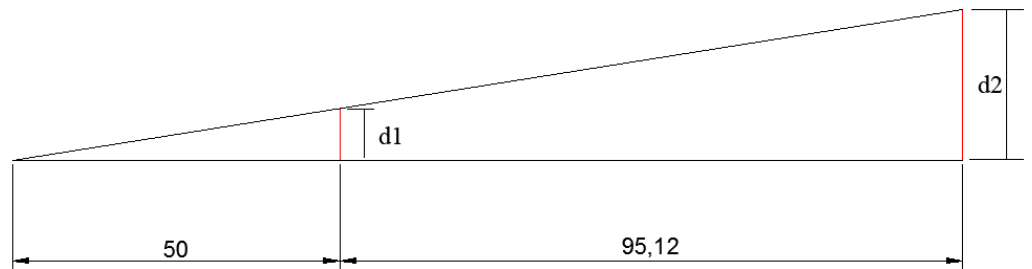


Fig. 29: Cantilever dimensional diagram (not to scale)

From Fig. 29:

$$\frac{57.97 \times 10^{-6}}{50} = \frac{d_2}{50 + 95.12}$$

$$d_2 = 168.25 \times 10^{-6}$$

A 10V signal from the control program is required to fully extend the piezo.

The effect of this at the end of the cantilever is as follows:

$$10V = 168.25 \mu\text{m}$$

$$1V = 16.825 \mu\text{m}$$

$$0.015V = 0.252 \mu\text{m} \text{ or } 252 \text{nm}$$

The 0.015V increment was originally chosen as a compromise between measurement speed and precision. With a target of measurement precision of 0.1 μm or better this increment was too large. However a smaller increment would also increase the time required for a single measurement, conflicting with the requirement for a high speed measuring system.

Ideally what would be needed is the ability to dynamically change the increment voltage during the measuring process. Of course the system cannot know how close it is to the sample unless it actually contacts the sample, so a program was developed to sense the initial touch, withdraw one “step”, and then step forward in a smaller increment. This is referred to as “multi-touch” measurement.

The program illustrated in Fig. 30 and Fig. 31 below was created as the first step to implementing this measurement strategy. The first part of the program compares the “current value” to the “target value” allowing for control limits. If the current value falls between the control limits then the comparison block passes a true signal to the case statement and the program ends. If the current value is outside of the range it is

being compared too then a false signal is sent to the case statement and the code held in the false frame is executed.

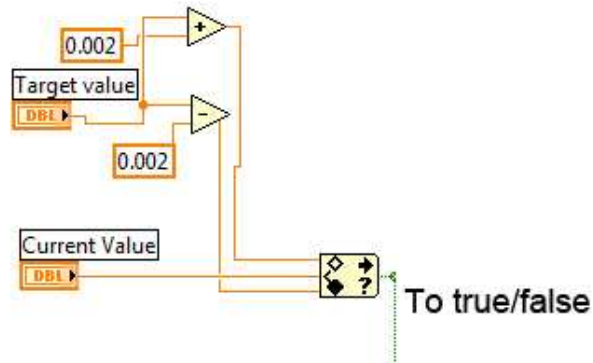


Fig. 30: Part one of changing step size program

When the false signal is detected by the case structure it first compares the target value and current value. Provided the current value is less than the target value it will continue to increment “current value” in steps as specified by the user. However when “current value” exceeds “target value” the program then decrements “current value” one step, reduces step size by the factor set on the front panel, and increments “current value” in the new smaller step size. This process is repeated until “current value” is within the control limits shown in Fig. 31 below.

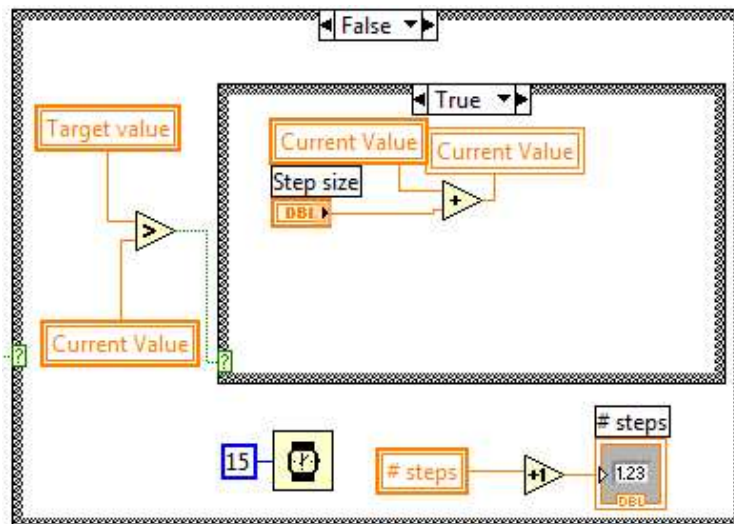


Fig. 31: Part two of changing step size program

Once testing of the operation of the multi-touch code was complete it was added to the control scheme in the LabVIEW control program. This required some modification as the program doesn't work to target values. Instead it senses touch when a strain gauge signal moves suddenly outside of control limits. The code above was

modified such that it would operate until the strain gauge signal was within a specified deviation from the control limits.

Fig. 32 below illustrates the differences in strain gauge feedback between the single touch and the multiple touch measurement schemes. As can be seen the single touch only crosses the control (detect touch) line once while the multiple touch plan crosses the same line several times in decreasing increments. This results in a smaller final step size than the single touch plan. Testing and results are discussed further in Section 6.

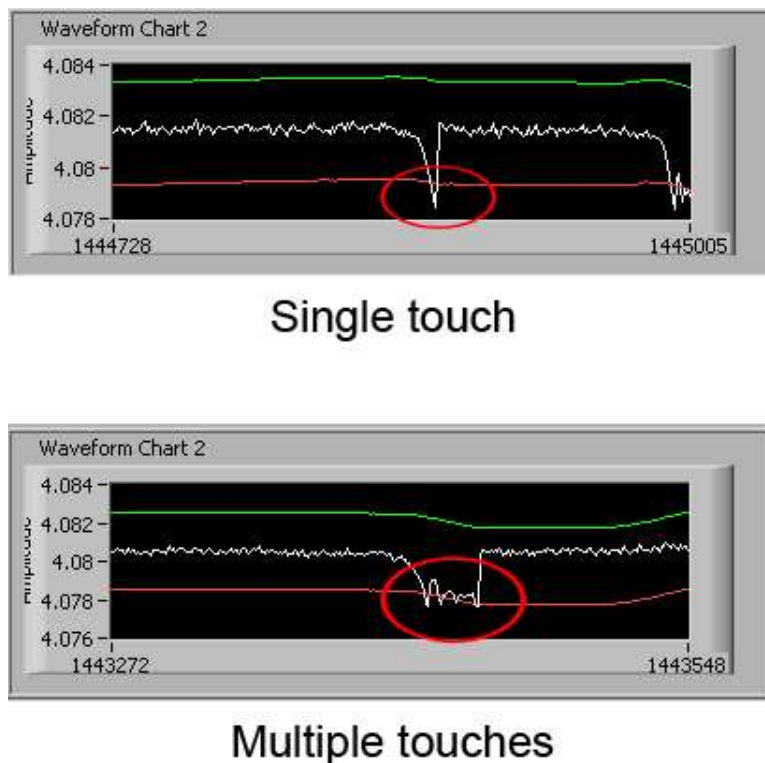


Fig. 32 Single vs. multiple touches

3.9. Additional sensors

3.9.1. Humidity and temperature

The sensitivity of the piezo actuators to humidity and the importance of fine temperature stability is discussed in Chapter 4. To monitor humidity and temperature a suitable sensor (Precon HS-2000V) was identified and added to the system. The Precon HS-2000V is a single sensor combining two functions; measuring relative humidity between 0-100% and temperature from -30degC to 100degC and outputting an analogue signal for each based on a percentage of the input voltage; so with an input voltage of

5V, and a RH value of 50%, the RH output would be 2.5V. The LabVIEW code was developed as shown in Fig. 33 below. The signals from each sensor were acquired through analogue inputs on the LabVIEW break-out box (BNC-2120).

Due to the relatively slow changing nature of the measurements LabVIEW was set up to take a small amount of samples (5) in at a very high rate (10 kHz). This sampling scheme means the program needs to spend very little time taking samples from these inputs and causes no slow down of other mission critical measurements; i.e. the strain gauge feedback from the piezos. Once the signals are acquired they must be processed by LabVIEW to produce a meaningful number. The first step is to convert the incoming waveform to DC values using the Basic DC/RMS VI. Once in this state, the values are smoothed using a moving average based on a set number of samples; 10 for humidity and 1000 for room temperature. The temperature value is smoothed more than the humidity value because it was observed to fluctuate more rapidly. From here, some basic mathematical operations give the relative humidity (%) and temperature (°C) values.

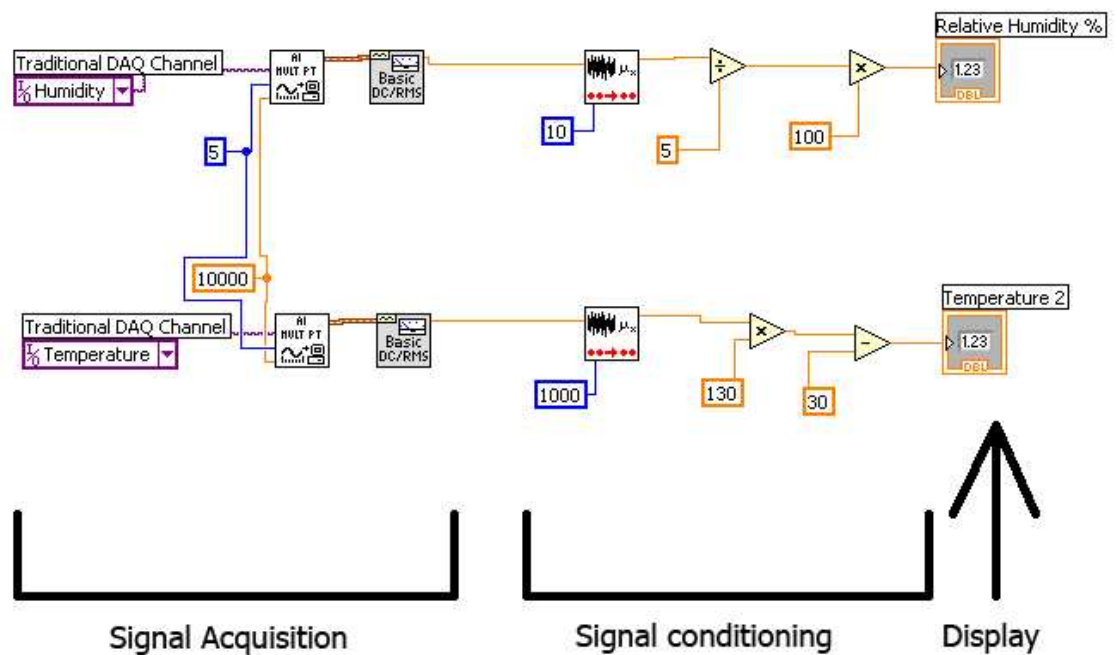


Fig. 33: LabVIEW code for humidity and temperature sensors

3.9.2. Fluid circulation status and air line pressure

Code was added to the LabVIEW program to monitor the status of the fluid circulation process, main air line pressure, and back up air line pressure. As well as

monitoring and displaying the status it also tracks the time at which any of the monitored lines fail.

Similar blocks of code were used for the three separate inputs. The code for monitoring the temperature normalising station process is illustrated in Fig. 34 below.

During normal operation the temperature normalising station PLC keeps a relay switched on, opening the normally closed connection and causing the digital line to be driven high, returning a true value which drives the corresponding Boolean indicator true and keeps the timer in the case structure running. If the process fails then the relay closes which completes the path to ground and the digital input is driven low; then the digital line will return a false signal and drive the Boolean indicator low. At the same time it will switch the case structure to the false case which will stop the timer in the true case from counting. The value of the timer in the case structure now loses synchronisation with the timer outside of the structure. This activates the down time display on the front panel and keeps count of the amount of time the system has been down for.

The blocks of code for the air line pressures work in exactly the same way. The only difference is the line from which the signal is read.

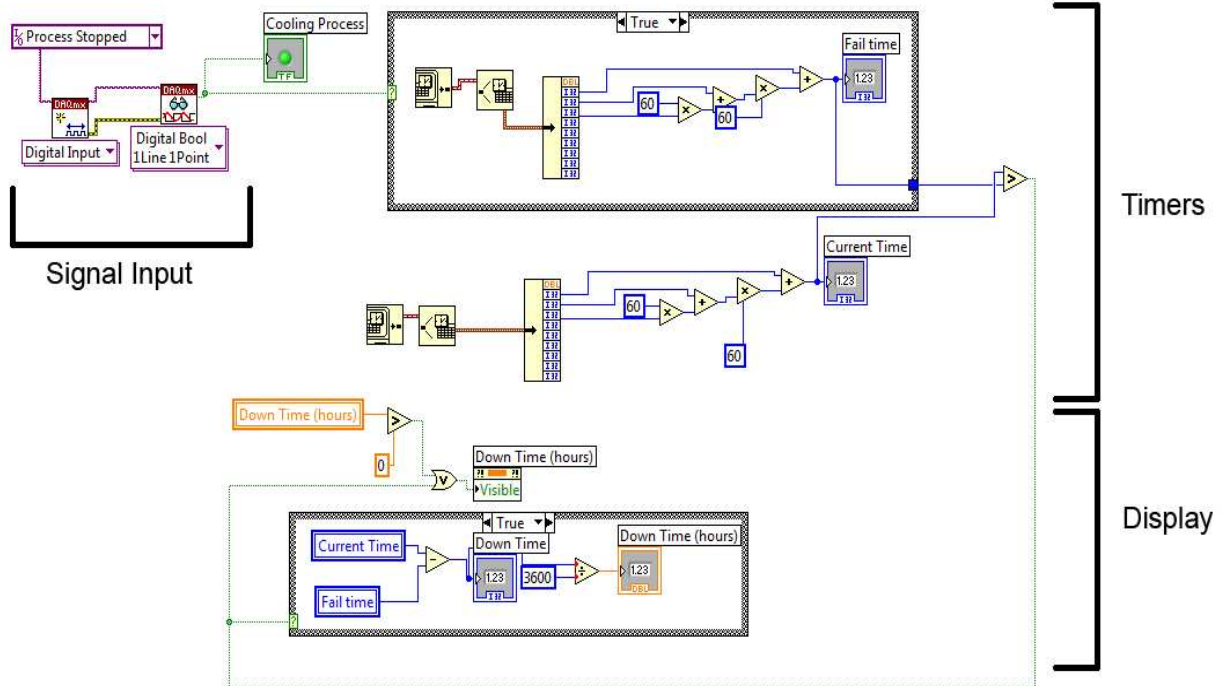


Fig. 34: LabVIEW temperature normalising process run status and down time counter code

3.9.3. Logging

In addition to logging the measured values of samples it was important to log the environmental conditions (humidity and temperature) at the time of measurement and the voltages detected during calibration. These values were added to the logging feature of the LabVIEW control program.

3.9.4. Status board and interface modifications

One of the interface improvements was the development of a status board which allows an operator to see at a glance the operational status of the system. Fig. 35 below shows the board when the main air has just failed. As can be seen the indicator turns red to warn of the failure and at the same time a timer is displayed along with a reset button to clear the timer once the fault has been rectified. The process and air line indicators are controlled by the code discussed in Section 3.9.2 above. The humidity

and temperature indicators are controlled by a comparison with the values returned in Section 3.9 above.

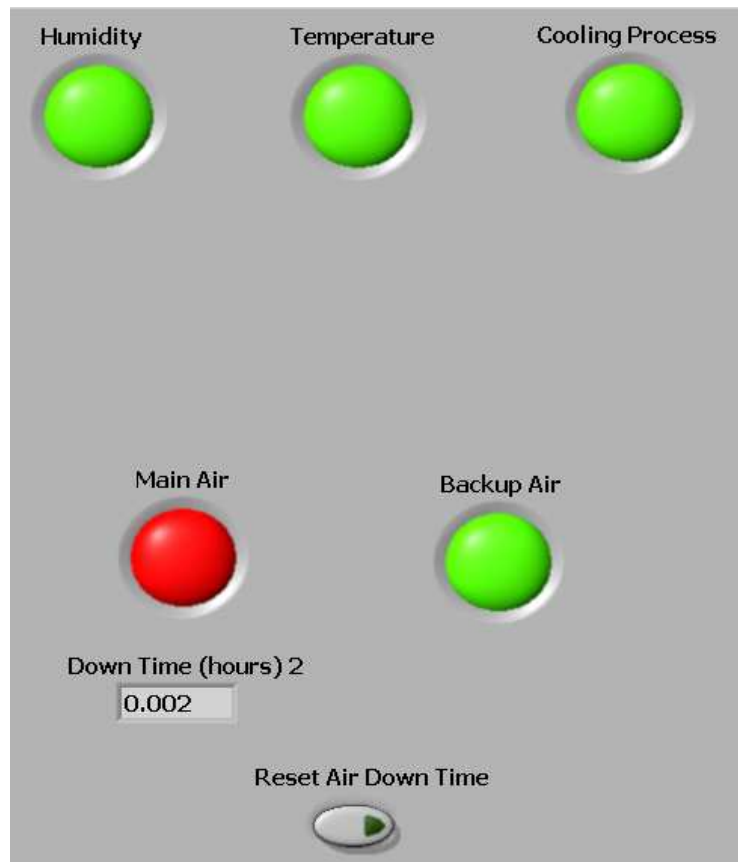


Fig. 35: LabVIEW status board showing main air failure

3.10. Conclusion

The hardware and software modifications discussed in this chapter have been put in place to provide improved measurement performance and improved reliability.

From a reliability point of view the sample circulation is now consistent (i.e. balls are delivered in the correct order) and no longer carries the risk of losing samples due to a break in a pipe or a sample bouncing out of the system somewhere. The extra monitoring functions in the LabVIEW control program provide the operator with a single point of information to ensure the system is running properly and the ability to quickly identify any errors.

The ability to measure the samples while immersed in temperature normalising fluid and a method of controlling the level of that fluid has been implemented.

The measurement capability of the equipment has been improved significantly by the addition of multi-touch measurement, as discussed further in Chapter 6.

4. Positive pressure piezo protection system

4.1. Introduction

This chapter describes the development and implementation of a positive pressure air flow system to protect the piezo actuators from excess humidity. The adverse effects of humidity have been discussed in Chapter 2.

Fig. 36 below illustrates the structure of a typical piezo actuator, showing the piezo layer and polymer insulation layer. It is when this polymer layer is exposed to humidity that breakdown occurs and current can leak through the insulator and cause a short between the working layers.

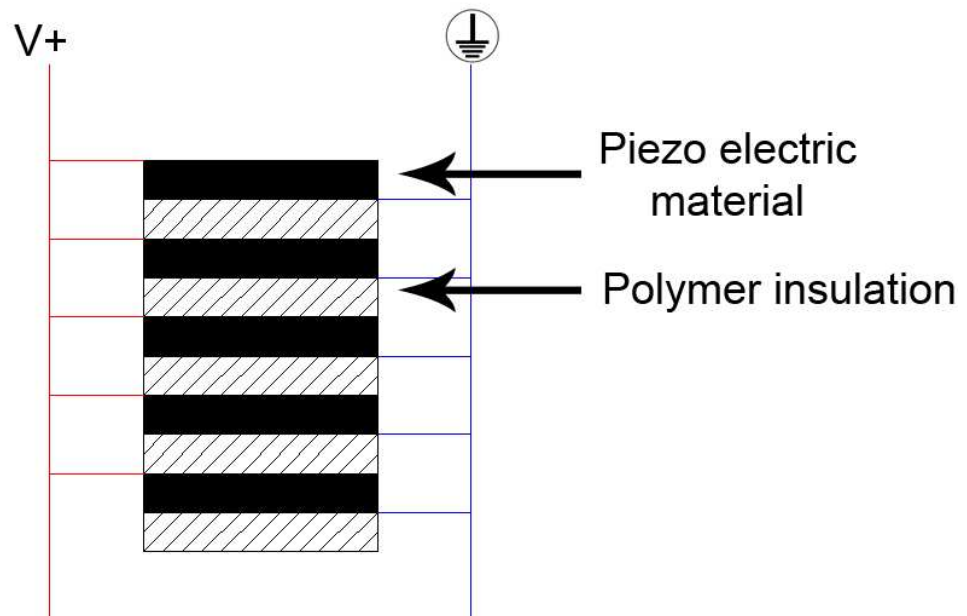


Fig. 36 Piezo electric actuator construction

The humidity protection for the piezo was studied and implemented in three stages: it was first demonstrated that a light air flow could prevent the ingress of water droplets into a chamber similar to that in which the piezos would be placed; second, this air flow principle was tested on an operating piezo and stage; it was implemented on the operational precision measurement stage. Finally due to the high cost of failure both in terms of down time and cost of piezo replacement, probable failure modes in the air protection system were identified and addressed.

4.2. Phase 1: Proof of concept

A model was constructed to simulate placing a piezo actuator in a high humidity environment. This was done to provide an initial indication as to the viability of air flow as a method of protecting the piezo actuators from humidity.

The assembly consisted of a hollow section 25*25*115mm steel tube (these are the dimensions of the chamber/enclosure for the “large” piezo as used in Section 4), closed at one end, with an inlet for an airline near the base. A 12mm diameter bar was placed in the tube to simulate the presence of a piezo actuator. It was supported above water in a bath using a steel support structure as illustrated in Fig. 37 below. There was a second air line placed in the tank to bubble air through water and thereby increase the water content in the air inside the system as much as possible and a Perspex cover (with some small holes for air exit) was placed over the top of the container in order to maintain a continuous high humidity level within the container.



Fig. 37: Mock-up piezo chamber in a water bath

A small piece of absorbent paper was placed in the base of the tube. The system was left running for 72 hours and then examined for signs of condensation and corrosion. It was noted that an abundance of water droplets had formed on the inside of the Perspex cover suggesting very high local humidity. Upon examination it was noted

that the steel tube had corroded over a large portion of its external surface area (it showed no signs of corrosion before the test). However the absorbent paper showed no sign of dampness and there was no corrosion on the inner walls of the tube, indicating that the air flow through the tube protected the contents of the enclosure.

From this it was judged that the risk of damaging a functioning piezo electric actuator in operation near the surface of a water bath would be minimised sufficiently to test the system on an older prototype piezo/monolithic flexure arrangement that was no longer in day to day use.

4.3. Phase 2: Prototyping

The next step in the development of the protection system was to prototype the system on a piezo. A protection system was installed on an existing flexure system incorporating a polymer insulated piezo. Fig. 38 below shows a Perspex enclosure around the piezo actuator in a flexure. The Perspex sheeting is affixed using a silicon based sealant as this flexure was not originally designed to allow for air flow across the piezo in this manner. It utilises a standard “push fit” air line fitting on the front of the housing as the entry point for the air pressure and uses small holes at the rear of the enclosure to release the air pressure.



Fig. 38: Front view of flexure with air protection system installed

Before immersing the flexure in water the system was tested in air with the air protection system running to prove that the water content of the compressed air was low enough to not cause any adverse functioning of the piezo actuator. The air input pressure was set at 6.9kPa and the system ran for several hours, during which time the

correct operation of the piezo was regularly checked by fully extending and retracting the piezo and monitoring the strain gauge output. No functional loss was observed.

Fig. 39 below show the flexure partially immersed in a water bath to mimic the planned immersion of the working system. The prototype protection system can be seen encasing the piezo electric actuator. Two air lines seen entering the image from the right supply air pressure to the system. The water level was set to just below the face of the measuring platen. A thermocouple which can be seen on the left hand side of the image was immersed in the water to monitor water temperature.



Fig. 39: Flexure in water bath showing water level and thermocouple

A programme was developed in LabVIEW to monitor and control the test; the water temperature and strain gauge feedback were recorded; automated on/off control of a water heater (around any selected set point) was implemented and manual selection of piezo extension and retraction was arranged.

In initial tests, the water bath was filled with cool tap water at 23°C, as measured by the thermocouple. The flexure was placed in the water bath with the air protection system running for several hours. Again the operation of the piezo was checked regularly by extending and retracting it and monitoring the strain gauge feedback. After eighteen hours, spread over three six hour sessions, the piezo showed no loss of function from being in the “cool” water bath. Following this, the water was exchanged for some “hot” water which was measured at an initial temperature of 57°C. The “hot” bath created a higher local humidity than would be seen using a bath at nearer room temperature due to a higher amount of evaporation from the hot bath and represented a worst case test for the system. Although the exact humidity figure could not be

determined this test is similar to the immersion planned for the working system except that it represents a worse scenario than the working system is ever likely to experience.

The system was run for several hours in this state with no observed functional loss giving the confidence necessary to install a similar air flow system on the working apparatus.

4.4. Phase 3: Primary equipment implementation

The installation consisted of front and rear Perspex panels secured to mounting points and sealed using silicon sealant such that only the ‘working end’ was open. As with the previous experimental prototypes this should ensure that the piezos are provided with sufficient protection from external humidity once the pressure flow maintains the positive pressure environment in the actuator enclosures. Fig. 40 below shows a computer generated render of the Perspex protection screens installed on the working stage. On the left of the image the large piezo is encased and sealed from the lower end (its fixed base) to close to the top, just below the level of the cantilever. The Perspex cover does not overlap any moving parts here so as not to create any movement errors due to friction between the fixed Perspex screen and the moving cantilever. Air pressure is supplied through a fitting at the base of the enclosure. The air rises upwards and exits through the top to provide protection against the ingress of moisture.

On the right of the image is the small piezo which is mounted upside down so it is encased and sealed from the top to just below the level of the bottom working end. It is not sealed at the lower end so that it does not impede the free movement of the flexure: the air exhausts at this end to again provide the protection against ingress of moisture.



Fig. 40 Render of air protection system as installed on working equipment

As an added precaution; a refrigerated air dryer (Dominik Hunter CRDC12) was incorporated in the air supply to guarantee a low humidity air supply.

To monitor the local humidity in and around the measuring tank a solid state humidity sensor (Precon HS-2000V) was installed. The outputs from this sensor were fed into the monitoring program so that both temperature and humidity could be monitored and logged. The installation and signal acquisition related to this sensor was discussed in further detail in Section 3.9.

Due to the crucial nature of maintaining the protective air flow (cost of failure in terms of time as well as money), a multi-level backup protection system was devised to protect the actuators even if the compressor supplying air to the system failed. The first part of the backup system was the installation of a secondary compressor which could take over pumping duties should the main compressor fail. Switching between the two was controlled by a pilot actuated spring return 5/2 way valve. This was chosen over electronically actuated valves to avoid unwanted switching in the case of electrical failure. Should both compressors fail (simultaneously) it was seen that there would be sufficient air reserve to continue to supply air to the system for approximately 3 hours (if full at time of failure). To protect the system, subsequent to this 3 hour period, a normally-open air controlled 2/2 way water valve was installed which would drain the

fluid content of the system into an external tank. The operation of the compressors and the valves was controlled by a PLC. Fluid inlets into the measurement system were arranged such that they would simultaneously be closed off by spring return (in case of general electrical failure); or in the event of loss of air pressure they are closed by the PLC.

4.5. System testing

The pneumatic system was tested extensively to ensure correct operation of the switchover from primary to secondary air supplies and proper operation of the emergency water drain. The testing revealed the need to add check valves to isolate the system from the compressed air supply to other parts of the facility in the event of main-air failure, as the secondary compressor is incapable of supplying the entire facility's air requirements and would deplete rapidly.

Further experimentation had shown that the most dangerous time for the piezo actuators is immediately after the temperature normalising fluid is removed from the system. The graph below, Fig. 41, shows the fluid in place for an initial thirty minutes. This established a normal humidity level in the atmosphere in the region of the stage. After this time the system was drained of fluid and the graph shows the subsequent relative humidity rises. The relative humidity is shown to peak at fifteen minutes after the fluid is drained from the holding tank. It takes a further ten minutes to reduce below the danger threshold of 70% as identified by PI [39]; and another forty-five minutes to return to pre-drain levels in the region of 60% relative humidity. This phenomena is caused by the exposure of additional wet surface area as the fluid is removed.

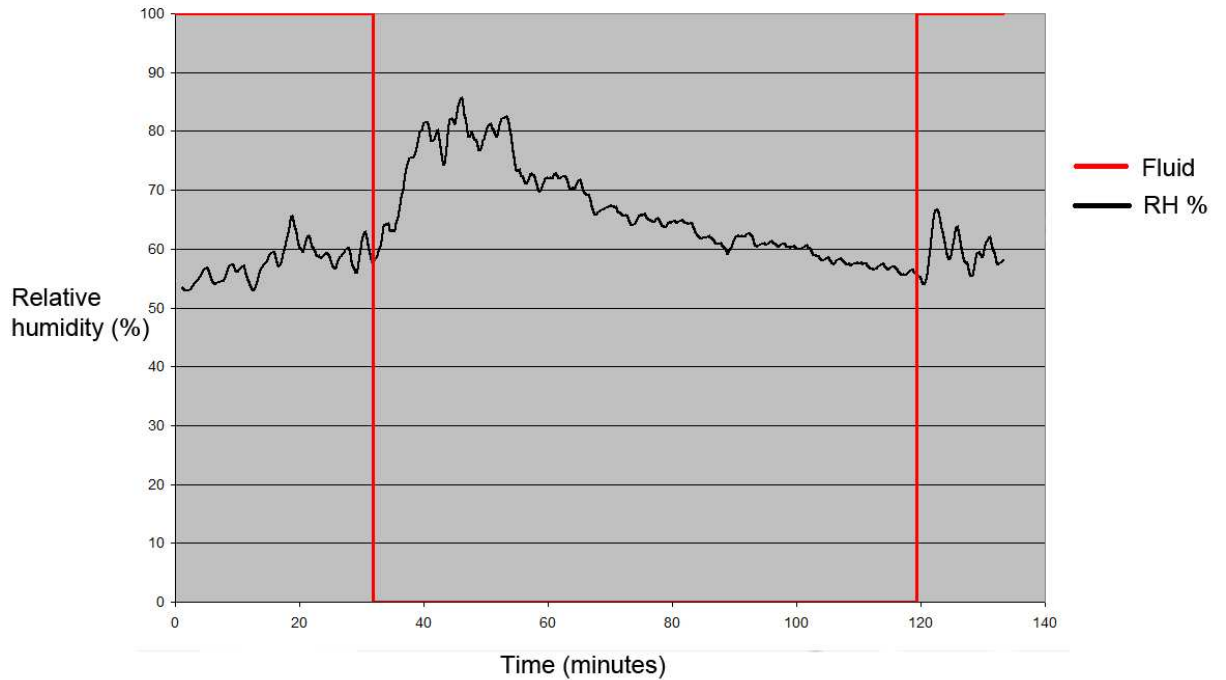


Fig. 41: Relative humidity (%) vs Time after fluid is drained

To overcome this issue of slow effective fluid extraction two options were examined. First coating the inner walls of the holding tank with a surface or finish that will encourage the fluid to run off it rather than adhere to it (as with the PVC tank walls); adhesive backed Teflon could be used to coat the walls of the holding tank for example. The other option was to revise the protection system control scheme so that if the primary compressor were to fail the 2/2 way water valve would be opened and the secondary compressor would be used only to provide air cover for the piezos during the draining as well as the period of high humidity that follows it. The latter option was implemented and tested.

4.6. Conclusion

This chapter has described the development of a simple and relatively inexpensive air flow protection system for polymer insulated piezoelectric component use in high humidity environments. This system entailed the construction of an air charging chamber around each of the piezo components, integration of a suitable air-flow supply and development of fail-safe mechanisms in the advent of system failure. Fluid dumping at the point of air loss was adopted as the key fail-safe scenario in the case of unattended system electrical or air supply loss. However it was found that

humidity levels peak some time after the fluid dump due to the exposure of additional wet-surface area and this high humidity takes some time to abate. Using the loss of main air supply pressure as the trigger for fluid dumping and preserving the residual compressor air reservoir capacity for the piezo protection, provided adequate air protection until the humidity returned to a safe level. The fully developed system has now been tested successfully over several months (and through several electrical and air supply failures) and has proven satisfactory.

An air-flow protection system is therefore shown to be a simple and very effective method of protecting sensitive polymer insulated piezoelectric components from harsh humidity conditions. It is felt therefore that there is now no overriding technical reason not to use the relatively cheap and available polymer insulated piezoelectric devices in high humidity environments.

5. Sample location and feed mechanism development

5.1. Introduction

A novel solution to the problem of positioning varying sized balls under the measuring platen has been developed using two spheres embedded into the base of the measuring platform to locate the sample [51]. This is a two degree of freedom holding method in that the samples are constrained in the X and Z axes. With the sample located by the embedded spheres its ability to move in the X axis is restricted and the force of gravity restricts movement in the Z axis. However the sample is still free to move in one direction along the Y axis as illustrated in Fig. 42 below. The sample is inserted along the Y axis and simply rests against the two spheres embedded in the measuring platform.

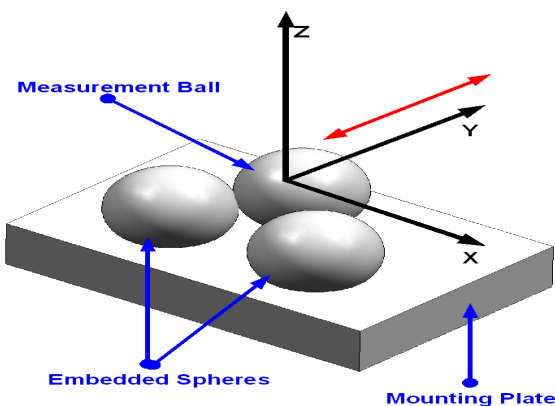


Fig. 42 Sample location diagram [51]

With the stage positioned at a slight incline there is a component of the force of gravity acting in the Y axis which helps to restrict movement in this axis.

However there has not been an examination of the magnitude of the forces involved nor is there significant knowledge regarding the magnitude of ‘upsetting’ forces. This means the measurement error arising from sample seating/location issues is relatively uncontrolled and may influence the results achieved from the measurement instrument.

This chapter examines two major changes to the way samples are handled by the system. The first is the introduction of a clamping mechanism to ensure consistent location of the samples at the point of measurement and to help reduce/negate the

influence of any vibrations during measurement. The second is the alteration of the queuing mechanism used to create a more reliable sample delivery system.

5.2. Clamping

A prototype clamping system to compliment the dual locating sphere system had been developed [51] but was never implemented on the working instrument due to space constraints and the question of clamping effectiveness was not addressed. The prototype is shown in Fig. 43 below. It was developed prior to the commencement of this work on the measuring instrument.

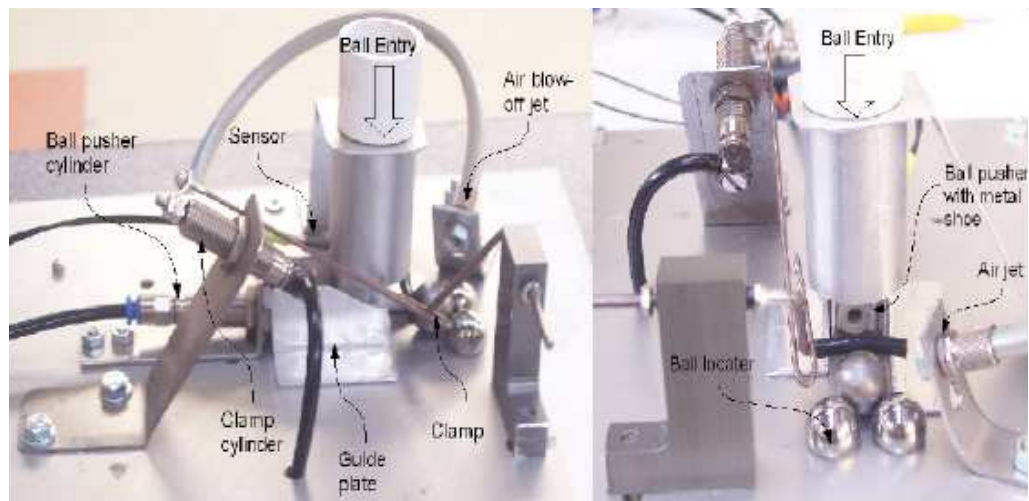


Fig. 43 Previous prototype clamp mechanism [51]

Despite the earlier decision not to implement the active clamping prototype on the working instrument it was felt that sample clamping could provide an additional balancing force to aid in the achievement of the sub-micron precision measurements along with the dual location sphere arrangement discussed above.

5.3. Clamping and sample location

During normal operation samples are held against two locating semi-spheres as outlined above. Fig. 44 below shows this in side elevation with a 13.5mm sample. Samples are held by gravity but are otherwise free to move. An analysis of the forces involved in the sample location was performed in order to study the stability of the system. The slope of the supporting surface is 6° , and (in the case of a 13.5mm sample ball (with a measured weight of 0.011kg) lying against the embedded 15mm diameter locating balls sitting approximately 5.5mm below the surface) the centre line of the locating and sample ball makes an angle of 60° to the vertical.

5.3.1. Locating forces analysis

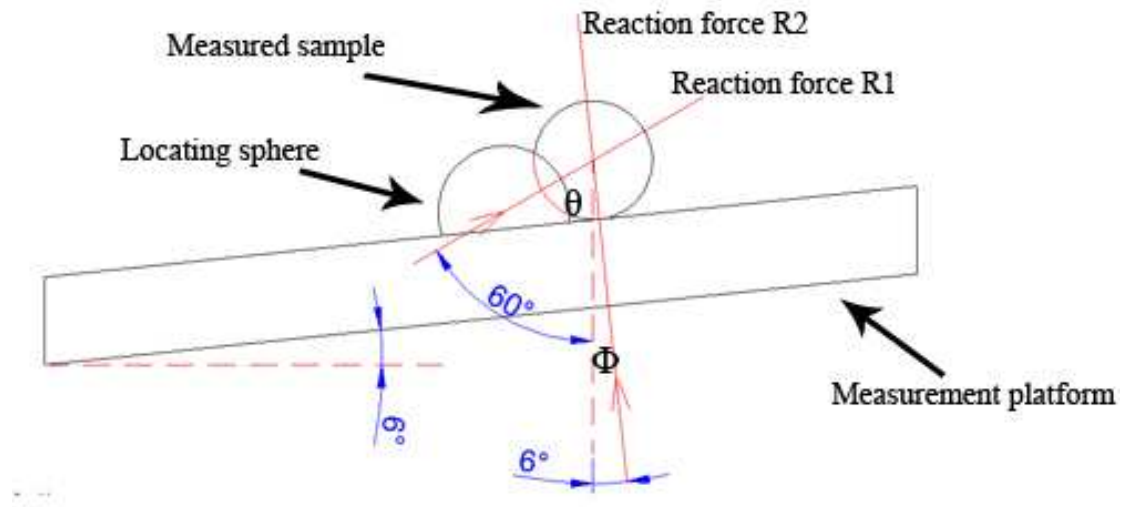


Fig. 44: Diagram illustrating 13.5mm sample and locating sphere relationship

The forces involved can be calculated as follows. First, consider the free body diagram about the sample, illustrated in Fig. 45 below. Note that the reactions from the embedded location spheres are not in the same plane as W and R_2 . In this treatment R_1 is considered as the resultant of the reaction forces acting in the plane common to W and R_2 ; and R_2 is the reaction force from the supporting base. θ is the angle between R_1 and W , 60° , and Φ is the angle between W and R_2 , 6° .

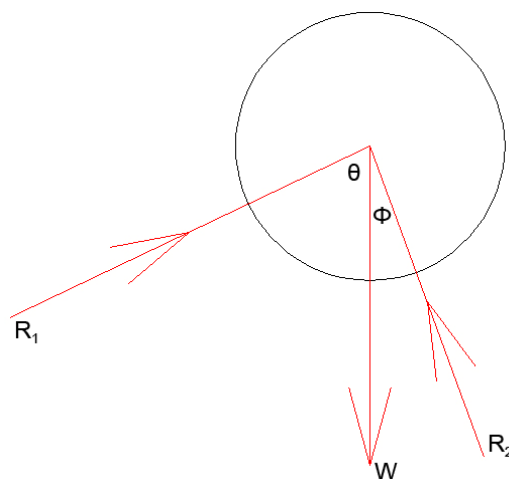


Fig. 45: Free body diagram about sample

The forces can then be resolved into their S-U components as shown in Fig. 46 below where the S and U axes are defined as parallel and perpendicular to the measuring platform respectively.

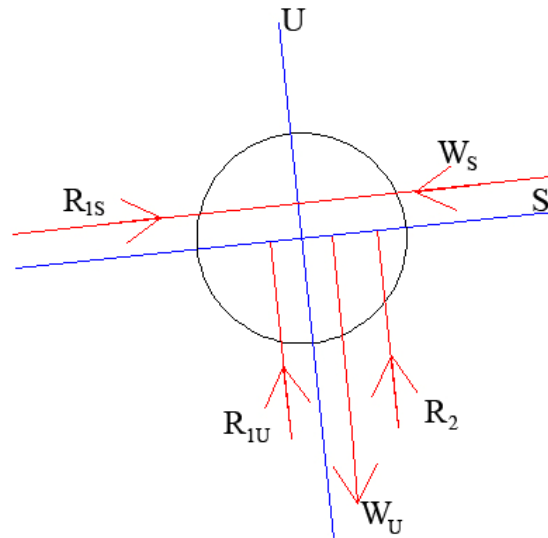


Fig. 46: Resolved forces about sample

For equilibrium:

$$R_{1S} = W_S \quad \text{Eq. 1}$$

$$R_2 = W_U - R_{1U} \quad \text{Eq. 2}$$

Also:

$$W = 0.011 * 9.81 = 0.1079 N$$

$$\cos 6 = W_U / W \Rightarrow W_U = 0.1079 * \cos 6 = 0.107 N$$

$$\sin 6 = W_S / W \Rightarrow W_S = 0.1079 \sin 6 = 0.011 N$$

From Eq. 1 $R_{1S} = 0.011 N$

And: $\cos 24 = R_{1S} / R_1 \Rightarrow R_1 = 0.011 / \cos 24 = 0.012 N$

$$\sin 24 = R_{1U} / R_1 \Rightarrow R_{1U} = 0.012 * \sin 24 = 0.005 N$$

From Eq. 2: $R_2 = 0.107 - 0.005 = 0.102 N$

From this we can see that the net locating forces are as follows:

- 0.102N perpendicular to the supporting surface

- 0.012N between the embedded locating spheres and the sample sphere, and acting at an angle of 60° to the vertical.

The largest ball nominal diameter is 13.5mm. However to view the effect of this passive ‘clamping’ across the complete range of diameters the smallest nominal diameter ball, 10.5mm, will now be considered.

Again the slope of the supporting surface is 6°, as stated, and (in this case of a 10.5mm sample ball (with a measured mass of 0.005kg) lying against the embedded 15mm diameter locating balls sitting approximately 5.5mm below the surface) the centre line of the locating and sample ball makes an angle of 63° to the vertical (Fig. 47).

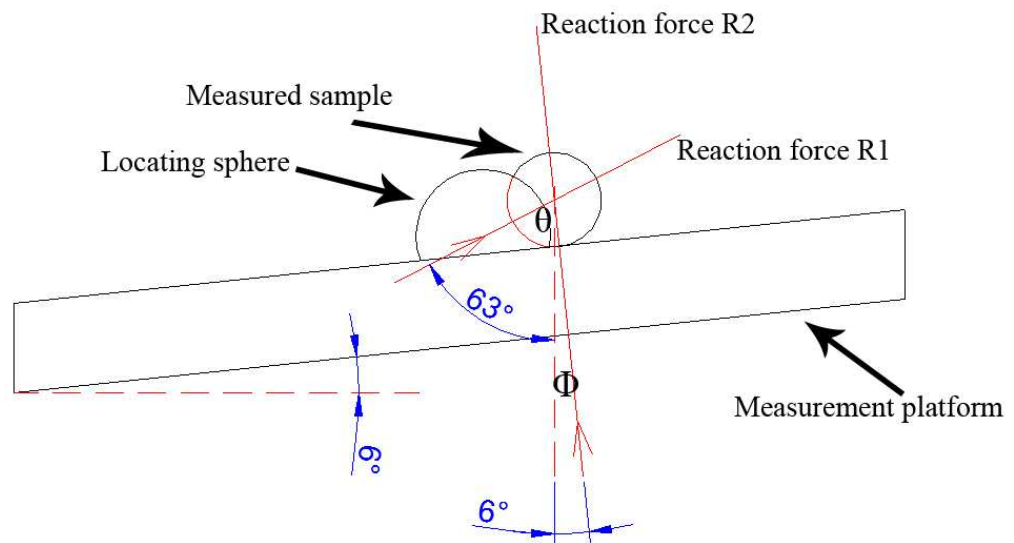


Fig. 47 Diagram illustrating 10.5mm sample and locating sphere relationship

For equilibrium:

$$R1_s = W_s \quad \text{Eq. 1}$$

$$R_2 = W_u - R_{1u} \quad \text{Eq. 2}$$

Also:

$$W = 0.005 * 9.81 = 0.04905 N$$

$$\text{Cos}6 = W_u / W \Rightarrow W_u = 0.04905 * \text{Cos}6 = 0.4878 N$$

$$\sin 6 = W_s / W \Rightarrow W_s = 0.04905 \sin 6 = 0.00513 N$$

From Eq. 1: $R_{1s} = 0.00513 N$

And: $\cos 21 = R_{1s} / R_1 \Rightarrow R_1 = 0.00513 / \cos 21 = 0.055 N$

$$\sin 21 = W_s / W \Rightarrow W_s = 0.00513 / \sin 21 = 0.0143 N$$

From Eq. 2: $R_2 = 0.055 - 0.0143 = 0.041 N$

From this it can be seen that the net locating forces are as follows:

- 0.041N perpendicular to the supporting surface
- 0.055N between the embedded locating spheres and the sample sphere, and acting at an angle of 63° to the vertical.

From this analysis the following can be concluded:

1. With passive ‘clamping’, there would be very little difference between the location stability across the range of balls.
2. The passive ‘clamping’ forces arising from gravity with the 6° inclined supporting surface are very small, especially the lateral force restraining the sample balls against the embedded location spheres (equivalent to a little more than a 1 gram mass on an 11 gram ball).
3. It can be observed that increasing the tilt angle of the stage (from 6° to say 12°) would increase the holding force against the embedded spheres, but the size of the force would still be small in relation to possible disturbing forces.
4. A more positive ‘active’ clamping force could be considered to augment this passive force.

Before considering an imposed ‘active’ clamping force system, it will be informative to review the additional force on the sample ball at the point of measurement when the top of the ball is contacted by the piezo electric driven measurement platen.

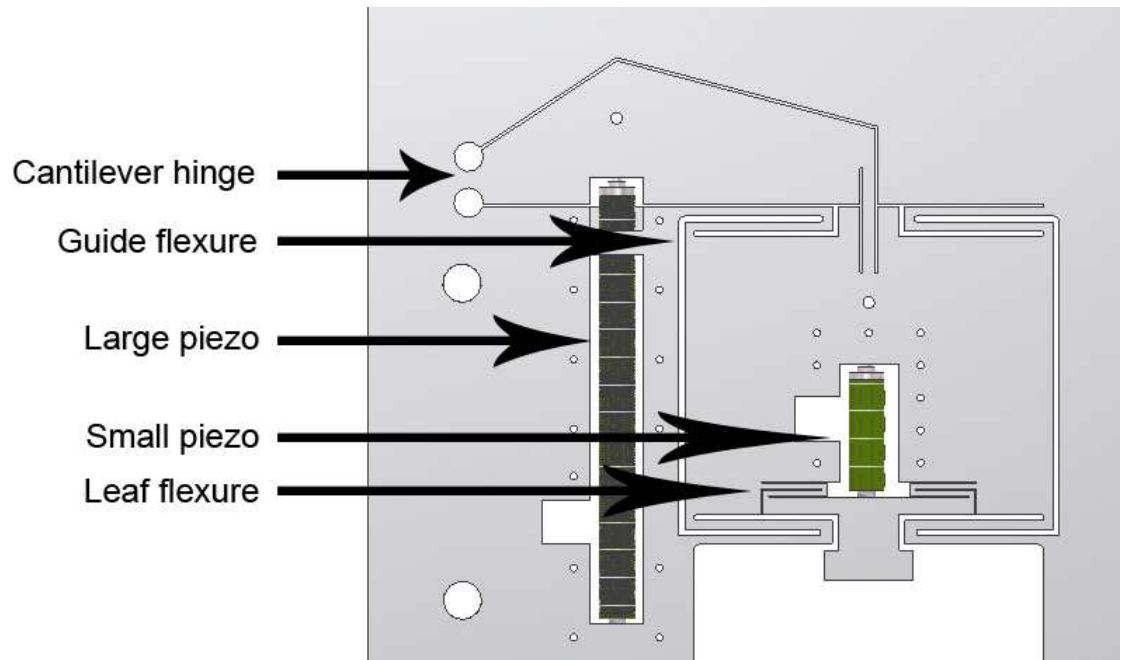


Fig. 48: Illustration showing flexures and piezos

The force applied to the sample at the moment of contact, due to stiffness of the flexure, will be imposed on the passive gravitational force as described above. This can be calculated as follows. First consider the stiffness of the flexures. The stiffness of the leaf flexures ($1.44\text{N}/\mu\text{m}$ [51]) and small piezo ($57\text{N}/\mu\text{m}$ [50]) must be considered (see Fig. 48 above for naming conventions). These are in series and so can be added together using the formula below to give theoretical stiffness, K_{C1} .

$$\begin{aligned} \frac{1}{K_c} &= \frac{1}{K_1} + \frac{1}{K_2} \\ &= \frac{1}{1.44} + \frac{1}{57} \\ K_{C1} &= 1.4045\text{N} / \mu\text{m} \end{aligned} \tag{Eq. 3}$$

The combined stiffness of the cantilever and guide flexure is $5.524861\text{N}/\mu\text{m}$ [51]. Using Eq. 3 again the stiffness of the cantilever, guide flexure, and leaf-flexure/small piezo combination can be added together to give:

$$\begin{aligned} \frac{1}{K_{C2}} &= \frac{1}{5.524861} + \frac{1}{1.4045} \\ K_{C2} &= 1.1198\text{N} / \mu\text{m} \end{aligned}$$

Finally the large piezo, which has a linear stiffness of $10\text{N}/\mu\text{m}$ [50], must be considered. The central axis of the large piezo is 50mm from the cantilever hinge and

the cantilever has an overall length of 145.12mm. This gives a ratio of $50/145.12 = 0.3445$. When applied to the stiffness of the large piezo, $3.445\text{N}/\mu\text{m}$ is the effective stiffness seen in the axis of movement of the measuring platen.

Combining this with K_{C2} above gives the overall stiffness, K_{C3}

$$\frac{1}{K_{C3}} = \frac{1}{1.12} - \frac{1}{3.445} \quad (\text{Minus because large piezo is in opposition to other stiffness})$$

$$K_{C3} = 1.659\text{N} / \mu\text{m}$$

By considering the movement of the large piezo it is possible to determine the maximum displacement of the various flexures during “touch”. In Section 3.8.1 it was shown that the 0.015V steps applied produced a vertical displacement at the measuring platen of $0.252\mu\text{m}$. The piezo cannot stop part way through a step and therefore when an object is encountered the maximum possible displacement beyond the point of touch is one full step, or $0.252\mu\text{m}$ (assuming contact is made at the very beginning of a step). This is then the maximum displacement experienced by the flexure system. As shown above the stiffness of the system is $1.659\text{N}/\mu\text{m}$. The maximum force of contact is then $1.659\text{N}/\mu\text{m} * 0.252\mu\text{m} = 0.418\text{N}$.

The maximum force of contact assumes the platform supporting the sample is infinitely rigid and does not absorb any displacement itself. This is not the reality. However calculating the movement in the platform support structure is not practical due to the high number of unknown variables in the structure.

There is a risk of the sample moving around during the measuring sequence due to this applied measurement force. This movement was observed previously when measuring using an oscillating piezo (in an attempt to improve the detection of the point of contact using a change in resonance frequency at the moment of contact [4]). In this case the touch-release-touch sequence of the changing step size control methodology was believed to cause the sample movement. This was thought to arise due to a slight misalignment between the sample seating surface and the touching surface or perhaps some element of stickiness at the touch point.

To counteract this phenomenon, it was decided to add an independent clamping system which would prevent inter-touch movement of the sample.

5.3.2. Active clamping design

Because of the extremely limited access to the measurement location for provision of an imposed load on the balls, as well as the limited area on the stage for mounting of any fixtures and fittings to implement an active clamping mechanism, a rough prototype clamp was created as a first step.

Factors requiring consideration at this stage included:

1. Hinge location and mounting:
 - a. The mechanism could rise and fall with the sample platform.
 - b. Alternatively the mechanism could be fixed to the stage structure if a common clamping height would suffice for the range of sample sizes
2. Clamp mechanism design: the ‘clamping head’ had to fit inside a tight working area close to the measurement point when lowered but also had to be removed from the sample entry path when retracted so as not to interfere with sample delivery.
3. System weight and load arrangement: the appropriate clamping load would be difficult to establish theoretically so it would be established experimentally. A method of easily varying the external mass on the clamp would therefore be necessary.

Fig. 49 below shows the concept clamp as constructed. A copper welding element was used to minimise the weight of the assembly. An arm was created on each side of the cantilever. It was seen that a single pneumatic actuator could be used to raise/lower the clamp head which would leave the opposite arm free to accommodate weights to adjust the load applied to the sample. As can be seen the prototype hinges were taped to the front of the face of the block of wood which was used to represent the face of the piezo driven stage. Being relatively satisfied with this prototype, the next step was to examine the design for implementation on the working equipment.



(a) Clamp position

(b) Insert/remove sample position

Fig. 49: Prototype/Concept clamp mechanism

5.3.3. Design study

The mechanism had to be designed to work with different sized samples and to work within the space constraints created by the measuring station arrangement.

A series of drawings were created to assist in the design of the clamping mechanism. One of the key metrics is the vertical distance above the centre of the sample where the clamp would be positioned. Option 1(b) above was seen as the most feasible solution as the system would have to work with various sized samples. A compromise clamping height would have to be identified to suit the full range of ball sizes. With this in mind the upper and lower heights for the clamp would have to be above the diameter of the largest sample to be measured (13.494mm) and below the tip of the smallest sample to be measured (10.5mm) with the actual working height somewhere in between.

The clamp was centred between upper and lower limits which were defined as $\frac{1}{4}$ the distance between the tip of the largest sample and its diameter below the tip of the sphere (upper limit) and $\frac{1}{4}$ the distance between the diameter and tip of the smallest sample above its diameter (lower limit) respectively. This creates a working range of 3.75mm as shown in Fig. 50 below.

Due to the moveable nature of the platform on which the samples rest the vertical position of the “clamp head” must be related to the base of the measuring platen. A vertical height of 3.2mm below the measuring platen (at contact) was chosen as the mid-point between upper and lower limits. In Fig. 50 the blue sphere represents a 10.5mm sample while the red sphere represents a 13.494mm sample.

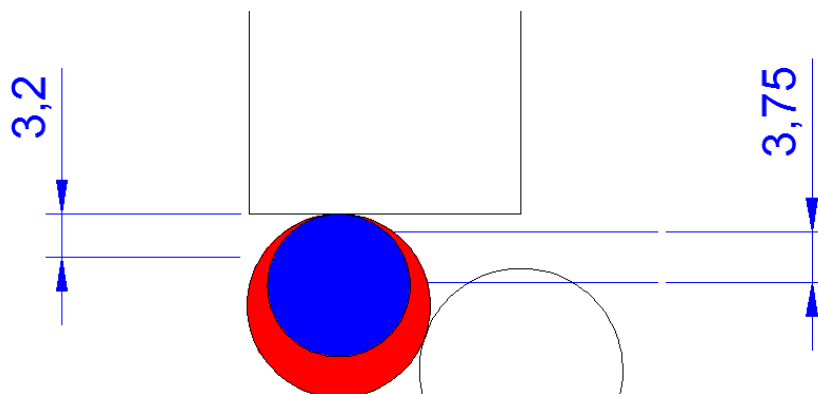


Fig. 50: Identification of clamp working height

The next step in the design phase was to select the hinge heights such that when raised there was sufficient clearance beneath the clamp to allow insertion/removal of samples. The lower tip of the clamp would need to rise at least 13.55mm above the measuring stage to allow for the insertion of the largest intended sample (note, although the largest sample ball has a nominal diameter of 13.494mm the large calibration ball for this size measures 13.55mm). This was modelled in AutoCAD and is illustrated in Fig. 51 below. A hinge height of 104mm perpendicular to the radius of the sample at contact height was found to be satisfactory when using a 22mm stroke pneumatic cylinder located 60mm from the hinge on the horizontal axis.

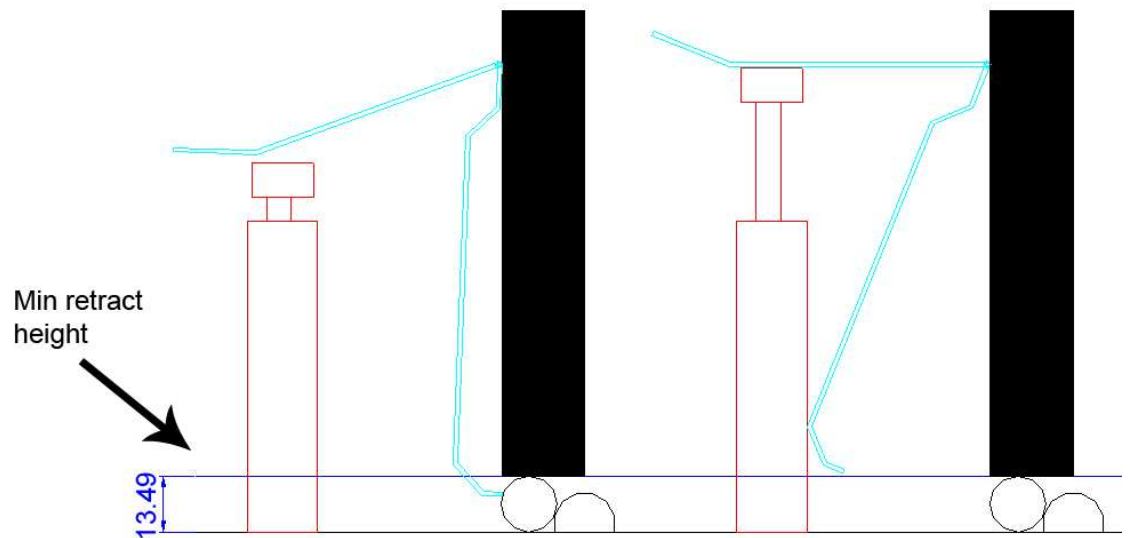


Fig. 51: Side elevation showing clamp position (left) and sample handling position (right)

Finally the issue of the force to be applied by the load was considered. Because the clamping force needed was unknown it would be established experimentally as suggested earlier. This would be achieved by loading the mechanism manually in a series of tests. The loads could be mounted on the outer arm of the wire mechanism as shown in Fig. 52 below.

If a nominal 10N load is considered the force applied to a 13.5mm diameter sample can be calculated by taking moments about P (Fig. 52):

$$\begin{aligned}
 d_1 * W &= d_2 * L \\
 L &= \frac{d_1 * W}{d_2} \\
 &= \frac{0.0682 * 10}{0.09906} = 6.885N
 \end{aligned}$$

where:

d_1 = perpendicular distance from load to pivot. (Fig. 52)

W = load. (Fig. 52)

d_2 = perpendicular distance from applied load to pivot point. (Fig. 52)

L = applied load.

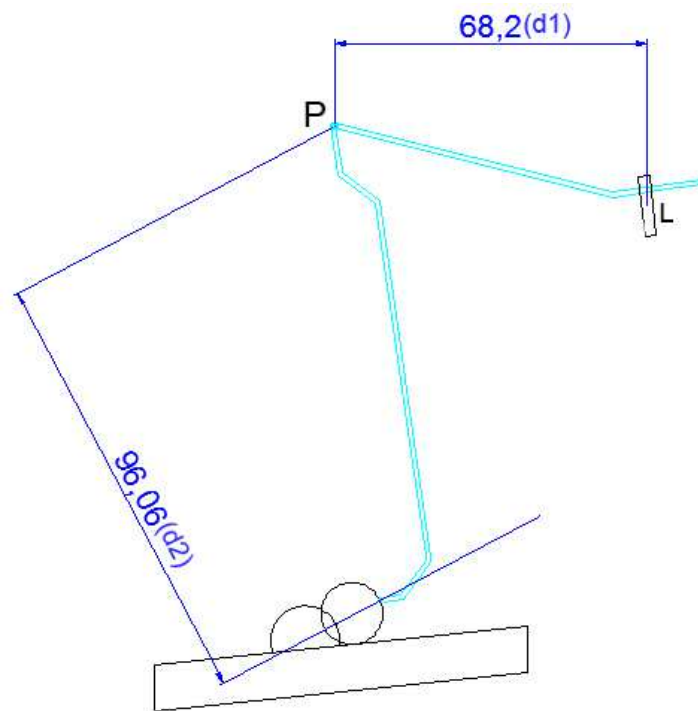


Fig. 52: Clamped 13.5mm sample showing perpendicular distances (mm) between pivot and forces

The reaction forces R_1 and R_2 were re-examined to determine the effect of this 'active' load. Here it is assumed that the loading source always acts through the centre of the sample. This will be true for an exactly cylindrical clamping end affecter.

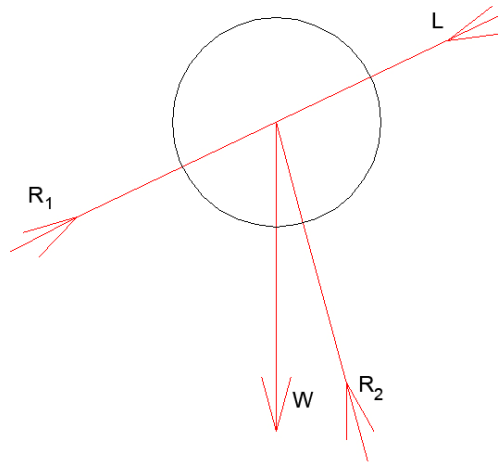


Fig. 53: Freebody diagram about 13.5mm sample with the clamping force L

The forces shown in Fig. 53 above can be resolved to component forces as shown in Fig. 54 below.

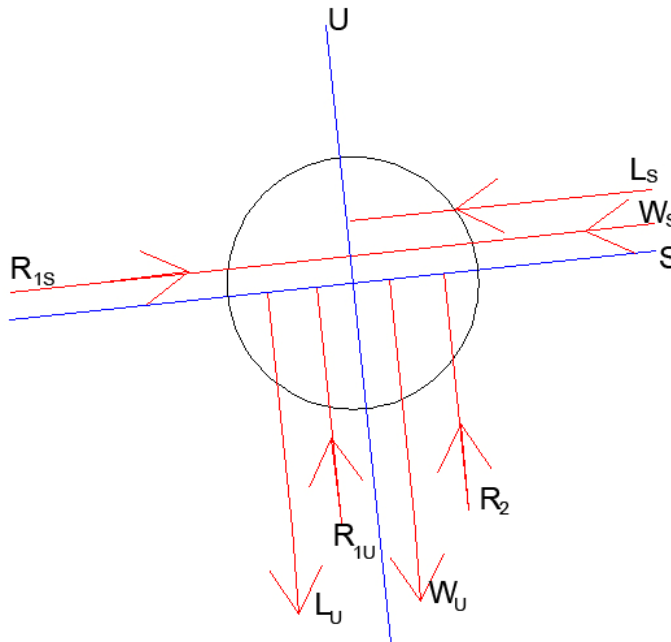


Fig. 54: Component forces

As before the slope of the supporting surface is 6° , and the centre line (and related reaction force) of the locating and sample ball makes an angle of 60° to the vertical. The external load L acts at an angle of 66° to the horizontal (height of contact = 2.97mm above the centre of the sample).

For equilibrium:

$$R_{1S} = W_S + L_S \quad \text{Eq. 4}$$

$$R_2 = W_U + L_U - R_{1U} \quad \text{Eq. 5}$$

Also:

$$W = 0.011 * 9.81 = 0.10791N$$

$$\text{Cos}6 = W_U / W \Rightarrow W_U = 0.1079 * \text{Cos}6 = 0.107N$$

$$\text{Sin}6 = W_S / W \Rightarrow W_S = 0.1079 * \text{Sin}6 = 0.011N$$

$$\text{Cos}66 = L_U / L \Rightarrow L_U = 6.885 * \text{Cos}66 = 2.899N$$

$$\text{Sin}66 = L_S / L \Rightarrow L_S = 6.885 * \text{Sin}66 = 6.29N$$

From Eq. 4: $R_{1S} = 0.011 + 6.29 = 6.301N$

And: $\text{Cos}24 = R_{1S} / R_1 \Rightarrow R_1 = 6.301 / \text{Cos}24 = 6.897N$

$$\text{Sin}24 = R_{1U} / R_1 \Rightarrow R_1 = 6.301 / \text{Sin}24 = 2.563N$$

From Eq. 5: $R_2 = 0.107 + 2.899 - 2.563 = 0.443N$

From this it can be seen that the net ‘clamping forces’ are as follows:

- 0.443N perpendicular to the supporting structure
- 6.899N between the embedded locating spheres and the sample sphere, and acting at an angle of 60° to the vertical

On this analysis it can therefore be concluded that: The active clamping using a 10N external cantilevered load in combination with the passive ‘clamping’, results in a net clamping effect perpendicular to the 6° inclined supporting surface of approximately 0.5N and a force of approximately 7N restraining the sample balls against the embedded location spheres. These restraining ‘clamping’ forces are significant in relation to the ball weight of approximately 0.1N and the estimated piezo-flexure touch force of approximately 0.4N.

As demonstrated in section 5.3.1 these forces differ slightly for a differently sized sample. On the smaller balls the imposed load will be the same but will act closer to the top of the ball. The reaction perpendicular to the supporting surface will therefore be increased and the transverse reaction will be lower than calculated above. However

they will both be still significant in relation to the ball weight and the piezo-flexure touch force.

5.3.4. Active clamp implementation

Once the designs were complete the solution was implemented on the main stage. The first problem to tackle here was the mounting and hinging of the swinging arm section. The original intention had been to hang two hinges from the top of the stage; however sourcing suitable hinges proved difficult. After some deliberation it was decided to use two lengths of M4 threaded bar to clamp two small pieces of aluminium to the stage. Through these pieces of aluminium a small hole was drilled, to act as a pivot point for the swinging arm. This is illustrated in Fig. 55 below.

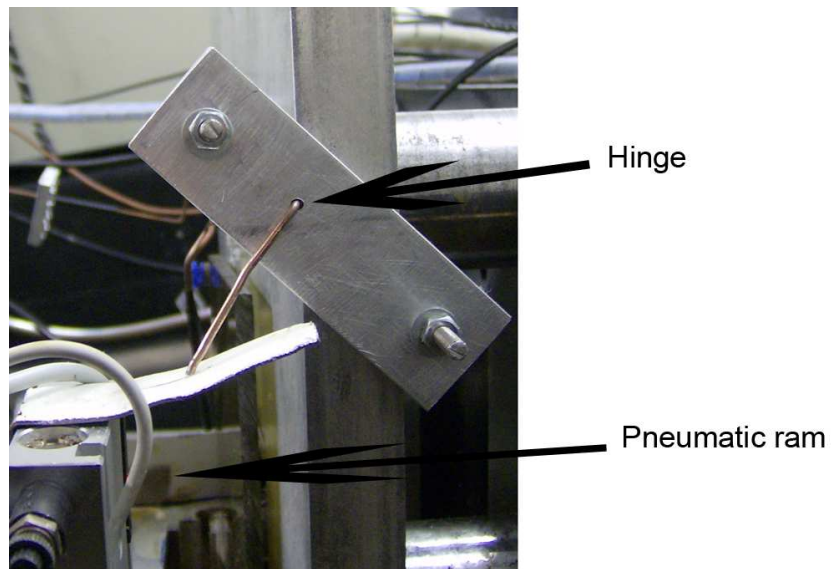


Fig. 55: Side view showing hinge and pneumatic ram

The swinging arm was constructed from a copper welding rod which could be easily shaped by hand as required. The shape can be seen in Fig. 56 and Fig. 57 below.

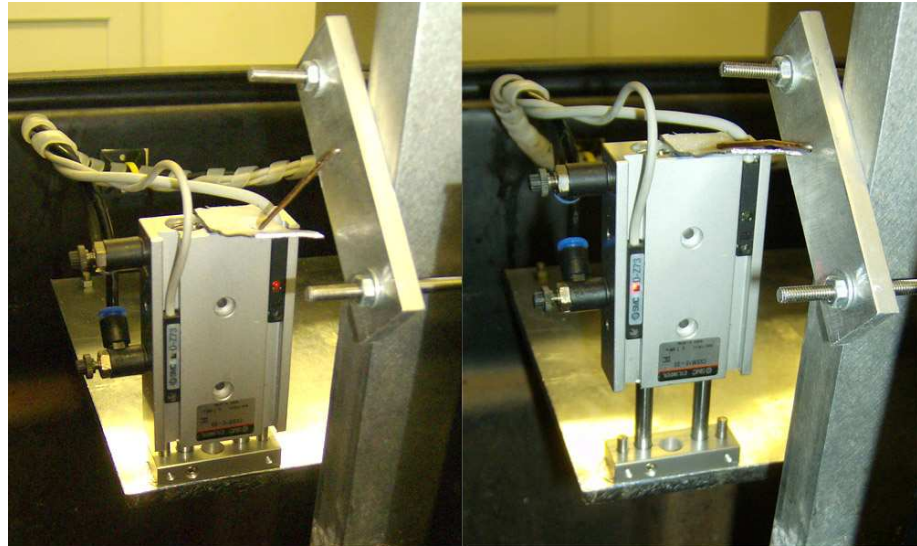


Fig. 56: Clamp in insert/remove position



Fig. 57: Clamp in home position with sample ball clamped

As part of the control of the clamping system it was important for the PLC to know which position it was in. Two magnetic reed switches were installed on the pneumatic ram and their outputs returned to the PLC. The program code running in the PLC was altered to control the up/down motion of the ram in addition to the sample insertion code already in place.



(a) Ram retracted and clamp in clamp position

(b) Ram extended and clamp in insert/remove position

Fig. 58: Pneumatic ram in both positions showing position sensors

5.3.5. Testing

The mechanism was tested with various weights in place of W in Fig. 52 above. It was found that too great a weight would cause the clamp to rise over the sample once inserted. Experimentation revealed a weight of approximately 10N to be suitable for clamping the sample without causing the clamp to rise over the sample.

Detailed test results showing the affect of the clamping mechanism on the measurement process capability are discussed in Chapter 6.

5.4. Sample insertion mechanism

5.4.1. First implementation & issues with

The original ball queuing and feeding mechanism, as developed by D. Madigan [51], is illustrated in Fig. 59 below. In this system all seven samples were delivered to the holding pipe at the same time and then fed into the measuring area individually by the pneumatic cylinder.

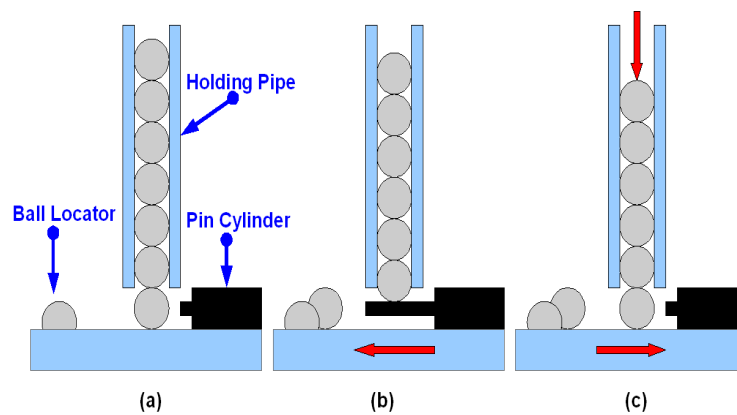


Fig. 59: Original vertical queue diagram [51]

It was found that it was possible for more than one sample to be inserted at one time. An attempt to solve this was made by adding a second cylinder as shown in Fig. 60 below as cylinder 2. In this case the second cylinder would extend to prevent a second ball rolling forward after the first had been pushed out.

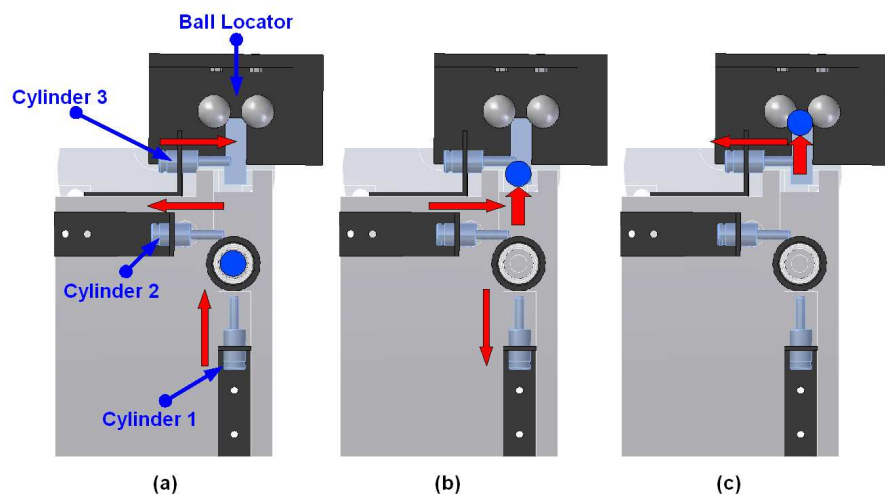


Fig. 60: Original queuing system overview showing working sequence [51]

In practice this did not always work as a second sample was often inserted at the same time as the first sample rather than immediately afterwards. A typical example of this “multiple sample insertion” is shown in Fig. 61 below.

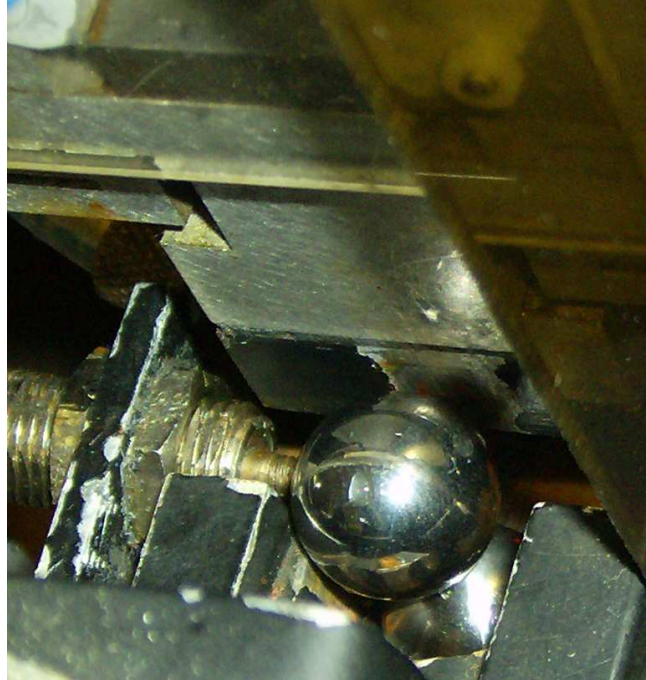


Fig. 61: Attempted multiple sample insertion

As part of the planned fluid immersion of samples (during the measurement process) it was also desirable to maintain fluid flow across the samples while queued for measurement (after removal from the temperature normalisation tank but before the samples are measured). While this is possible with the original implementation there were concerns about fluid flow in close proximity to the measuring platens causing vibrations/ripples and affecting the result. With this in mind it was also considered important to move the queuing mechanism further away from the measuring platen and stage.

5.4.2. Design study

It became apparent that the only way to completely solve the problem of the mechanism inserting more than one sample at a time was to store each sample separately prior to measurement.

Approaches to the implementation can be classified under headings of: rotary, vertical, or horizontal.

5.4.2.1. Rotary

The concept of a rotary indexer was dismissed previously as “*too elaborate*” and “*unreliable*” due to poor construction of a prototype [51]. However; it still warranted further exploration when considering an alternative to the existing ball queuing system.

In the system illustrated in Fig. 62 below the samples would be delivered to the indexer at one side and released to the measuring station after rotating through 180 degrees. The indexer position would be counted using a hole in the indexer to allow a thru-beam optic sensor to function. Knowledge of absolute rotational position would not be required. Instead it is sufficient to know when the indexer has a bay in the eject position.

Upon the arrival of samples at the indexer entrance point; the indexer would load 3 samples before delivering the first to the measuring station. Thereafter it would load and eject one sample per index.

The single biggest stumbling block with this approach is the need to use an electrical motor to drive it. As the intention is to have the samples immersed in fluid for the maximum possible time the chance of damaging or destroying any electrical motors are quite high; even proximity to high humidity environments can cause the motors to seize, as discussed previously in Chapter 2.6.

While the motor could be mounted remotely and the shaft driven by a belt this would be undesirable as it would add unnecessary complication to the system by requiring tensioning devices and extra programming to ensure that any slippage of the drive belt is compensated for by driving the motor further to ensure proper indexing.

This system would also require more maintenance than either horizontal or vertical systems as shafts and any bearings used would need to be lubricated at regular intervals. This lubricant could easily be washed away by the constant flow of fluid through the system; causing premature oxidation/failure of the parts and contaminating the temperature normalising fluid.

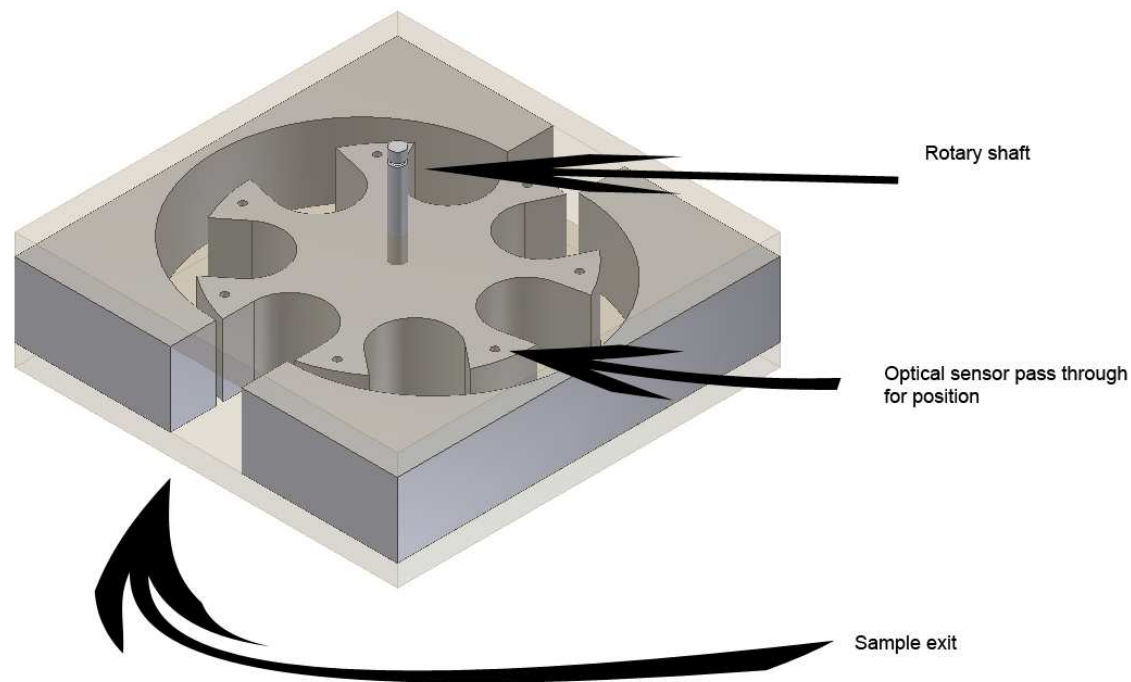


Fig. 62: Render of rotary indexer

5.4.2.2. Vertical

The vertical gravity feed queuing system already in place was reasonably successful when it came to delivering the balls to the measuring area and so an updated version with individual sample storage was designed. In this version the seven samples are still queued vertically but now are separated by sorting pins. This type of separated storage would require a sorting mechanism further back in the system to ensure only a single sample is delivered to each storage area. Otherwise two or more may fall into one area leaving the sorting pins unable to close properly and resulting in the multiple insertion issue of the original system.

Temperature normalisation of the samples using the temperature normalising fluid is also more difficult with this arrangement as it would simply flow past the samples and the flow rate required could be far too high to be sustainable.

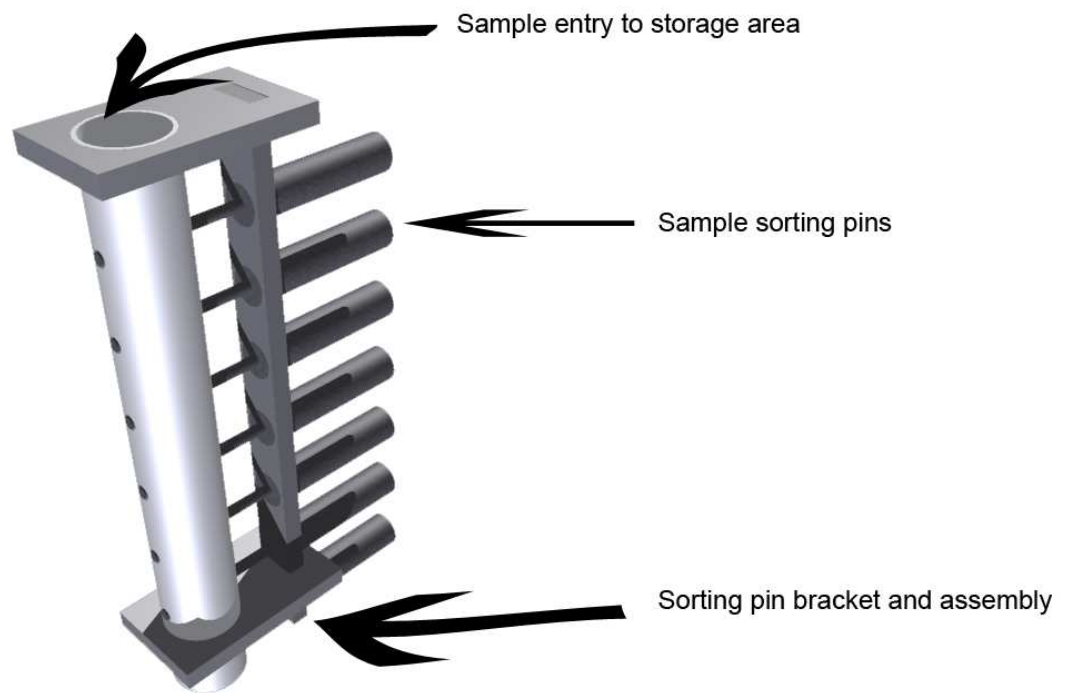


Fig. 63: Render of vertical feeding and storage mechanism

5.4.2.3. Horizontal

With the issues presented by rotary and vertical solution, a horizontal queuing system was envisioned which would use sliding doors to separate individual storage compartments. This is illustrated in Fig. 64 below. As with the vertical queuing system this arrangement would also require a separate mechanism to prevent the full sample set from attempting to feed in at once. This would require at least two more pneumatic cylinders or re-using the existing queuing system to feed the new storage system. This configuration is also the easiest to apply partial fluid immersion of the samples to as an overhead sprinkler system can be installed which can use a sustainable flow rate while keeping the samples covered in a film of temperature normalising fluid. This low flow rate coupled with sufficient distance from the measuring platens also address the ripple/vibration issue in as much as is possible with this particular implementation.

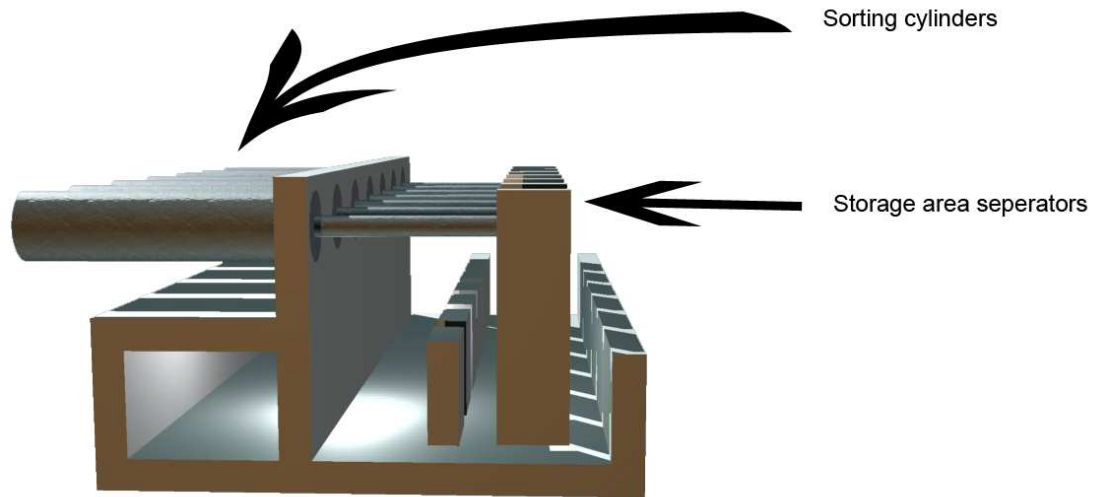


Fig. 64: Render of horizontal storage showing all areas open

5.4.3. Implementation

Based on the design study, the horizontal implementation was chosen because it offered the best compromise of functionality, complexity and reliability.

The system was constructed from Perspex and is illustrated in Fig. 65 below. When installed it is mounted at a slight angle to allow the balls to roll out of the system accelerated by gravity rather than forcing them out with a pneumatic cylinder as the original implementation did. At the time of writing this mechanism had not been installed primarily due to space constraints in the measuring tank and limited PLC output availability. A future project should address the redesign of the space in the measuring tank to accommodate the queuing mechanism. This has not been possible in this project due to time constraints created by the necessity to advance the primary objective of the project (improvement of the measurement capability of the apparatus).

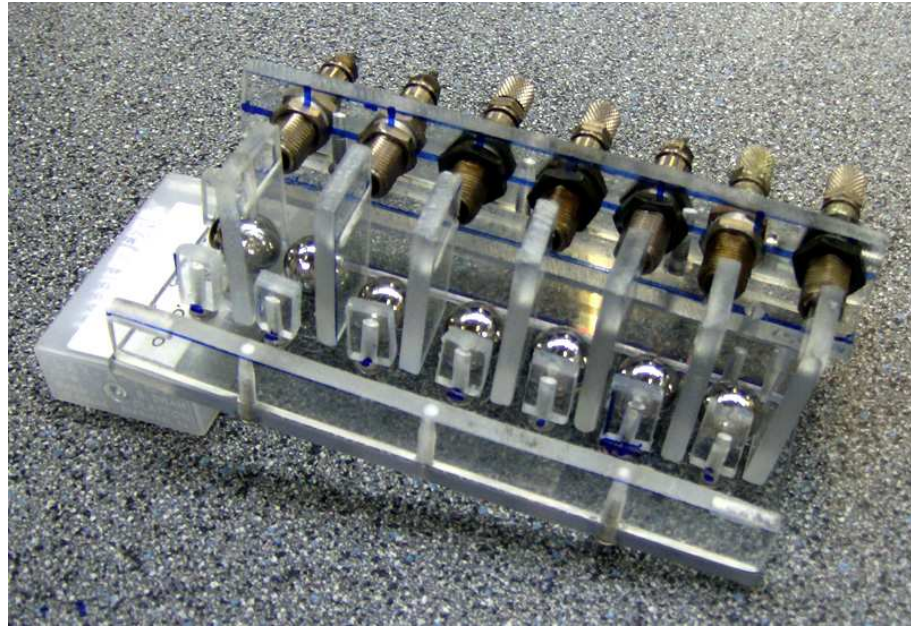


Fig. 65 Horizontal sample insertion mechanism

5.5. Conclusion

A method for actively clamping the full range of balls has been developed. The clamping mechanism has been installed, tested, and found to be reliable.

The effect of this active clamping on the accuracy of measurement is outlined in Chapter 6.

The issue of sample feeding reliability has been examined and a new mechanism constructed. However space and PLC wiring constraints mean that this solution has not been implemented as of time of writing. A suggested solution to the PLC wiring issue is discussed in Section 7.4.6.

6. Progressive measurement improvements

6.1. Introduction

A major facet of this project is the improvement in measurement precision and accuracy of the apparatus.

The first step towards achieving these improvements was the identification of as many sources of error as possible. An examination of sources of error was undertaken and those considered key error sources were actively addressed using a process of experimentation and testing.

A summary of the results are presented in Section 6.4.

6.2. Sources of measurement error

The sources of error (Fig. 66) have been divided into four key areas: electrical, mechanical, environmental, and sample/product errors.

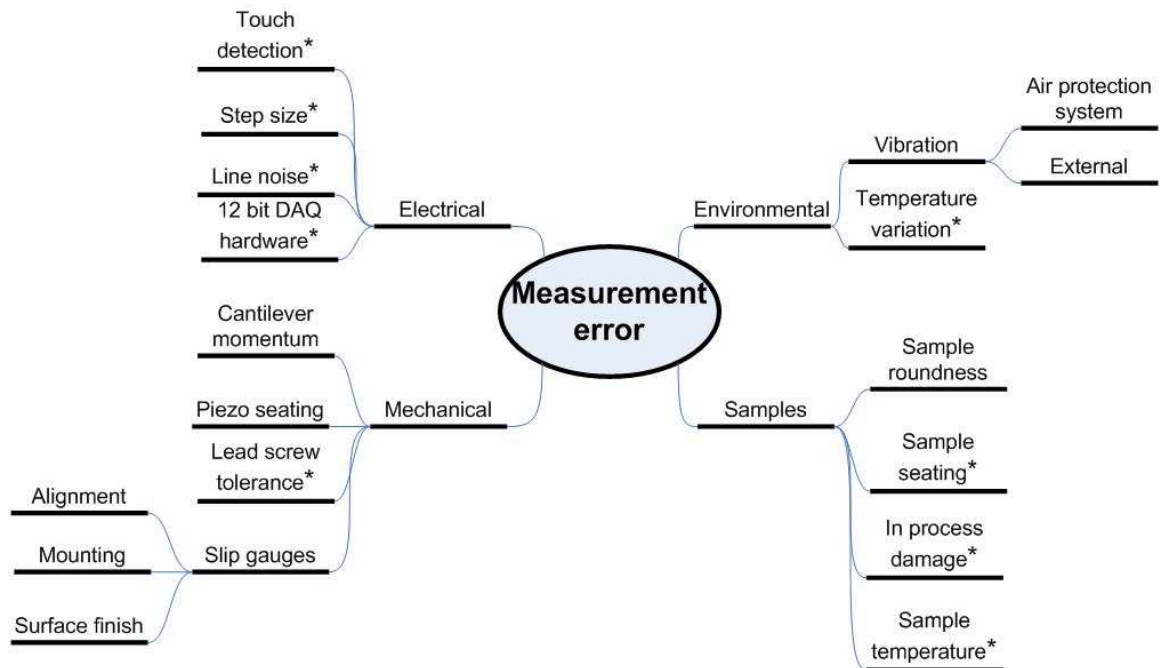


Fig. 66 Perceived causes of measurement error

The sources of error marked (*) above are discussed in more detail in the following section. These error sources were identified because of the perceived likely contribution they would make to the overall error in the system. Due to the limited time

scale of this project it was seen that only a limited number of sources of error could be investigated experimentally.

6.2.1. 12bit DAQ hardware

Ultimate measurement resolution is limited by the data acquisition hardware in use. The 12 bit PCI-6024e (and accompanying BNC-2120 breakout box) from National Instruments are used in this project. The PCI-6024e is a 12bit device which means it can detect 4096 discrete values between 0V and 10V. The smallest observable/controllable increment is then $10/4096 = 2.44\text{mV}$. Taking the 10V range to cover the $167\mu\text{m}$ measurement range then 2.4mV equates to a maximum theoretical measurement precision of $0.04\mu\text{m}$. A measurement precision of $0.01\mu\text{m}$ would be strictly necessary to provide the targeted measurement accuracy of $0.1\mu\text{m}$. However precision of $0.04\mu\text{m}$ is probably acceptable (readings would be to $0.1\mu\text{m} \pm 0.04\mu\text{m}$). A 16bit DAQ device would be capable of detecting 65536 discrete values across the 10V input range, or every 0.15mV . This would theoretically enable the hardware and control program to see 2.5nm . However the piezo actuator has a step response of 2mV [50] and so the smallest possible step observable is 33.4nm (at the end of the cantilever). So while moving to a 16 bit platform would see an improvement in measurement precision the cost of such a hardware change would far outweigh the benefits.

6.2.2. Touch detection and step sizing

One of the uncertainties associated with the measurement strategies presented in this thesis is where exactly in a ‘step’ (i.e. the distance traversed when the control program sends a move instruction to the piezo controller) the measuring platen makes contact with the sample. As the actuator cannot make a partial step it is very difficult to establish the exact point during a given step at which contact is made with the sample. The signal from the strain gauge incorporated into the ‘small’ piezo is used to detect ‘touch’. ‘Touch’ is said to have occurred when the strain (reduction in length due to compressive forces) experienced by the small piezo crosses a predetermined threshold. When ‘touch’ occurs the voltage from the ‘large’ (driving) piezo strain gauge is captured and processed. Touch can occur at any point during a step of the large piezo. The control program is setup to step the piezo in 0.015V increments. This translates to 252nm vertical displacement of the measuring platen for each increment and means that contact can occur anywhere inside a 252nm window.

Errors can be introduced at this point if there is any lag in the system, either on the hardware or software side. As more subroutines are added to a LabVIEW program it is able to devote fewer resources to each task. In a large control program there can be a considerable slow down in the acquisition and processing of data from inputs while the program is completing other tasks (subroutines). As the number of tasks (subroutines) performed by the control program increases, so too does the likelihood of slow down and associated error occurring. One such error which can arise from this lag is the possibility of the driving piezo continuing to extend beyond the initial touch and further compressing the small piezo. The effect this may or may not have on the results is unknown and suggestions to improve this are dealt with in section 7.4.7.

There is also a question as to how tight the touch threshold (i.e. what level of strain is interpreted as contact between measuring platen and sample) on the data from the ‘small’ piezo strain gauge should be to have a minimal rise time. Fig. 67 below illustrates the time taken from initial touch to ‘detected’ touch. The rise time is from the visible increase in strain (on the graph) to the point where the voltage crosses the detection threshold. The overshoot caused by the inability of the large (driving) piezo to make partial steps can be seen as the portion of the strain gauge signal which is below the detection threshold (red line).

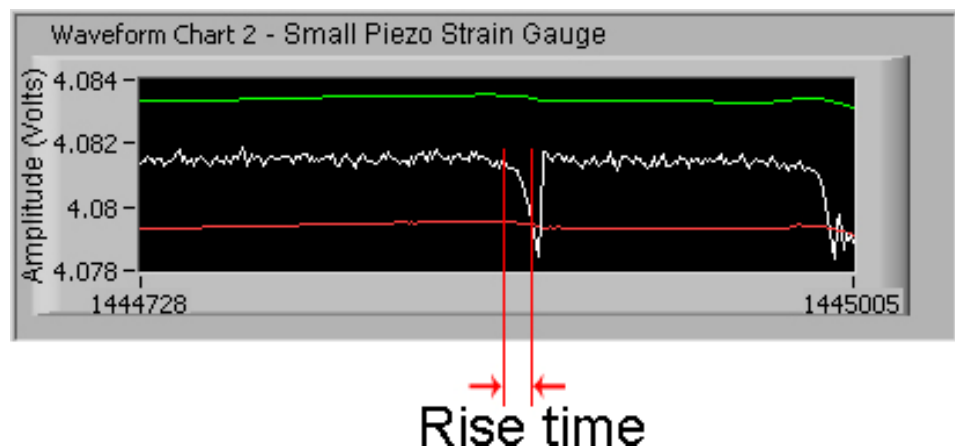


Fig. 67 Rise time during a single touch measurement

To reduce the rise time/overshoot observed in Fig. 67 two approaches must be taken. The first is to narrow the touch detection thresholds in the monitoring program to reduce rise time. This could lead to false positives due to vibration from external sources or even line noise in extreme cases. A system of trial and error has identified suitable threshold levels. The second approach is the implementation of the multiple touch detection discussed in Section 3.8.1 which while not reducing initial overshoot

does reduce the effect of overshoot by detecting the sample multiple times while decreasing step size and therefore reducing observed overshoot. Again trial and error was used to establish suitable thresholds for detection.

6.2.3. Line Noise

The strain gauge used to measure position is an integrated component of the large/moving piezo. The output from this strain gauge covers a range from 0-10V which must represent the 167 μ m effective working distance

The existing control box was built to limit as much as possible the effects of electrical interference on the control circuitry[51]. These measures included:

- Cable lengths minimised.
- Each signal outgoing and return (positive and negative) lines are run together.
- All cables are screened and the screen is grounded.
- There are steel dividing walls within the cabinet between both piezo drivers and the power supply.
- All the equipment is mounted on a grounded EMC (Electromagnetic Compatibility) compliant back plate.
- Cables from different cable groups are physically separated. Cables can be categorised into four groups: I, II, III, IV.

Group I: Very susceptible (analog signals, instrument lines)

Group II: Susceptible (digital signals, sensor cables, 24vDC switching signals, communication signals, e.g. field buses)

Group III: Noise source (control cable for inductive loads, unswitched power cables, contactors)

Group IV: Strong noise sources (output cables from frequency converters, supply cables for welding equipment, switched power cables)

- Noise generating and susceptible cables are crossed at right angles; cross lines from Group I, II and III, IV at right angles
- Cable screens are grounded at control cabinet entry and exit and to the devices

Fig. 68 below shows the level of background noise while the piezo is in its home position with all equipment powered up as normal (power to PC, two PLCs, two

piezo controllers, and various other hardware with ‘normal’ activity levels in the laboratory). This background noise is in the range of $\pm 0.25\text{mV}$ around the average. 1mV represents 16.7nm and so this approx 0.5mV line noise can cause approximately 8nm error in readings. This is acceptable in the context of the measurement precision target of $0.1\mu\text{m}$.

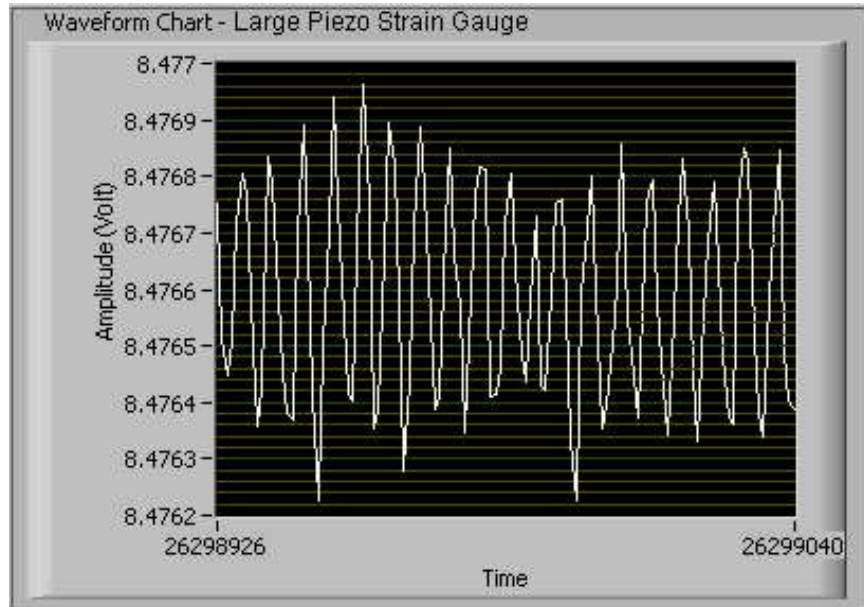


Fig. 68: Large strain gauge line noise

6.2.4. *Measuring platform locking mechanism*

The measuring platform is mounted on a lead screw which allows for height adjustment to accommodate differently sized samples. The lead screw introduces an unknown amount of variation though both a lack of ultimate rigidity (in comparison to a fixed height platform for example) and an unspecified tolerance required to allow the stage move on the lead screw. The forces applied to the sample during the measurement process are transmitted to the platform and could potentially generate movement on the lead screw. However as the ‘touch’ force (0.418N) estimated in the previous chapter is very small in relation to the mass of the measuring platform (approx 150g); this is not expected to be a very significant factor.

Platform ‘settling’ after positioning for a particular ball size could also introduce error. Here the stage is moved up and down on the lead screw during the self calibration routine performed by the hardware prior to each set of measurements. It is also possible that vibrations introduced by other moving parts in the system (fluid circulation pumps and valves, active clamping control cylinder movements, sample

circulation valves) could cause some small degree of movement of the stage on the lead screw. The weight of the platform will be significant in eliminating these latter effects.

The weight of the stage has been one of the setup variables tested in the experimentation to determine the influence this factor has on the measurement results achieved (by comparative performance testing with imposed dead loads on the platform) – see Section 6.3.

6.2.5. *Sample seating*

The issue of sample seating was dealt with in Section 5.3. It is difficult to say with certainty that all seating related errors have been eliminated. However the active clamping ensures a tightly held sample. Any micro or macro dust or particles around the seating area or on the samples will of course affect the seating and lead to measurement errors. One of the advantages of under fluid measurement is the continuous washing of these areas. It demands comprehensive filtering of course to ensure an absolute minimum of particles suspended in the temperature normalisation fluid.

Despite the advancements made in Chapter 5 poor surface finish of the measurement platens could adversely affect measurements taken from the stage by causing the samples to sit in/on different peaks/troughs on the surface. This issue arises because the apparatus was developed to measure samples from production where the unfinished samples are likely to be differently sized or not perfectly round and so each different size will have a slightly different seating position relative to the embedded spheres used to locate the sample. Fig. 69 below shows an exaggerated example of this different positioning. In the diagram the red sample has a diameter of 11mm while the blue sample has a diameter of 13.5mm. It can be clearly seen that the centre point of each sample sits in a different position. The same would be true of samples that are only very slightly differently sized. The effect would simply be less pronounced.

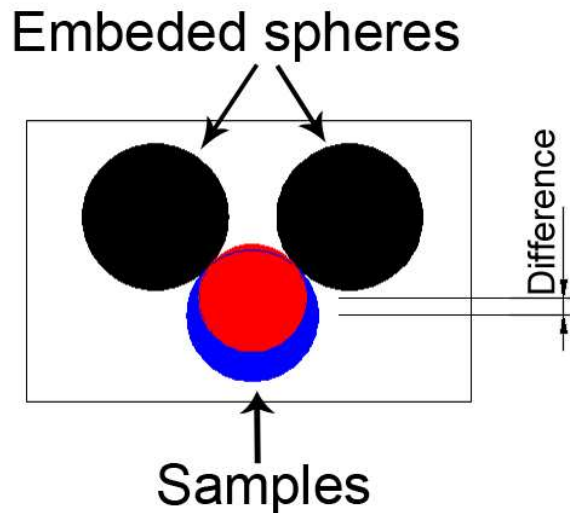


Fig. 69 Plan view of measuring platform showing location of different sized samples

In this situation it is possible that two slightly differently sized samples could be seated at a different height relative to each other on the locating platform due to irregular peaks and troughs and be touched by a corresponding irregular peak or trough on the surface of the measuring platen as illustrated in Fig. 70 below.

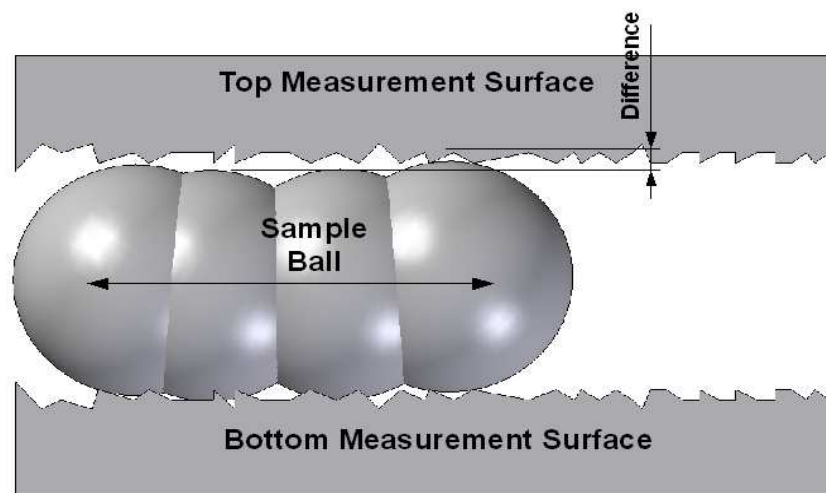


Fig. 70 Surface roughness illustration [51]

Machining the surfaces of both the measuring platen and the sample holding base to a high quality surface finish is an expensive and time consuming option. It would also be difficult to ensure both surfaces were perfectly parallel to each other as the base was to be attached to a lead screw to give an adjustable height.

To reduce costs and minimise production time two precision machined slip gauges were purchased and installed; one in the moving platen and one in the stage on which the sample rests, as illustrated in Fig. 71 below. These gauge blocks were

bonded in place using an adhesive. Questions arose as to the possible movement of these gauge blocks as the measurement force is applied due to the elasticity of the adhesive used.

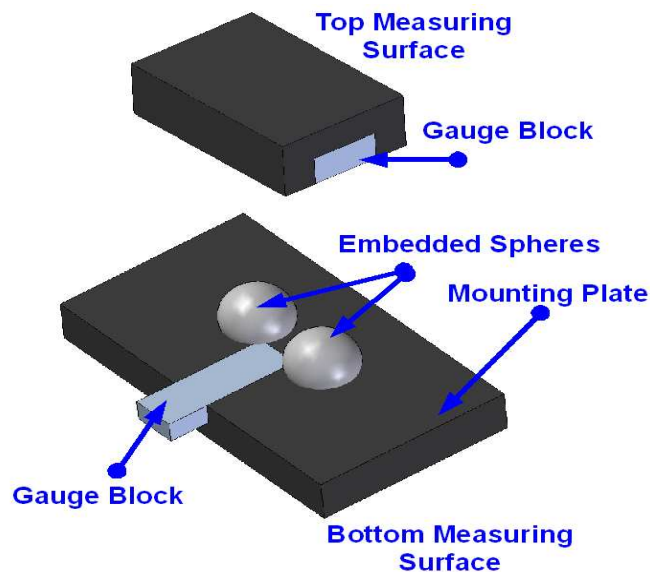


Fig. 71 Slip gauges installed [51]

There are two key lessons to be learned from this section which are important to this project:

1. Misalignment between the measuring platen and the support platform may cause the measuring platen to have to travel further than necessary to make contact with the sample. If this were the case it could create significant error in the measurement result. It is possible that any error here is 'calibrated out' (if the error remained constant for a set of measurements) when measuring the two reference balls however it is impossible to put a number on the magnitude of this error (if any).
2. The adhesive used to bond the slip gauges to the support and measurement platens may compress during the measurement sequence. If this were the case it would absorb some of the movement that would otherwise be transferred to the 'detection piezo' via the flexure system. Again it is possible that any error here is absorbed during calibration. However the concern is that the error may not be constant and is not easily quantifiable.

6.2.6. In process damage

Fig. 72 below illustrates damage to sample balls discovered during examination of the balls after testing. This sort of visible flat spotting on the sample could very easily result in bad data which may not be evident without a physical examination of the samples. Various steps were taken to improve the sample handling and thereby reduce damage to samples. The various sample handling improvement are discussed in detail in Section 3.3.

Also visible in Fig. 72 is the early onset of oxidation of the sample. As mentioned in Chapter 2.6 an anti-oxidant was added to the water coolant used in the laboratory in an attempt to counteract this oxidation.



Fig. 72 Damage to sample

6.2.7. Sample temperature variation

Using a comparative measurement system, it is important that samples are measured at the same temperature as the reference balls. In this implementation the calibrated and sample balls spend varying amounts of time exposed to air at room temperature while queuing to be measured in sequence. Temperature change can also occur due to friction during the ball delivery to the measuring tank, though this and other related ‘movement’ frictions should be consistent for all balls. Temperature

variations in the normalising fluid and variations in soaking times of the balls could have significant impact on the achieved measurements when the goal of sub-micron measurements is considered. The magnitude of the potential error has been identified earlier (Section 2.5) and is shown here again.

$$\Delta L = L_0 \alpha_l \Delta T$$

Where: ΔL = change in length; L_0 = Original length; α_l = coefficient of thermal expansion; 10.6×10^{-6} [52]; ΔT = change in temperature

$$\Delta L = 0.013494 * 10.6 \times 10^{-6} * 1 = 143 \text{nm}$$

So a 1°C change in temperature of the sample translates to a diameter variation of 143nm or 0.14µm for a 13.494mm ball. Section 2.5.2 details the methods of thermal control utilised by the apparatus.

6.2.8. Environmental temperature

While measuring the samples immersed in the temperature normalising fluid will help correct errors caused by thermal variation, exposure of the samples to air while queuing for measurement can present thermal stability issues as is suggested in Section 6.2.7 above. Fig. 73 below shows the room temperature (as monitored by the Prescon HS2000V sensor) over a period of 48 hours. A 100 point moving average was applied to the raw data to generate the graph shown. The mean temperature was 23°C with a peak temperature of 24.15°C and a minimum of 21.5°C over the measurement period. This suggests roughly typical “office” level control of the room temperature, as described in Table 5 below.

Table 5: Temperature control "rules of thumb" [unknown source]

Control level	Tolerances
“No” temperature control	± 25°C
“Office” temperature control	± 2°C
“Good” temperature control	± 1°C
“Very good” temperature control	± 0.1°C
Using air shower	± 0.05°C
Using oil shower	± 0.01-0.001°C [53]

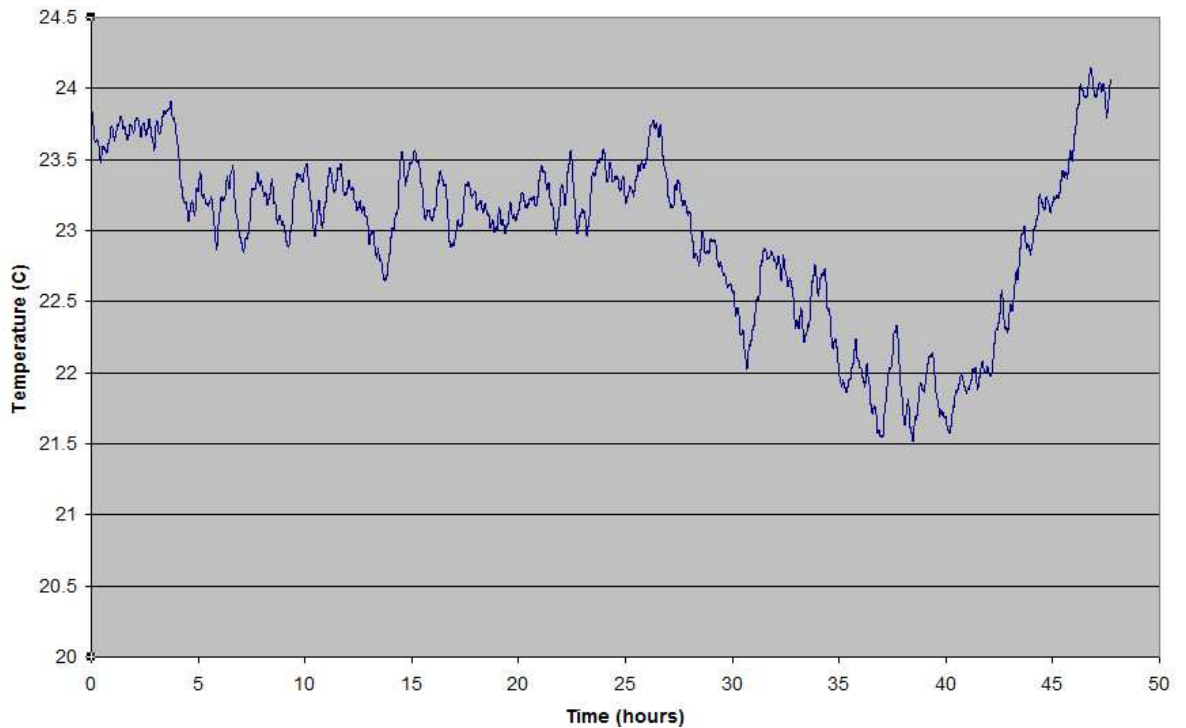


Fig. 73 Temperature log over 48 hour period

However, thermal stability during a measurement sequence is more important than over a lengthy period of time. So picking a random 5 minute window from the above gives an average temperature of 23.8°C with a range of 0.12°C during the period (see Fig. 74 below). This suggests that, while the system is subject to “office” levels of control over the medium to long term, in the short term the temperature stability of the equipment surroundings could be classed as ‘very good’. In a one minute window (within which a set of samples and reference balls could be measured) the maximum temperature range as shown in Fig. 74 is approximately 0.035°C. A measurement time of 15 seconds would bring the temperature ‘drift’ close to the 0.01°C required to limit the diameter change on the 13.5mm balls to the 0.01µm targeted for the 0.1µm accuracy objective. This then sets a measurement cycle objective 15 seconds for measurement in air (i.e. not under fluid) which is highlighted as one of the recommendation for future work on the stage (see Section 7.4.2). The measurement cycle time in the experimentation reported below was between 3-5 minutes per measurement set: this suggests a temperature range of 0.12°C for the air based measurement which on the basis of this data corresponds to 17.16nm drift. This is negligible in the context of a 0.01µm precision target.

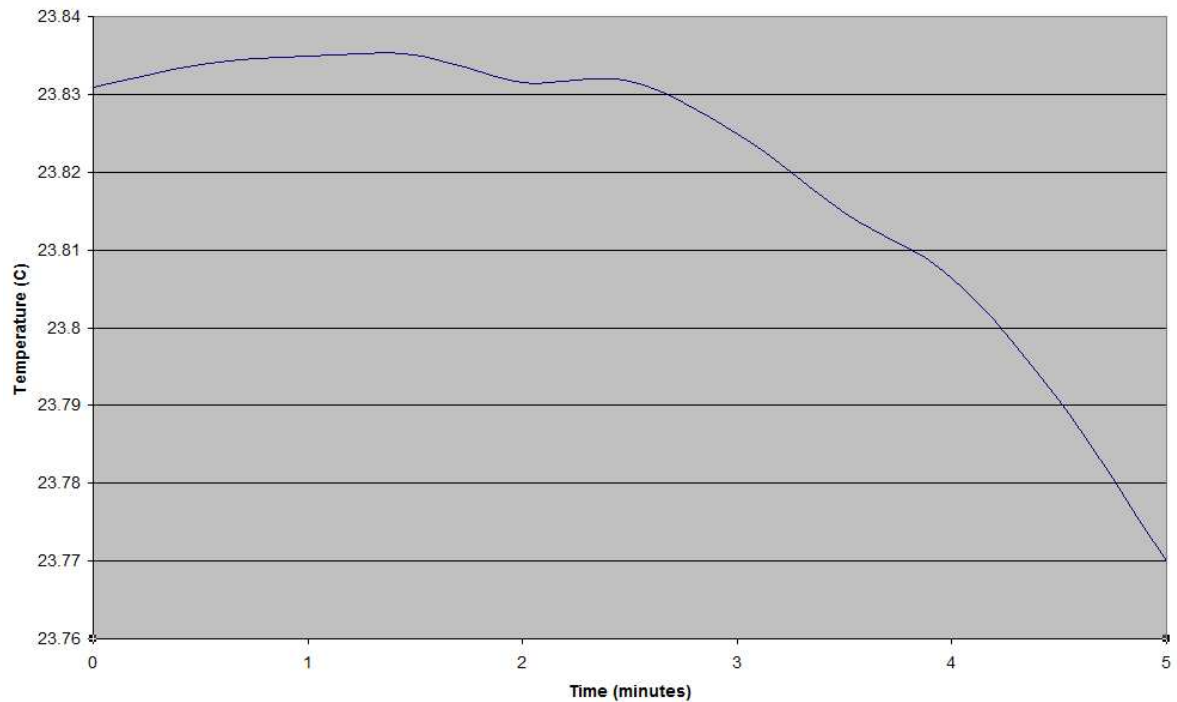


Fig. 74 Temperature over randomly selected five minute period

6.3. Experimentation

The variables of single/multi-touch, under fluid measurement, weighted measuring platform, and passive/‘active’ sample clamping touch measurement as discussed in the previous section as well as earlier in this thesis were tested in a series of measurement tests. The tests were carried out in the following 6 configurations:

- Single touch measurement.
 - Movement piezo steps in 0.015V (0.135 μ m) increments. This is the benchmark test.
- Multiple touches measurement (as discussed in detail in Section 3.8.1.):
 - The “Large” piezo steps in 0.015V increments until initial touch. It is pulled back one step then stepped forward again in a step half as large (i.e. 0.0075V). This cycle of touch-step size reduction-touch is repeated until strain gauge signal is within specified control limits.
- Multiple touches measurement with samples immersed in temperature normalisation fluid.
- Multiple touches with weighted measuring platform (as mentioned in Section 6.2.4).

- Multiple touches with ‘active’ sample clamping as described in Chapter 5.
- Multiple touches with ‘active’ sample clamping, weighted platform, and fluid immersion

6.3.1. Measurement strategy and test methodology

The statistical process control system in use by NN Euroball was based on measuring the diameter of three components per hour from a production lot. The grind process would typically run for 12 hours. This meant a total of 36 samples per process lot would have been measured by the measurement technician.

During the initial design stages for the new piezo measurement system a decision was taken to move to taking measurements from five components twice hourly; a change to 120 measured components from the lot. This was chosen arbitrarily as a ‘reasonable’ inspection level given the planned capacity of the measurement apparatus.

Further research in the area has revealed that a general rule of thumb for choosing sample sizes is to use the Normal Inspection, Level IV sample size table from the old US military standard MIL-STD-414 [54]. This table gives code letter ‘O’ for a lot between 22001 and 110,000 components. Code letter ‘O’ on table C1 of MIL-STD-414 gives a sample size of 115. This sample size can be split into sub-groups as required for SPC purposes and so 120 components over the 12 hour production cycle is sufficient. It is worth noting that the 36 components originally measured during the production cycle is consistent with the figures from the table for reduced inspection level from MIL-STD-414.

For these experiments three calibrated (UKAS certified) samples purchased from OPUS Metrology Ltd. were used [55]. These were sized 13.45mm ($\pm 0.0001\text{mm}$), 13.55mm ($\pm 0.00005\text{mm}$), and 13.50mm ($\pm 0.00005\text{mm}$). The 13.45mm and 13.55mm sized samples were used to calibrate the stage before each set of measurements. The 13.50mm sample was then measured five times (in accordance with MIL-STD-414) without removal from the stage. The samples were returned to the temperature normalisation tank after use. This was repeated 50 times for each of the variable configurations listed above

The improvement between single and multiple touch measurement was such that it was felt further experimentation with single touch measurement would not be a productive use of time and so all further experimental setups were based around the multiple touch measurement strategy.

6.4. Results

The full test results are presented in Appendix A. This section presents a discussion and interpretation of the results under the headings of repeatability and reproducibility, ANOVA analysis, and regression analysis.

6.4.1. Accuracy and Precision

Fig. 75 below is used by Montgomery [41] to illustrate the concepts of accuracy and precision (note that precision is often labelled as repeatability in other literature). He defines accuracy as *'the ability of the instrument to measure the true value correctly on average'* while precision is defined as *'a measure of the inherent variability in a measurement system'*. In this example the best performing system would be one which has the tightest spread of figures closest to the 'bulls eye' i.e. diagram (a), Fig 63.

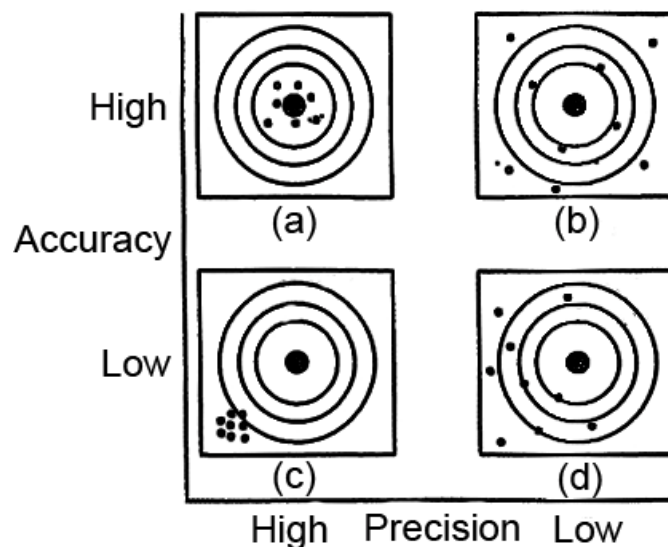


Fig. 75 Accuracy vs. precision diagram[41]

Table 6 below is an extract (for discussion purposes) of four of the fifty measurement test results for one of the six experimental setups. Measurements 1-5 are the readings taken in sequence by the apparatus without recirculation of the samples or recalibration of the Volts/mm relationship.

Table 6: Extract from results (13.50mm ball)

#	Meas. 1	Meas. 2	Meas. 3	Meas. 4	Meas. 5	Xbar	Range
1	13.501759	13.501287	13.501049	13.500811	13.500341	13.50105	0.001418
2	13.500998	13.500751	13.500267	13.500511	13.500509	13.50061	0.000731
3	13.501887	13.501558	13.501317	13.501072	13.50083	13.50133	0.001057
4	13.501949	13.501702	13.501703	13.501448	13.501448	13.50165	0.000501

By taking the range of the five figures from each measurement set (where a ‘measurement set’ is defined as a 5 measurements of the same sample ball without removal and without recalibration of the volts/mm relationship) and averaging this range figure over the 50 iterations per experiment a figure for precision is obtained. In other words the average range figure is the ‘*inherent variability in the measurement system*’. These results are summarised in Table 7 and show graphically in Fig. 76 below.

Table 7: Precision

Experimental Setup	Range
Single touch	0.004464
M. Touch	0.000888
M. Touch Under fluid	0.000699
M. Touch Weighted	0.000689
M. Touch weighted clamped fluid	0.000378
M. Touch Clamped	0.000159

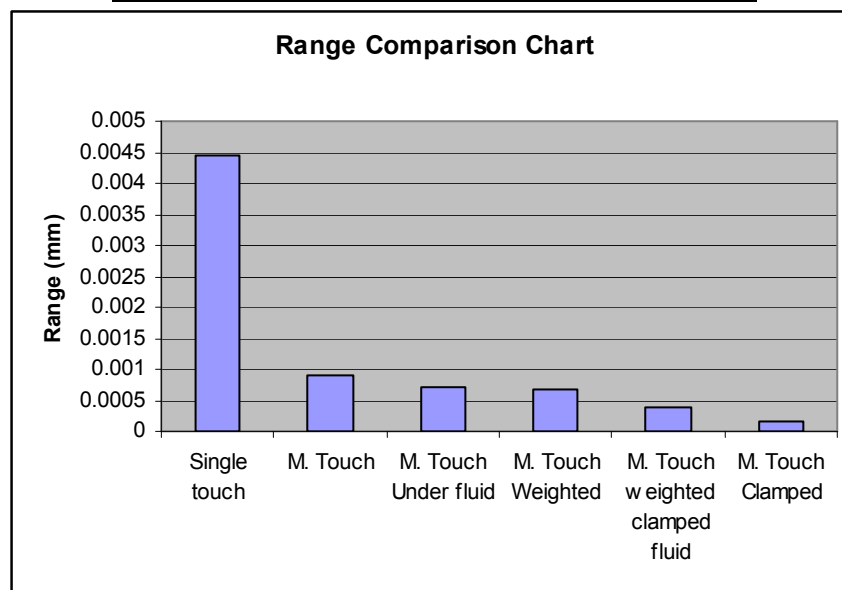


Fig. 76 Comparison of measurement range (precision)

To get a figure for accuracy take the same five figures from a ‘measurement set’ and get their average (Xbar in Table 6). The difference between the maximum and minimum Xbar figures from the experimental data gives the accuracy figure. These are presented in Table 8 and graphically in Fig. 77 below.

Table 8: Accuracy (13.50mm sample ball)

Experimental Setup	Xbar max	Xbar min	Accuracy
Single touch	13.5123828	13.45648	0.055907
M. Touch	13.5469394	13.49342	0.053521
M. Touch Weighted	13.506064	13.49499	0.01107
M. Touch Clamped	13.505241	13.49612	0.009122
M. Touch weighted clamped fluid	13.5020558	13.49758	0.004475
M. Touch Under fluid	13.5025482	13.49877	0.00378

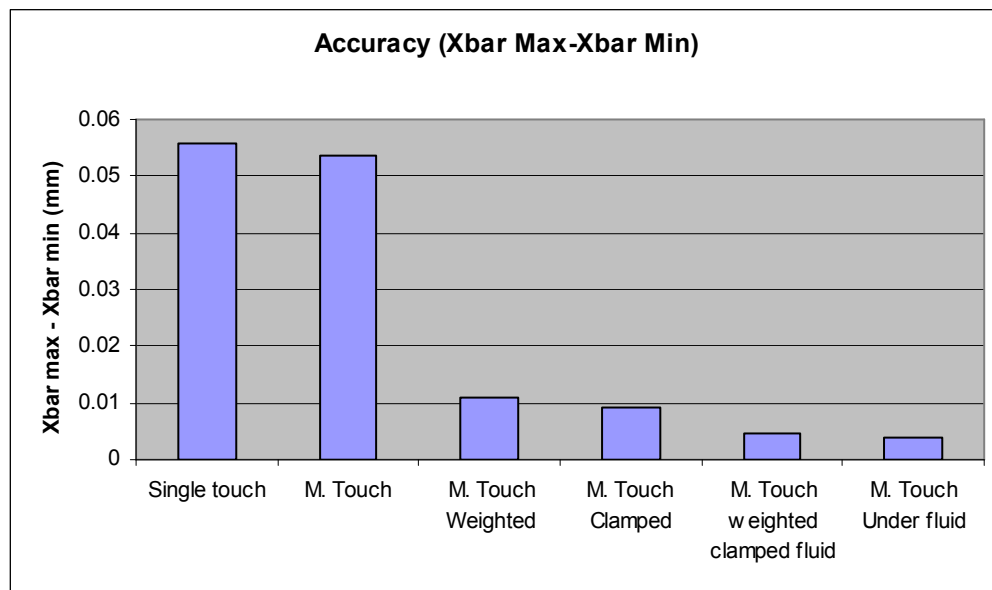


Fig. 77 Accuracy comparison chart

Table 9 below summarises the accuracy and precision data presented above. The results from ‘multi-touch under fluid’ (3rd row) and ‘multi-touch with weight stage, active clamping, and under fluid measurement’ (5th row) can be picked out as combining very good precision with the best accuracy figures found. In terms of these results the choice then is between these 2 configurations. The poorer figure for accuracy in the latter can perhaps be accounted for by the additional experimental setup factors involved which adds complexity to the multiple (50 off) sets of experiments; the

tighter figure for precision suggests improved results due to these factors when the weighting is on the 5 off single set-up measurements.

Table 9: Combined precision and accuracy

Exp Setup	Precision (mm)	Accuracy(mm)
Single touch	0.00446374	0.0559066
M. Touch	0.000887796	0.0535212
M. Touch Under fluid	0.000699245	0.0037798
M. Touch Weighted	0.000688745	0.0110702
M. Touch weighted clamped fluid	0.00037846	0.0044754
M. Touch Clamped	0.000158755	0.0091215

6.4.2. ANOVA Analysis

To identify the source of variance an ANOVA analysis was carried out for each experimental setup using the Minitab statistical software package. The data presented in Table 10 below shows the results of ANOVA analysis on the ‘single touch’ experiment.

At a typical significance level of 0.05 (i.e. P values below 0.05 represent significance) the ANOVA analysis points to calibration as a significant source of variance while variance from the part is not significant. The expectation was that part variation would be nil, minimal, or insignificant once examined because a single calibrated sample was used for the test.

Table 10: ANOVA analysis of 'single touch' experiment

Source	DF	SS	MS	F	P
Part	4	0.0001538	0.0000384	0.30542	0.874
Calibration	24	0.0141039	0.0005877	4.66892	0.000
Repeatability	221	0.0278166	0.0001259		
Total	249	0.0420742			

Table 11 below presents a compilation of P values for the range of experiments performed (see Section 6.3). As can be seen results correspond with Table 10 for all but one experiment. The reason for this is unknown and if time constraints permitted the experiment would have been repeated to validate the result.

Table 11: Compiled 'P values'

Exp Setup	Part P Value	Calibration P Value
Single touch	0.874	0.000
M. Touch	0.992	0.000
M. Touch Under fluid	0.004	0.000
M. Touch Weighted fluid	0.345	0.000
M. Touch weighted clamped fluid	0.345	0.000
M. Touch Clamped	0.957	0.000

6.4.3. Regression Analysis

To explore calibration error a regression analysis was carried out on available data. By comparing the figures used to calculate the sample diameter from detection voltages and the reported Xbar value (the average of 5 measurements) Minitab generated a formula to determine the correction factor that would need to be applied to have the system report the nominal diameter of the sample. Correction formulae for available data are presented in Table 12 below. This suggests there is a unique calibration error for each experimental setup. It should be noted that as measurement performance improves for different experimental setups that the calibration error correction factor also decreases.

Table 12: Regression formulae

Test condition	Formula
Multiple touch	$\phi = Xbar + (0.000478 * volts / mm)$
M. touch, fluid	$\phi = Xbar + (0.000314 * volts / mm)$
M. touch, clamped	$\phi = Xbar + (0.000267 * volts / mm)$
M. touch, clamped, weight, fluid	$\phi = Xbar - (0.000183 * volts / mm)$

6.5. Conclusion

Experimental results summarised in this chapter show significant increases in the precision and accuracy of the apparatus.

- Measurement precision in the sub $1\mu\text{m}$ range has been achieved. $0.1\mu\text{m}$ is targeted however not achieved with the closest result being $\sim 0.15\mu\text{m}$.
- Measurement accuracy has seen an approximate 14.7x improvement (from 0.0559mm to 0.00378mm) however is not in the sub-micron range targeted.
- Despite improvements in accuracy and precision the best results under both categories are not achieved in the same experimental setup. The ‘multiple touch under fluid’ and ‘multiple touch under fluid with active clamping and weighted platform’ achieve the best overall results, $0.7\mu\text{m}$ and $0.4\mu\text{m}$ and $3.8\mu\text{m}$ and $4.5\mu\text{m}$ precision and accuracy respectively, where other setups may have a higher precision but lower accuracy or vice-versa.
- ANOVA analysis has identified the main source of measurement variation as the stage calibration i.e. the results achieved when the apparatus performs a ‘self calibration’ using a large and small calibration ball to determine a ‘volts/mm’ figure which is then used to calculate the diameter of measured samples. It is important to be aware that ‘calibration’ error actually incorporates all conceivable errors that occur during the measurement process (i.e. any error not directly attributable to the sample).
- The aberrant result from one set of data in the ANOVA analysis indicates that at the very least the test producing this result (multiple-touch under fluid) needs to be re-run to confirm the data. Due to time constraints it was not possible to redo this experiment. This deviant result also casts some doubts over the validity of results from the other experimental setups. If, after re-running, the results of the deviant test did not fall into line with other experiments then the entire series should be re-tested to confirm the results.
- Regression analysis demonstrates a basis for further improving gauge results. Applying the correction factors identified could see an improvement in the accuracy figure. It is also important to note that this would need to be monitored carefully and that more than 50 results may be required to calculate a suitable correction factor. This is given further consideration in Chapter 7.

7. Outcomes, Conclusion, and Further Work

7.1. Introduction

The intention had been for this project to pick up where the previous projects (D. Madigan[51] and C. Shouldice[52]) finished. Unfortunately circumstances at NN Euroball Kilkenny (plant closure) meant further plant integration was impossible and so the apparatus was transferred back to the Ultra Precision Research Laboratory at Waterford Institute of Technology for further improvements. The focus of this project became the upgrading of the measurement station in the laboratory for both reliability and measurement accuracy; both factors which were less than satisfactory in the on-site implementation.

This chapter presents the outcome of this upgrade work and presents recommendations for future work to further enhance the performance of the apparatus.

7.2. Objectives and outcomes

1. To improve the overall reliability of the station.

Outcome: The upgrades presented in Chapter 2.6 contributed to significantly improved reliability of the working system. Sample circulation pipe breakages were eliminated. Samples are now delivered in a consistent and controlled order to the measuring station.

Positive pressure piezo protection discussed in Chapter 4 effectively removed the risk to the piezos caused by the high local humidity created by the water bath in which the stage was partially immersed.

The issue of sample queuing and insertion has been examined and a new queue/feed mechanism constructed although installation is pending. This was presented in Section 5.4.3.

2. To establish a benchmark for measurement performance.

Outcome: Initial testing produced a set of results which were used as a benchmark for system capability at the outset of this project. This benchmark was referred to as ‘single touch’ or ‘single touch measurement’ throughout this thesis.

3. To investigate and implement methods of improving measurement performance

Outcome: A number of potential problem areas were identified (presented in Fig. 66) which allowed the selection of a number of improvements to the apparatus and its environment through which were likely to see an improvement in the measurements achieved from the station. Each was implemented and tested in turn. The improvements achieved are quantified in Section 6.4.

4. To redefine instrument capabilities, post improvements.

Outcome: The benchmark testing set instrument repeatability (precision) and reproducibility (accuracy) at 0.004464mm and 0.055907mm respectively. Documented improvements have seen these figures improve to 0.000159mm and 0.00378mm for repeatability (precision) and reproducibility (accuracy) respectively. However these figures are not taken from the same experimental setup. The “multiple touches clamped” setup gave the best repeatability (precision) while the “multiple touches under fluid” setup provided the best reproducibility (accuracy) figure. The results from ‘multi-touch under fluid’ and ‘multi-touch with weighted stage, active clamping, and under fluid measurement’ can be picked out as combining very good precision with the best accuracy figures found.

7.3. Conclusions

The principle objectives of this project were the improvement in overall measurement and temperature normalisation station reliability and improvements in measurement performance (accuracy and precision) of the apparatus.

Although reliability improvements are difficult to quantify, demonstrable improvements have been achieved. The sample return mechanism no longer regularly breaks down and leaks from the fluid circulation system have been repaired.

From a measurement perspective there have been significant improvements. Sub-micron precision has been achieved though is still short of the 0.1 μ m targeted. Sub-micron accuracy has not been achieved however the significantly improved precision should make it possible to program around the accuracy problems (effectively shifting the ‘bulls eye’ spoken about in section 6.4). This is discussed briefly in section 7.4.3.

7.4. Recommendations for future work to achieve aims and objectives

7.4.1. Temperature normalisation fluid filtration

With a measurement precision of 0.01 μm necessary to provide the targeted measurement accuracy of 0.1 μm , particles suspended in the temperature normalising fluid greater in size than 0.01 μm could cause a decline in instrument performance if they attach to the surface of the reference/sample balls or become lodged on the measurement platform.

To rectify this situation an in-line filtration system capable of removing 'nuisance' particles needs to be installed.

7.4.2. Cycle time

Thermal stability is an important theme running through this project. Section 6.2.8 above details the environmental temperature stability over time. From these results it can be concluded that the quicker a set (2 reference balls, 5 sample balls) of measurements are completed the lower the environmental thermal variation the set is exposed to. This creates a 15 second target cycle time for operation in air. At present it takes approximately 4 minutes to complete a set of measurements.

Methods of improving this cycle time may include:

- Step size investigation: The measuring platen is moved forward in 252nm steps. If this step size were increased it would take fewer steps to reach the sample.
- Step speed: A higher specified computer in combination with a control program less resource intensive may allow the piezo to increment more frequently than the current setup (see Section 7.4.7).
- High speed feeding: At present samples are gravity fed (allowed to roll) into the equipment. A method of positioning the samples using driven systems could provide some cycle time improvements. This combined with a reduction in the distances samples need to move may result in significant improvements. However it is important to note that the key to cycle time improvements lie

firstly with the time taken to measure each sample and that component handling is a secondary concern.

7.4.3. Accuracy improvement - regression analysis

The regression analysis carried out in Section 6.4.3 demonstrated a method that could be used to improve upon the accuracy results achieved by the apparatus. With two setups returning excellent precision it should be possible to determine a suitable correction factor to improve the accuracy. This may require a more detailed study with a larger sample size than undertaken in this project.

7.4.4. Rebuild sample return system

Despite the work done to improve the sample return system it is still quiet violent and resource intensive in use. A re-designed system could use long travel pneumatic rams with a suitable pallet attached or a pulley system and electric motors to simultaneously reduce the systems consumption of compressed air and create a quieter work space with less risk of damage to sample/calibration balls.

An alternative configuration could use a SCARA robot to move sample and reference balls between measuring and temperature normalising tanks.

7.4.5. Sample queuing upgrade

Issues related to the installation of the upgraded queuing mechanism discussed in Section 5.4 need to be further examined. The most obvious solution to the issue of lack of space is a larger tank. A greater problem is presented by the shortage of PLC outputs available to control the new queue mechanism. A possible solution to this issue is described in Section 7.4.6.

7.4.6. PLC wiring/communication

At present the measuring station PLC and the cooling station PLC communicate with each other by turning on/off an output for each signal they need to send. This approach uses up inputs/outputs that could be used for other purposes. A method of

reducing the number of inputs/outputs required should be examined. One such method would involve using a group of inputs/outputs on each PLC to create a simple binary exchange. Four inputs/outputs on each, for example, would allow for the exchange of 2^4 (16) different signals between the PLCs and free up ports for other uses.

Alternatively an examination of current PLC function may reveal that the smaller (16 input 16 output) PLC used to control various measuring station functions is surplus to requirements and that the system could be rewired for full control from the cooling station PLC.

7.4.7. LabVIEW control improvements

As discussed in Section 6.2.2 a large LabVIEW program consumes a lot of resources and can cause resource management issues with enough subroutines. Eventually this can lead to a point where there is a significant reduction in program performance which can cast doubts over the quality of results attainable.

Many of the subroutines of the existing control program are sufficiently intertwined as to make simply removing parts at will a practical impossibility. Therefore a rewrite is required. One suggested method is to have a control program which can open and run blocks of code only as they are required. This would allow each subroutine to run efficiently as LabVIEW would not have to scan through large amounts of code during program iterations. Fig. 78 and Fig. 79 show two possible approaches to this method of simplifying the LabVIEW control program. The first shows the program running on a single workstation. In this instance there would be a master control program which calls other functions as necessary. In the second diagram there are two workstations; one dedicated to the measurement function, and one dedicated to the process control function, both sharing information via a database which can be stored on either workstation or directly tied into an enterprise resource management package.

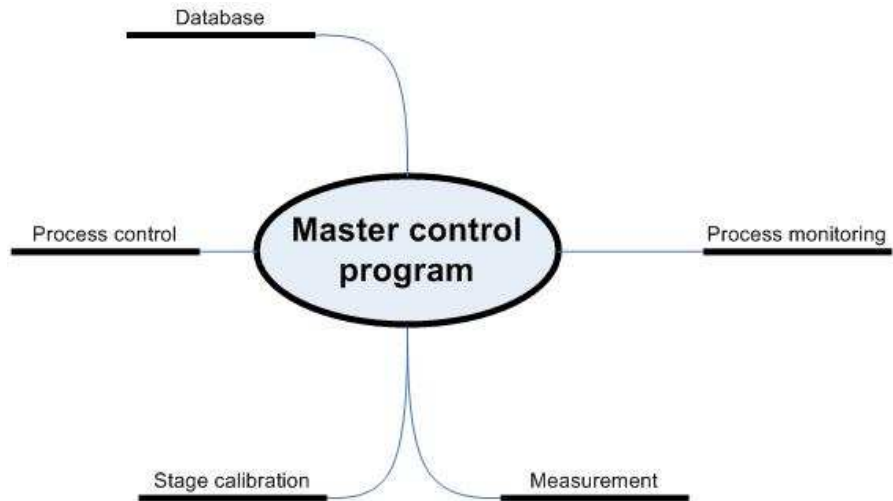


Fig. 78 Suggested program layout for a single workstation

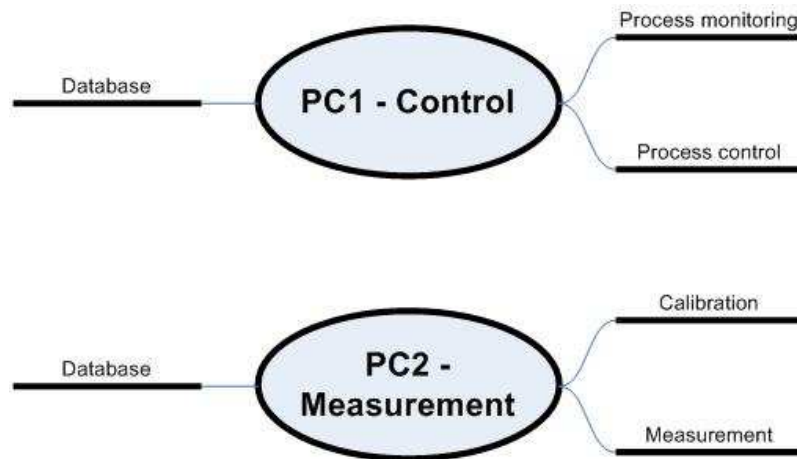


Fig. 79 Twin workstation program layout

7.4.8. Temperature normalising station reconstruction

The temperature normalising station was originally designed to accept samples directly from production where heat dissipation was a much greater issue. As samples are no longer arriving hot from machining the temperature normalisation system could be greatly reduced in size/temperature normalising capacity. Also the system should be rebuilt so that the tanks can be covered to help prevent evaporation or the temperature normalising fluid. A rebuild would also give the opportunity to work on the problem described in Section 7.4.1 above and ideally both issues would be tackled at the same time.

7.4.9. Secondary position measurement

At present all measurements taken by the equipment are relative measurements. The LabVIEW control program calculates the diameters of the sample balls based on voltages observed from known calibration balls. To enhance this, two high precision distance measurement devices could be added. The first would measure the height of the measuring stage from a known point, e.g. from the base of the aluminium flexure. The second would measure the distance moved by the measuring platen before the strain gauge detects contact with the sample being measured. Again this would be an absolute measurement from a known point. By combining both of these measurements the measurement provided by the strain gauge could be confirmed. This strategy has the added benefit of measuring any backlash from the measurement platform at the instant of touch. The key requirement for any extra measuring system would be zero friction added to the system. To this end LDVT (linear variable differential transformer) or multi-pass laser interferometry would be suitable although not necessarily compatible with the stage in its current implementation.

7.4.10. Improved stage height locking mechanism

At present the measuring stage is held in place by a lead screw which can be used to raise and lower the stage to allow different sized samples to be measured. However lead screws introduce an unknown amount of variability in the form of unknown rigidity (or lack of) and unspecified manufacturing tolerance to allow movement between the lead screw and the stage it is holding. This combination of unknowns can allow for undesirable movement during positioning and measurement which can introduce inaccurate results. A locking mechanism which holds the stage in place against the lower edge of the screw could be implemented and this would ensure there is no movement during the measuring cycle.

7.4.11. Temperature control of normalising fluid

At present the temperature of the normalising fluid in which the samples are held can be increased using a 3kW heating element installed in either the measuring tank or the storage tank. These elements are large, power hungry, and make precise temperature control difficult.

A new system could make use of a higher number of smaller heating elements, a two way water-air heat exchanger, or Peltier junctions.

7.4.12. Mass based measurement

An alternative measurement system which would remove the necessity for careful thermal control by measuring a property of the sample(s) which does not change with temperature could be considered. By measuring the mass of the samples it is possible to calculate their diameter though this approach assumes a homogenous lot and perfectly round balls. However for a desired detectable difference of 1 μ m any measurement system would need to be able to detect a difference in mass of 2.1×10^{-7} kg (assuming a material density of 7800 kg/m³ for chrome steel 52100 and based on a 13mm diameter sample). To make a system such as this practical it could require 1000 samples be weighed at a time to make the differences detectable. Taking 1000 samples reduces the measurement requirement to 0.0002kg (0.2g) but forces the system to be heavily reliant on averages and assumptions about the homogeneity of the lot.

Despite the drawbacks of this approach it could prove useful to control the “first grind” (see section 1.3) production phase if the system were to be implemented in a production environment. During the first grinding phase ball finish is rough enough that there is little benefit gained by using the high precision stage to control the process.

8. References

- [1] Dorsey Metrology, available: <http://www.dorseymetrology.com/> [accessed 05 October 2009]
- [2] Automation and Metrology, Inc. available: http://www.auto-met.com/heidenhain/Length_Gages/index.htm [accessed 05 October 2009]
- [3] Madigan, D., Phelan, J. (2007) *Flexural-hinge guided stage for sub-nicom precision measurement*, IMC24, Waterford Institute of Technology.
- [4] Wemyss, T., Phelan, J. (2007) *Development of a flexure based componenet measurement instrument for use in a noisy environment (Paper 2)*, IMC24, Waterford Institute of Technology.
- [5] Gong, S. (2003) *A conceptual development of novel ultra-precision dimensional measurement technology*, Measurement 33 347-357
- [6] Tian, Y., Shirinzadeh, B., Zhang, D. (2009) *A flexure-based mechanism and control methodology for ultra-precision turning operation*, Precision Engineering 33 160-166
- [7] Nikon D3x Preview, available <http://photo.net/equipment/nikon/D3X/preview/> [accessed 01 September 2010]
- [8] Oka, T., Nakajima, H., Tsugai, M., Hollenbach, U., Wallrabe, U., Mohr, J., (2003) *Development of a micro-optical distance sensor*, Sensors and Actuators A 102 261-267
- [9] Hsu., C., Lu, M., Wang, W., Lu, Y., (2009) *Distance measurement based on pixel variation of CCD images*, ISA Transactions 48 389-395
- [10] Finkelstein, L. (2003) *Widely, strongle and weakley defined measurement*, Measurement 34 39-48
- [11] BIPM, IEC, IFCC, ISO, IUPAC, IUPAP, OIML: International Vocabulary of Basic and General Terms in Metrology, 2nd edition 1993, ISBN 92-67-01075-1
- [12] Bullock, R., Deckro, R. (2006) *Foundations for system measurement*, Measurement 39 701-709
- [13] Suppes, P., Zinnes, J.L. (1962) *Basic Measurement Theory*, available http://suppes-corpus-stanford.edu/techreports/IMSSS_45.pdf [accessed 16 August 2010]
- [14] <http://dictionary.reference.com/browse/isomorphism>
- [15] <http://dictionary.reference.com/browse/homomorphism>
- [16] ISO 5725-1 Accuracy (trueness and precision) of Measurement Methods and Results Part 1; General Principles and Definitions 1994

- [17] Measurement Systems Analysis Work Group, *Measurement Systems Analysis Reference Manual*, third edition, Daimler Chrysler Corporation, Ford Motor Company, General Motors, 2002
- [18] Marriott F.H.C. “*A Dictionary of Statistical Terms*”, 5th edition, The International Statistical Institute, Published by Longman Scientific and Technical
- [19] Prittschow, G., (1998) *A comparison of linear and conventional electromechanical drives*, Annals of the CIRF 2 541-548
- [20] Hai-Hua Mu, Yun-Fei Zhou, Xin Wen, Yan-Hong Zhou, (2009) *Calibration and compensation of cogging effect in a permanent magnet linear motor*, Mechatronics 19 577-585
- [21] Baldor, available http://www.baldor.com/products/linear_motors.asp [accessed 28 July 2010]
- [22] Physik Instrumente, (2009) Piezoelectrics in Positioning
- [23] Physik Instrumente, M-663 PILine data sheet, available http://www.physikinstrumente.com/en/pdf/UMP_linear_datasheet.pdf [accessed 29 July 2010]
- [24] Goethals, P., Sette, M., Reynaerts, D., Van Brussel, H., (2007) *Tactile sensing technology for robot assisted minimally invasive surgery*, Journal of Biomechanics 40 S647
- [25] Muhammad, H.B., Oddo, C.M., Beccai, L., Adams, M.J., Carrozza, M.C., Huskins, D.W., Ward, M.C., (2009) *Development of a Biomimetic MEMS Based Capacitive Tactile Sensor*, Procedia Chemistry 1 124-127
- [26] Del Castillo-Castro, T., Castillo-Ortega, M.M., Herrera-Franco, P.J., (2009) *Electrical, mechanical and piezo-resistive behaviour of a polyaniline/poly(m-butyl methacrylate) composite*, Composites Part A 40 1573-1579
- [27] Shikida, M., Shimizu, T., Sato, K., Itoigawa, K., (2003) *Active tactile sensor for detecting contact force and hardness of an object*, Sensors and Actuators A 103 213-218
- [28] Dagahi, J., (1999) *A piezoelectric tactile sensor with three sensing elements for robotic, endoscopic and prosthetic applications*, Sensors and Actuators 80 23-30
- [29] Vidic, M., Harb, S.M., Smith, S.T., (1998) *Observations of contact measurements using a resonance-based touch sensor*, Precision Engineering 22 19-36

- [30] Woody, S.C., Smith, S.T., (2003) *Resonance-based vector touch sensors*, Precision Engineering 27 221-233
- [31] Wemyss, T., Phelan, J. (2007) *Development of a flexure based component measurement instrument for use in a noisy environment (Paper 1)*, IMC24, Waterford Institute of Technology.
- [32] Gao, W., Hocken, R.J., Patten, J.A., Lovingood, J., Lucca, D.A., (2000) *Construction and testing of a nanomachining instrument*, Precision Engineering 24 320-328
- [33] Salapaka, S., Sebastian, A., Cleveland, J.P., Salapaka, M.V., (2002) *Design, identification and control of a fast nanopositioning device*, Proceedings of the 2002 American Control Conference 1966-1971
- [34] Yang, H-J., Nyberg, S., Riles, K., (2007) *High-precision absolute distance measurement using dual-laser frequency scanning interferometry under realistic conditions*, Nuclear Instruments and Methods in Physics Research A 575 395-401
- [35] Wang, X., Wang, X., Lu, H., Qian, F., Bu, Y., (2001) *Laser diode interferometer used for measuring displacements in large range with a nanometer accuracy*, Optics and Laser Technology 33 219-223
- [36] Omega.com, available
<http://www.omega.com/literature/transactions/volume3/strain.html> [accessed 27 July 2010]
- [37] PI Datasheet, available
<http://www.physikinstrument.com/en/products/prdetail.php?sortnr=400600.30> [accessed 16 August 2010]
- [38] Cadiergues, L., Baviere, Ph, Le Letty, R. (2007) *Evaluation of piezoceramic actuators*, ESMATS, Liverpool.
- [39] PI, Environmental conditions and influences, available:
<http://www.physikinstrumente.com/en/products/prdetail.php?sortnr=400715> , [accessed 07 May 2009].
- [40] King-Fu Hii, Vallance, R.R., Pinar, M.M, (2009) *Design, operation, and motion characteristics of a precise piezoelectric linear motor*, Precision Engineering 34 231-241
- [41] Montgomery, D. C., (2005) *Introduction to Statistical Quality Control*, fifth edition, United States of America: John Wiley & Sons, Inc.

- [42] Shouldice, C., Walsh, D., Phelan, J., (2007) *Product temperature control for sub-micron inline measurement*, IMC24, Waterford Institute of Technology.
- [43] Harvey, M. E., (1967) *Precision temperature-controlled water bath*, Review of Scientific Instruments 39 13-18.
- [44] Ogasawara, Hiromitsu, (1986) *Method of precision temperature control using flowing water*, Review of Scientific Instruments 57 3048-3052.
- [45] Hoque, E., Mizuno, T., Ishino, Y., Takasaki, M., (2010) *A six-axis hybrid vibration isolation system using active zero-power control supported by passive weight support mechanism*, Journal of Sound and Vibration 329 3417-3430
- [46] Chen, K.T., Chou, C.H., Chang, S.H., Liu, Y.H., (2008) *Intelligent active vibration control in an isolation platform*, Applied Acoustics 69 1063-1084
- [47] Hongling, S., Kun, Z., Haibo, C., Peiqiang, Z., (2007) *Improved Active Vibration Isolation Systems*, Tsinghua Science and Technology 12 533-539
- [48] Kawashima, K., Kato, T., Sawamoto, K., Kagawa, T. (2007) *Realization of virtual sub chamber on active controlled pneumatic isolation table with pressure differentiator*, Precision Engineering 31 139-145
- [49] Engineering Toolbox, Equivilant pipe lengths, available:
http://www.engineeringtoolbox.com/equivalent-pipe-length-method-d_804.html
 [accessed 19 August 2009].
- [50] PI Datasheet, available
<http://www.physikinstrumente.com/en/products/prspecs.php?sortnr=101000> [accessed 24 September 2008]
- [51] Madigan, D. (2008) *Piezo actuated flexural stage for sub-micron measurement*, (MEng), Waterford Institute of Technology.
- [52] Shouldice, C. (2008), *Total automation of an industrial in-line quality measurement system*, (MEng), Waterford Institute of Technology.
- [53] Yong Zhao, Trumper, D. L., Heilmann, R K., Schattenburg, M. L., (2007) *Optimization and temperature mapping of an ultra-high thermal stability environmental enclosure*, Precision Engineering 34 164-179
- [54] MIL-STD-414: Sampling procedures and tables for inspection by variables for percent defective (1957) United States of America: Department of Defence
- [55] Opus Metrology Ltd calibration certificates. 1st April 2009.

Appendix A – Test Results

Appendix A.1: Single sample, single touch

Humidity	Temperature	M1	M2	M3	M4	M5
61.29199	26.12753	13.51836	13.51928	13.51882	13.52017	13.52018
60.95215	26.23672	13.48998	13.48979	13.48979	13.4898	13.4898
61.73535	26.33931	13.56632	13.56147	13.53458	13.53724	13.5379
60.08496	26.28513	13.50121	13.5012	13.50145	13.50145	13.50145
56.67969	26.35221	13.49889	13.49913	13.49913	13.49913	13.49913
58.65332	26.44406	13.54919	13.55047	13.49239	13.49264	13.49287
57.46777	26.31694	13.49581	13.49559	13.49559	13.49582	13.49559
59.02539	26.32044	13.49683	13.49683	13.49661	13.50136	13.50114
58.3125	26.31397	13.50565	13.50491	13.50491	13.50491	13.50447
58.12891	26.32396	13.49754	13.49708	13.49685	13.49661	13.49684
56.32422	26.32646	13.49505	13.49481	13.49481	13.49458	13.49458
56.92188	26.30563	13.4568	13.4564	13.4564	13.4564	13.45639
57.11621	26.38782	13.49902	13.4988	13.49861	13.49861	13.4984
57.2959	26.44999	13.49684	13.49659	13.49637	13.49613	13.49591
58.99121	26.43056	13.49384	13.49384	13.49406	13.49406	13.49406
57.96094	26.43991	13.49599	13.49599	13.49577	13.49577	13.49577
57.78027	26.43449	13.49599	13.49599	13.49599	13.496	13.49577
56.65625	26.45091	13.49645	13.49645	13.49646	13.49646	13.49645
57.31348	26.49992	13.4948	13.4948	13.49458	13.49458	13.4948
57.14746	26.56428	13.49599	13.49578	13.49555	13.49555	13.49533
58.7002	26.51205	13.49602	13.49579	13.49535	13.49535	13.49513
54.50293	26.57973	13.49182	13.49182	13.49182	13.49181	13.49182
57.84961	26.56771	13.4969	13.4969	13.4969	13.4969	13.4969
57.60156	26.53138	13.49567	13.49589	13.49567	13.49567	13.49545
57.63379	26.56315	13.49851	13.49803	13.4978	13.49755	13.49756
58.07422	26.58008	13.50127	13.50078	13.50078	13.50078	13.50078
54.36231	26.57359	13.5017	13.5017	13.50123	13.50099	13.50122
54.72461	26.60187	13.50254	13.50226	13.50198	13.50171	13.50143
54.85254	26.54629	13.49675	13.49675	13.49675	13.49675	13.49675
55.89453	26.61938	13.50082	13.50036	13.50013	13.49989	13.49989
57.23828	26.55942	13.49685	13.49664	13.49663	13.49638	13.49638
55.06445	26.59089	13.50091	13.50091	13.50114	13.50137	13.50137
54.90137	26.55515	13.50231	13.50231	13.50285	13.50285	13.50258
55.71582	26.51278	13.50328	13.50354	13.50328	13.50354	13.50354
57.21973	26.62198	13.49958	13.49915	13.49889	13.4989	13.49866
57.19824	26.6331	13.50138	13.50104	13.50081	13.50081	13.5008
55.52832	26.58192	13.50387	13.50388	13.50387	13.50388	13.50364
56.43164	26.6093	13.50332	13.50332	13.50355	13.50355	13.50379
54.55371	26.56581	13.50975	13.51281	13.51312	13.51312	13.51312
55.7334	26.62007	13.50205	13.50205	13.50146	13.50121	13.50146
54.86035	26.57719	13.49742	13.4971	13.49686	13.49686	13.49637
55.1416	26.6155	13.49782	13.49737	13.4976	13.49692	13.49692
56.97461	26.60012	13.49703	13.49681	13.49659	13.49681	13.49658
54.50879	26.5988	13.49825	13.49825	13.49825	13.49802	13.49802
55.55371	26.63856	13.50037	13.50014	13.49989	13.49965	13.49966
56.06055	26.60129	13.49907	13.49876	13.49876	13.49852	13.49829
53.86426	26.55843	13.49989	13.49989	13.49965	13.49942	13.49942

Humidity	Temperature	M1	M2	M3	M4	M5
54.47852	26.59532	13.50006	13.49973	13.49949	13.49949	13.49949
53.38086	26.60999	13.50076	13.50052	13.50029	13.50028	13.50005
54.02832	26.56502	13.5006	13.40036	13.50013	13.49989	13.49989

Appendix A.2: Single sample, multiple touch

Humidity	Temperature	M 1	M 2	M 3	M 4	M 5
58.83594	25.51117	13.49304	13.49297	13.49256	13.49255	13.49256
57.91797	25.530884	13.49898	13.49819	13.4985	13.49795	13.49795
58.91504	25.527469	13.4989	13.49874	13.49897	13.49852	13.49851
56.85547	25.543008	13.49754	13.4973	13.49715	13.49576	13.49568
59.25391	25.501824	13.50139	13.50197	13.50106	13.50089	13.5009
57.09473	25.535276	13.49997	13.4995	13.49925	13.49917	13.49876
57.16797	25.52526	13.54699	13.54699	13.54699	13.54699	13.54675
56.54883	25.537219	13.49914	13.49922	13.49953	13.49905	13.49873
57.5	25.619192	13.4968	13.49725	13.49681	13.49703	13.4968
57.75879	25.669872	13.50024	13.49901	13.49924	13.49969	13.49909
55.24707	25.680168	13.49967	13.49959	13.49951	13.49951	13.49935
55.63281	25.571356	13.49914	13.49883	13.49883	13.49876	13.4986
56.15234	25.735735	13.51342	13.51366	13.5122	13.51111	13.51017
56.70996	25.780575	13.50092	13.49931	13.49875	13.49797	13.49788
56.61035	25.788408	13.49327	13.49327	13.49368	13.49341	13.49347
56.23145	25.7765	13.49834	13.49801	13.49786	13.49761	13.49753
55.5332	25.754969	13.50283	13.50236	13.5029	13.50244	13.50267
54.67578	25.817963	13.4987	13.49831	13.49824	13.49824	13.49823
55.92285	25.7903	13.50005	13.49902	13.49902	13.49902	13.49886
55.12695	25.844356	13.49914	13.49906	13.49906	13.49898	13.49898
54.79688	25.820972	13.4985	13.49789	13.49781	13.49796	13.49789
54.85156	25.75408	13.49957	13.4995	13.49973	13.49926	13.49926
66.57324	24.555135	13.4986	13.4986	13.49852	13.49836	13.49836
64.22363	24.503465	13.49958	13.49951	13.49927	13.49927	13.4992
65.29492	24.619449	13.49936	13.4992	13.49897	13.49897	13.49896
66.3252	24.683446	13.49844	13.49828	13.49851	13.49805	13.4979
64.82617	24.733161	13.50083	13.50053	13.49989	13.49873	13.49873
66.54981	24.858362	13.49893	13.49845	13.49854	13.49822	13.49821
65.55078	24.833149	13.51372	13.51347	13.51347	13.51324	13.51315
66.26563	24.869141	13.50064	13.5004	13.50009	13.50001	13.49993
66.05176	24.949426	13.49946	13.49908	13.49893	13.499	13.49923
66.16992	24.900231	13.49835	13.49827	13.49866	13.49866	13.49819
67.34863	25.041441	13.49824	13.49801	13.49785	13.49777	13.49762
65.80078	24.934839	13.49993	13.49962	13.4997	13.4997	13.4997
65.78027	25.030092	13.49485	13.49509	13.49426	13.49409	13.49451
66.26465	25.073599	13.49959	13.49943	13.4992	13.49943	13.49919
64.43652	25.123225	13.4984	13.49817	13.4981	13.49795	13.49794
66.18457	25.198343	13.49902	13.49933	13.49886	13.49886	13.49878
65.87988	25.205186	13.49576	13.49569	13.49569	13.49548	13.49548
64.13477	25.288518	13.50009	13.49985	13.49962	13.49954	13.49962
63.66699	25.301695	13.50881	13.50243	13.50604	13.50597	13.50604
62.81641	25.353645	13.49942	13.49919	13.4995	13.49926	13.49895
64.08984	25.357098	13.49943	13.49942	13.49966	13.49911	13.49888
64.71484	25.430756	13.50179	13.50179	13.50179	13.50164	13.50156

Humidity	Temperature	M 1	M 2	M 3	M 4	M 5
63.74023	25.368473	13.50225	13.50241	13.50265	13.50265	13.50289
62.70898	25.493813	13.5059	13.50632	13.5066	13.5066	13.5066
62.95703	25.543592	13.50007	13.5003	13.50054	13.50031	13.50031
62.24121	25.546728	13.50035	13.50082	13.50082	13.50098	13.50082
62.03906	25.592723	13.49732	13.49815	13.49877	13.49778	13.49824
61.79785	25.688306	13.50083	13.50115	13.50114	13.50114	13.50114

Appendix A.3: Single sample, multiple touch, under fluid

Humidity	Temperature	M 1	M 2	M 3	M 4	M 5
72.58594	25.525856	13.50176	13.50129	13.50105	13.50081	13.50034
75.96875	25.493991	13.501	13.50075	13.50027	13.50051	13.50051
75.85352	25.511625	13.50189	13.50156	13.50132	13.50107	13.50083
74.6709	25.537308	13.50195	13.5017	13.5017	13.50145	13.50145
79.29688	25.69869	13.49994	13.49969	13.4992	13.49944	13.49944
77.60645	25.569186	13.49896	13.49872	13.49872	13.49872	13.49872
75.42285	25.655361	13.50228	13.50228	13.50228	13.50203	13.50203
74.61816	25.605316	13.50133	13.50109	13.50109	13.50109	13.50084
76.28711	25.650359	13.50175	13.5015	13.50126	13.50126	13.50101
74.87109	25.662496	13.50022	13.49997	13.49948	13.49973	13.49924
74.99707	25.684916	13.50034	13.5001	13.49986	13.49962	13.49962
78.56738	25.648925	13.49998	13.49974	13.49928	13.4995	13.4995
79.39941	25.537104	13.49962	13.49938	13.49938	13.49892	13.49915
77.10938	25.824895	13.5007	13.50046	13.50022	13.49975	13.49998
73.27148	25.706028	13.50058	13.50034	13.5001	13.5001	13.49962
74.95508	25.807959	13.49986	13.49986	13.49938	13.49962	13.49962
74.15039	25.702524	13.49945	13.49921	13.49921	13.49921	13.49872
71.98438	25.716705	13.49985	13.49961	13.49961	13.49936	13.49936
73.78418	25.811996	13.50014	13.4999	13.49942	13.49966	13.49966
70.99512	25.981364	13.49964	13.4994	13.4994	13.49884	13.4994
69.5127	25.935737	13.49998	13.49928	13.49952	13.49952	13.49952
69.91992	25.322439	13.5001	13.49962	13.49986	13.49986	13.49938
71.80371	25.418695	13.49951	13.49975	13.49975	13.49928	13.49928
70.58203	25.428585	13.50002	13.50002	13.49978	13.49978	13.49978
70.85254	25.501545	13.5007	13.49998	13.50022	13.49974	13.49998
69.875	25.326083	13.50262	13.50237	13.50212	13.50213	13.50188
71.75293	25.380368	13.50042	13.50018	13.4997	13.49994	13.49994
72.54395	25.45913	13.50307	13.50257	13.50232	13.50207	13.50182
70.76465	25.536978	13.5006	13.50035	13.50035	13.5001	13.5001
71.11621	25.837945	13.50128	13.50104	13.50081	13.50081	13.50081
74.5957	25.754207	13.50284	13.5026	13.5026	13.50235	13.50235
72.82422	25.759019	13.49921	13.49945	13.49897	13.49921	13.49921
74.49023	25.763525	13.49998	13.49998	13.4995	13.4995	13.49974
74.10645	25.865342	13.50112	13.50088	13.50039	13.50063	13.50063
75.30566	25.746501	13.50284	13.50207	13.50183	13.50157	13.50131
73.38965	25.855186	13.50075	13.5005	13.50024	13.50024	13.50024
75.32813	25.785463	13.50007	13.49982	13.49956	13.49956	13.49956
73.0293	25.811425	13.50152	13.50127	13.50103	13.50077	13.50053
74.75488	25.834937	13.5012	13.50095	13.50037	13.50061	13.50061
73.42578	25.871728	13.50052	13.50028	13.50028	13.50028	13.50028
76.45508	25.82219	13.5015	13.50099	13.50075	13.50025	13.50049

Humidity	Temperature	M 1	M 2	M 3	M 4	M 5
71.80078	25.841398	13.50113	13.50088	13.50088	13.50064	13.50063
72.61621	25.933427	13.50116	13.50066	13.50041	13.49983	13.50007
73.47656	26.031155	13.50095	13.50037	13.50061	13.50061	13.50061
73.96973	26.056812	13.50117	13.50066	13.50041	13.50041	13.50041
71.06348	26.007707	13.50062	13.50037	13.50037	13.49986	13.50012
73.3418	26.035675	13.50269	13.50244	13.50218	13.50193	13.50193
74.28125	26.023741	13.5026	13.50234	13.50209	13.50209	13.50209
72.60938	26.080692	13.50152	13.50103	13.50127	13.50127	13.50127
73.11328	26.044498	13.50145	13.50119	13.50093	13.50093	13.50067

Appendix A.4: Single sample, multiple touch, active clamping

Humidity	Temperature	M 1	M 2	M 3	M 4	M 5
51.17188	24.47245	13.49989	13.49966	13.49966	13.49951	13.49943
51.25195	24.627117	13.49827	13.49798	13.49798	13.49805	13.49805
51.1709	24.581554	13.49889	13.49897	13.49889	13.49889	13.49873
52.48633	24.593627	13.49933	13.49955	13.49948	13.49941	13.49948
51.66406	24.571271	13.50122	13.50097	13.50073	13.50073	13.50073
52.90527	24.594871	13.49841	13.49833	13.49809	13.49801	13.49793
53.85742	24.597524	13.50026	13.49962	13.49946	13.49978	13.49946
52.64844	24.587762	13.5011	13.50064	13.50041	13.5001	13.49986
50.98535	24.737021	13.49612	13.49611	13.49589	13.49597	13.49627
50.31836	24.701689	13.50024	13.49932	13.49925	13.49894	13.49886
52.23047	24.754921	13.49771	13.49747	13.49747	13.49747	13.49771
50.05762	24.728489	13.49916	13.49908	13.49908	13.499	13.49931
51.37402	24.766829	13.50057	13.50033	13.5008	13.50064	13.50056
51.6416	24.792296	13.49939	13.49954	13.49947	13.49931	13.49977
50.54199	24.857474	13.49839	13.49847	13.49885	13.49831	13.49839
50.26465	25.031971	13.49949	13.49941	13.49972	13.49972	13.49941
50.54199	24.995776	13.49914	13.49915	13.49914	13.49915	13.49915
49.9209	25.008484	13.49809	13.49817	13.49793	13.49793	13.49816
49.83984	24.961842	13.50117	13.50088	13.50073	13.50088	13.50138
52.47266	25.01289	13.50125	13.50066	13.50066	13.50081	13.50125
49.60742	24.96645	13.49939	13.49931	13.50008	13.49978	13.49978
48.43457	25.090763	13.49768	13.49721	13.49697	13.49681	13.49674
51.48828	25.247664	13.49845	13.49792	13.49776	13.49753	13.49746
49.24023	25.154887	13.49923	13.49923	13.49916	13.49969	13.49923
50.17578	25.180404	13.50044	13.50029	13.5002	13.5002	13.50012
50.01074	25.19767	13.50048	13.50072	13.50025	13.50025	13.50017
50.16211	25.194179	13.49888	13.49896	13.49896	13.49896	13.49872
50.16406	25.202126	13.49939	13.49923	13.49932	13.499	13.49901
51.06055	25.206442	13.50267	13.50213	13.50213	13.50236	13.50189
50.14063	25.230995	13.49904	13.49889	13.49866	13.49866	13.49842
49.54785	25.283236	13.50025	13.50017	13.50025	13.50001	13.5
49.98731	25.269246	13.49888	13.49904	13.49903	13.49926	13.49888
49.12793	25.194966	13.49997	13.49927	13.49927	13.49927	13.49927
48.63672	25.294814	13.49985	13.49986	13.49969	13.49978	13.49986
50.60352	25.334297	13.49923	13.49923	13.49899	13.49899	13.49899
51.12891	25.29696	13.49935	13.49935	13.49935	13.49936	13.49958
50.30078	25.28528	13.49891	13.49946	13.499	13.499	13.49922
50.53711	25.245709	13.49806	13.49798	13.49798	13.49798	13.49822
49.4082	25.260283	13.49695	13.49694	13.49695	13.49717	13.49687
48.33789	25.218211	13.49872	13.49863	13.49848	13.49848	13.49848

Humidity	Temperature	M 1	M 2	M 3	M 4	M 5
50.18945	25.260956	13.49958	13.4995	13.49934	13.49965	13.49935
49.52832	25.406673	13.50537	13.50537	13.50528	13.50528	13.5052
51.32031	25.477843	13.49853	13.49852	13.49853	13.49853	13.49852
57.66309	24.630253	13.50013	13.49989	13.49989	13.49989	13.49989
56.38965	24.645538	13.5027	13.50269	13.5027	13.5027	13.5027
56.69434	24.723195	13.50171	13.50194	13.50194	13.50193	13.50194
58.24512	24.797234	13.50103	13.50103	13.50118	13.50118	13.50118
57.36426	24.705904	13.50167	13.5019	13.5019	13.5019	13.5019
56.21387	24.798187	13.50113	13.50128	13.50136	13.50159	13.50136
57.54883	24.653955	13.50167	13.50159	13.50167	13.50167	13.50167

Appendix A.5: Single sample, multiple touch, weighted stage

M 1	M 2	M 3	M 4	M 5
13.49908	13.49885	13.49885	13.49885	13.49908
13.49848	13.4984	13.4984	13.4984	13.4984
13.50641	13.50547	13.50547	13.50648	13.50648
13.49929	13.49913	13.49936	13.49881	13.49882
13.49857	13.49842	13.49835	13.4982	13.4982
13.49584	13.49569	13.49554	13.49575	13.49547
13.49863	13.49887	13.49856	13.49863	13.49863
13.49565	13.49531	13.49505	13.49487	13.49435
13.50031	13.50085	13.50101	13.50124	13.50124
13.50147	13.50162	13.50178	13.50177	13.50185
13.5009	13.50098	13.5013	13.50145	13.50146
13.49821	13.49821	13.49875	13.49891	13.49845
13.49944	13.49921	13.49968	13.49991	13.49991
13.50525	13.50331	13.50371	13.50379	13.50331
13.49984	13.50046	13.50054	13.50054	13.50054
13.50239	13.50223	13.50224	13.502	13.50199
13.49734	13.4985	13.49858	13.49866	13.49921
13.50024	13.49947	13.49916	13.49955	13.49955
13.4992	13.49927	13.4988	13.4988	13.49889
13.49819	13.49819	13.4982	13.49866	13.4982
13.4997	13.49907	13.49891	13.49884	13.49891
13.49946	13.4993	13.49906	13.49898	13.49906
13.49758	13.49734	13.49718	13.49718	13.49718
13.49868	13.49844	13.49844	13.49844	13.49844
13.49907	13.49875	13.49851	13.49851	13.49875
13.50013	13.49965	13.49942	13.49918	13.49919
13.5045	13.50402	13.50378	13.50353	13.5033
13.49895	13.49872	13.49848	13.49847	13.49848
13.49793	13.49793	13.49746	13.49769	13.49769
13.49931	13.49907	13.49884	13.49837	13.4986
13.49942	13.49895	13.49917	13.49871	13.49871
13.49896	13.49872	13.49848	13.49848	13.49848
13.4989	13.49889	13.49889	13.49889	13.49841
13.49977	13.49953	13.49953	13.49953	13.49906
13.49915	13.4989	13.4989	13.49867	13.49867
13.50013	13.49989	13.4999	13.49966	13.49966
13.49865	13.49842	13.49819	13.49818	13.49818

M 1	M 2	M 3	M 4	M 5
13.49953	13.49931	13.49907	13.49907	13.49907
13.49511	13.49511	13.49511	13.49482	13.49482
13.50321	13.50298	13.50276	13.50276	13.50253
13.49853	13.4983	13.4983	13.4983	13.49806
13.4986	13.49813	13.49813	13.49813	13.4979
13.49697	13.49675	13.49653	13.49653	13.49653
13.49645	13.49601	13.49623	13.4958	13.496
13.50046	13.50022	13.50022	13.49974	13.49998
13.49999	13.49976	13.49952	13.49929	13.49929
13.49951	13.49927	13.49904	13.49904	13.49904
13.49848	13.49825	13.49825	13.49771	13.49771
13.50342	13.50238	13.50238	13.50238	13.50186
13.49867	13.49843	13.49843	13.49819	13.49819

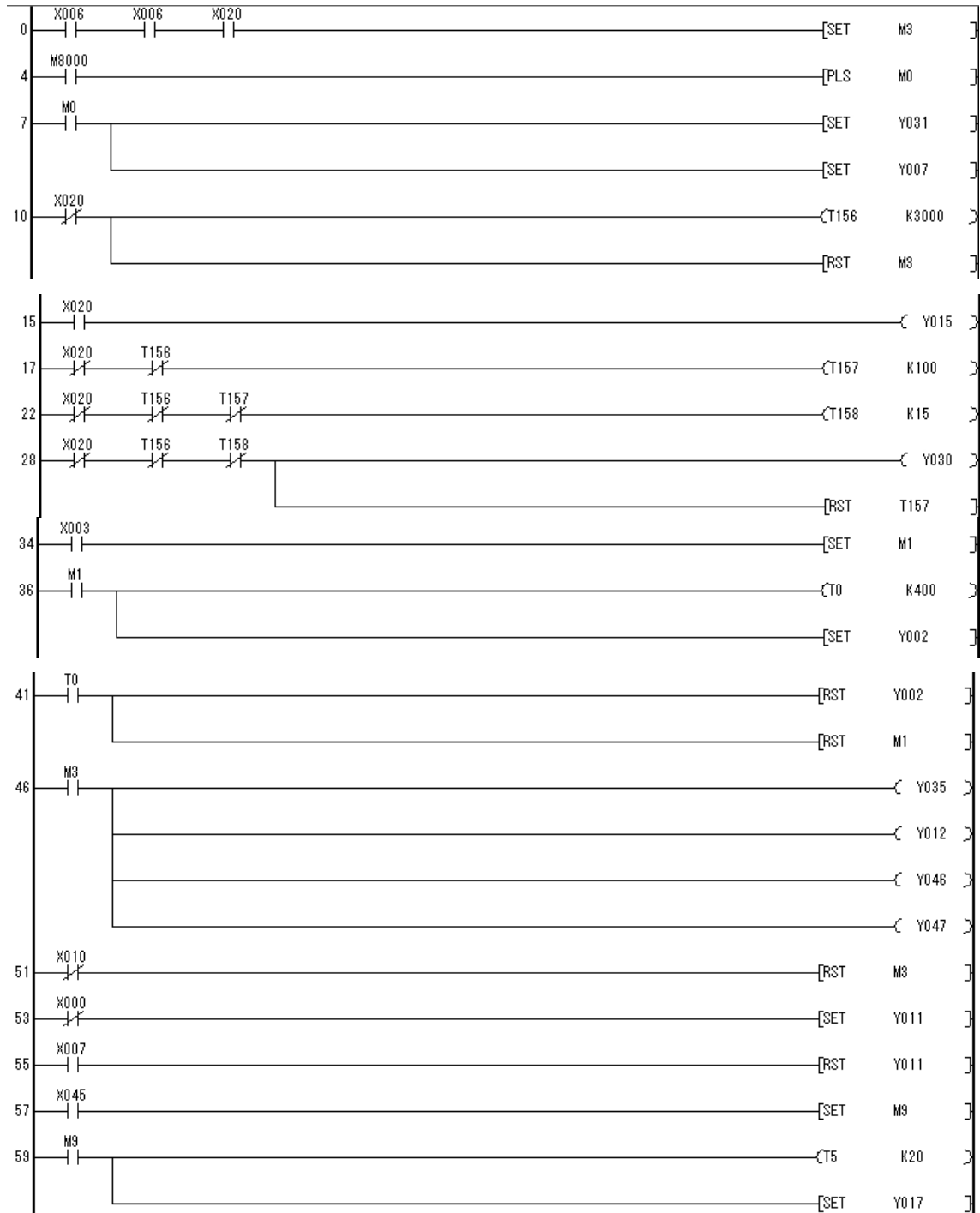
Appendix A.6: M. touch, weighted stage, active clamping, under fluid

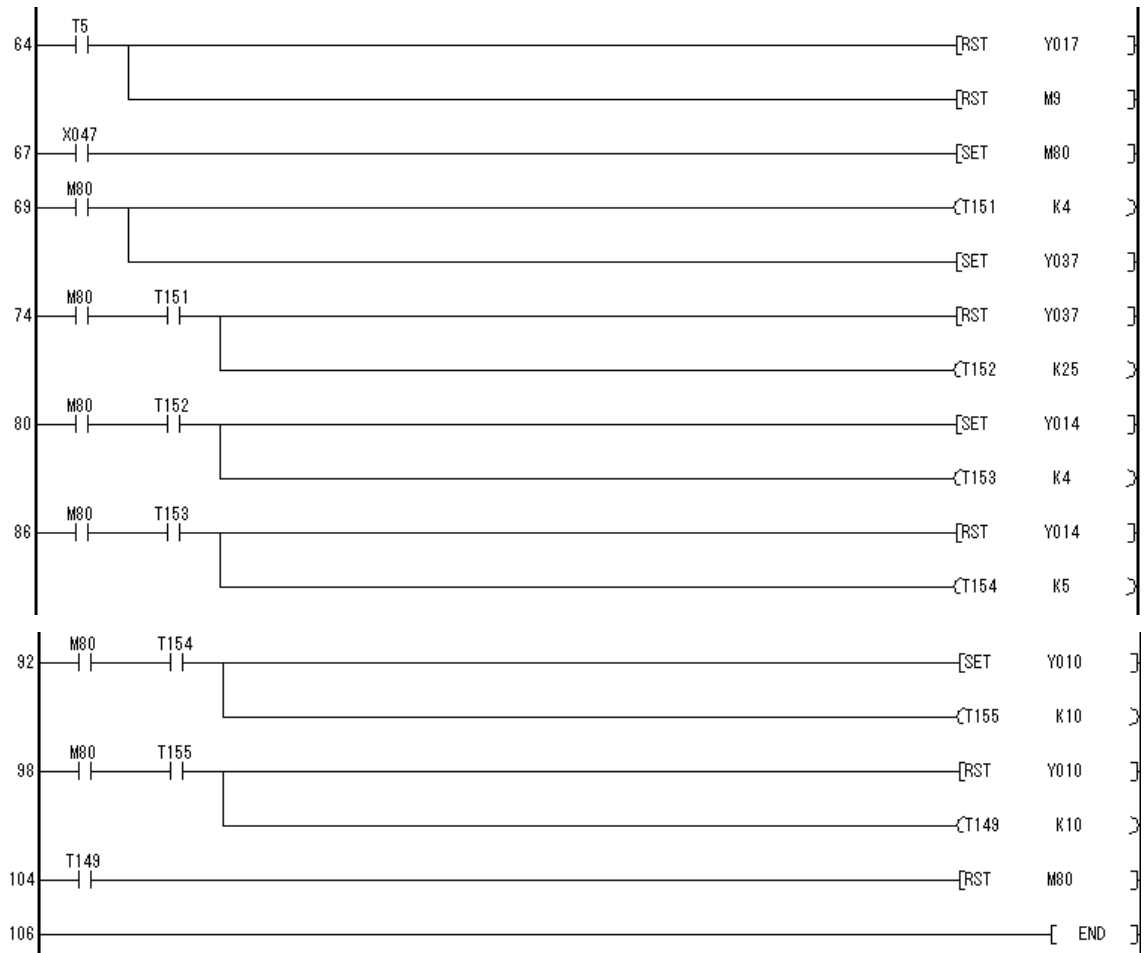
Humidity	Temperature	M 1	M 2	M 3	M 4	M 5
62.75488	20.767349	13.49866	13.49866	13.49866	13.49866	13.49866
63.43066	20.956433	13.49971	13.49917	13.49947	13.49948	13.49947
63.51074	21.081812	13.49966	13.49921	13.49943	13.49944	13.49943
63.18262	20.959657	13.49921	13.49944	13.49921	13.49943	13.49921
62.49414	20.98077	13.49909	13.49931	13.49931	13.49931	13.49931
64.53027	21.033519	13.50047	13.50023	13.50023	13.49978	13.5
63.26953	21.036756	13.50001	13.49978	13.49977	13.49977	13.49978
63.20313	21.020138	13.49848	13.49849	13.49848	13.49803	13.49803
61.83887	21.096906	13.50205	13.50206	13.50206	13.50206	13.50206
62.76758	21.039003	13.50255	13.50208	13.50185	13.50185	13.50161
63.73242	21.124899	13.49882	13.49859	13.49834	13.49859	13.49858
61.14844	21.308867	13.49865	13.49865	13.49865	13.49865	13.49865
61.31738	21.173929	13.49906	13.49883	13.49883	13.49883	13.49883
61.83301	21.39305	13.49895	13.49872	13.49872	13.49872	13.49872
60.18555	21.199675	13.49872	13.49849	13.49795	13.49796	13.49796
62.03809	21.224304	13.49797	13.49796	13.49797	13.49796	13.49797
62.41602	21.318097	13.49939	13.49939	13.49939	13.49939	13.49893
60.99023	21.278805	13.4992	13.49875	13.49897	13.49897	13.49897
60.95606	21.278805	13.49954	13.49932	13.49908	13.49908	13.49908
58.15137	21.365539	13.49909	13.49886	13.49886	13.49842	13.49863
60.6543	21.386283	13.49859	13.49813	13.49836	13.49836	13.49836
59.05273	21.599971	13.49922	13.49876	13.49899	13.49899	13.49898
61.04102	20.215242	13.49943	13.4992	13.49899	13.49898	13.49898
58.16504	20.235377	13.49954	13.49933	13.49933	13.49933	13.49933
57.86816	20.445941	13.49884	13.49861	13.49861	13.49861	13.49861
58.87891	20.438756	13.49794	13.49749	13.49749	13.49749	13.49749
57.28418	20.392621	13.49943	13.4992	13.49873	13.49896	13.49897
57.3877	20.893578	13.49989	13.49965	13.49966	13.49965	13.49965
53.73047	20.695176	13.49989	13.49944	13.49966	13.49966	13.49966
54.1709	20.803035	13.49931	13.49931	13.49932	13.49931	13.49931
54.13574	20.750883	13.49942	13.49919	13.49919	13.49919	13.49919
53.82227	20.950288	13.49908	13.49908	13.49862	13.49908	13.49862

Humidity	Temperature	M 1	M 2	M 3	M 4	M 5
53.23438	20.981328	13.4992	13.49874	13.4992	13.4992	13.49919
54.6709	21.026295	13.50013	13.50036	13.50036	13.50036	13.50036
54.63867	21.059861	13.4995	13.49904	13.49904	13.49926	13.49926
54.38672	21.273206	13.50097	13.50074	13.50074	13.50074	13.50097
52.85059	21.222603	13.49886	13.49833	13.49864	13.49864	13.49834
49.93555	21.822418	13.49897	13.49897	13.49897	13.49897	13.49897
50.96777	21.881045	13.49832	13.49855	13.49855	13.49855	13.49856
50.52539	21.877541	13.49908	13.49909	13.49862	13.49863	13.49862
51.36719	21.817975	13.49996	13.49949	13.49973	13.49973	13.49973
51.62695	21.915005	13.49849	13.49804	13.49826	13.49803	13.49827
51.64551	21.734681	13.4994	13.49939	13.49939	13.4994	13.49917
49.40332	21.845143	13.49778	13.49778	13.49733	13.49778	13.49778
50.94238	21.8692	13.49889	13.49888	13.49842	13.49842	13.49843
51.25	21.822088	13.49876	13.4983	13.4983	13.49853	13.49853
51.36328	21.890465	13.49939	13.49962	13.49962	13.49962	13.49962
51.79395	21.890465	13.49913	13.49859	13.49882	13.49882	13.49882
50.51465	21.946616	13.4992	13.49866	13.49866	13.49866	13.49866
50.32227	21.851376	13.50046	13.50103	13.50103	13.50078	13.50079

Appendix B – PLC Programs

Appendix B.1: Cooling station PLC program





Appendix B.2: Measurement station PLC program

